ABSTRACT

Title of Thesis:	Evaluation of Roadside Soil Compaction and Restoration Practices on Vegetation Growth and Water Quality
	Mikayla Cunningham
	Master of Science, 2024
Thesis Directed By:	Professor Allen P. Davis and Professor Ahmet H. Aydilek
	Department of Civil and Environmental Engineering
	University of Maryland, College Park

The construction of roads using heavy equipment and cut-and-fill methods leads to heavily compacted roadside soils with low fertility, sparse vegetation, low water infiltration rates, and high erodibility. Poor post-construction vegetation and soil quality lead to higher runoff volumes with higher sediment and nutrient loads to local water bodies. Cost-effective methods are needed to restore roadside soils, establish sufficient vegetative cover, and maintain runoff water quality. A research project was undertaken to assess topsoil application, tillage, and yard waste compost amendment as means of restoring roadside soil quality. A 28-week pot study was used to test how topsoil depth, initial soil density, compaction from mowing equipment, and compost amendment influenced long-term soil density, hydraulic conductivity, and vegetation establishment. A 12-week mesocosm study with weekly simulated storm events was conducted to further examine the effects of soil type and soil bulk density on vegetation on a larger scale. Water quality testing of the simulated rainfall and runoff samples was also implemented to measure soil erosion and nutrient leaching. Compost-amended subsoil improved vegetation (biomass and grass heights) compared to subsoil, but it did not perform as well as topsoil. The yard waste compost was selected and applied at a rate designed to limit nitrogen and phosphorous losses, and it was successful, given that the compost-amended mesocosms did not export higher nutrient loads than mesocosms with inorganic fertilizer. Hydraulic conductivity was observed to primarily depend on soil density. A series of recommendations for highway projects to effectively restore roadside soil quality to improve vegetation and stormwater management are provided. A low-density layer of topsoil at least 20 cm deep is ideal. Yard waste compost should not be applied at a rate that raises soil organic matter by more than 2%.

EVALUATION OF ROADSIDE SOIL COMPACTION AND RESTORATION PRACTICES ON VEGETATION GROWTH AND WATER QUALITY

by

Mikayla Cunningham

Thesis submitted to the Faculty of the Graduate School of the
University of Maryland, College Park, in partial fulfillment
of the requirements for the degree of
Master of Science
2024

Advisory Committee:

Professor Ahmet H. Aydilek, Co-Chair

Professor Allen P. Davis, Co-Chair

Assistant Professor Guangbin Li, Committee Member

© Copyright by
Mikayla Cunningham
2024

Acknowledgements

I would like to thank the Iowa Department of Transportation for the funding support for this research. I would also like to thank my advisors Dr. Allen Davis and Dr. Ahmet Aydilek for their constant support and guidance throughout my degree. Further, I would like to extend my gratitude to Dr. Guangbin Li for serving on my committee and to my collaborators at Michigan State University: Dr. Bora Cetin, Oguzhan Saltali, and Dr. Angela Farina. I also really appreciate all the help that my undergraduate research assistants, Bryce Brown and Ashwini Mariappan, provided me with during my mesocosm study. Furthermore, Dr. Sai Pamuru, Marya Anderson, and Meghan Fisher Holbert all provided me with assistance during my research, for which I am incredibly grateful. Finally, I would also like to thank my parents and sister for their support.

Table of Contents

List of Figures

List of Tables

Chapter 1 Introduction

The construction of roads using heavy equipment and cut-and-fill methods leads to heavily compacted roadside soils with low fertility, low infiltration rates, high erodibility, and sparse vegetation (Bochet and Garcia-Fayos, 2004; Haynes et al., 2013). The removal of topsoil during construction results in the remaining soil having minimal organic matter and nutrients. Compaction increases bulk density and root penetration resistance, and it reduces porosity and precipitation storage capacity (Richard et al., 2001; Zhang et al., 2006). If a soil has high bulk density relative to its texture, then plant roots will be affected, and at a certain density, root growth will be restricted (NRCS Soil Quality Institute, 1999). Vegetation intercepts rainfall and reduces erosion and the roots of plants create channels in soil that can increase infiltration rate over time (Hino et al., 1987). Poor post-construction vegetation and soil quality lead to higher runoff volumes and higher sediment and nutrient loads to local water bodies than conditions prior to construction or of typical vegetated spaces. Furthermore, climate change is making extreme precipitation events more common while continued urban development leads to increasing areas of disturbed soil (Wang et al., 2017). Hence, sufficient stormwater infiltration is more important than ever to protect the health of water bodies.

Structural solutions to manage stormwater, like bioretention basins, can be too expensive to build and maintain to be practical for wide-spread roadside applications. In contrast, vegetated stormwater control measures (SCMs) are cost-effective and can still be successful at reducing stormwater runoff and its associated pollution. In SCMs, processes like filtration, biological transformation and uptake can improve water quality (Hunt et al., 2012; Vogel et al., 2015). Vegetated SCMs rely on adequate infiltration and vegetation establishment to function. Thus, soil

quality restoration practices, such as tillage, are often required to achieve desired performance from vegetated SCMs in roadside applications.

Tillage is a possible approach to reducing soil compaction and increasing infiltration rate by altering the pore structure of a soil (Lipiec et al., 2006). Mohammadshirazi et al. (2017) found that tillage increased infiltration rate so that it was generally 3-4 times that of compacted soils after about two and a half years. Moreover, Haynes et al. (2013) showed that deep tillage prior to seeding on construction sites can lead to high infiltration rate and successful vegetation growth. However, rapid and robust vegetation establishment was required to sustain these results in the long-term. Over time, use of routine mowing equipment can lead to reconsolidation of the soil (Oliveira & Merwin, 2001). Other studies have found that benefits of tillage on soil density and infiltration rate are maintained only if tillage is coupled with compost amendment as initial benefits of the tillage alone can be lost within two years (Olson et al., 2013; Schmid et al., 2017). Rivers et al. (2021) found that tillage increased runoff sediment concentration and did not decrease the volume of runoff from roadside soils, but tillage with compost amendment decreased runoff volume which in turn decreased net sediment transport.

Compost amendment can also improve nutrient concentrations and organic matter content of deficient soils, further aiding vegetation establishment. Compost amendment to soils has been found to improve several soil properties including decreasing bulk density (Landschoot and McNitt, 1994; Cogger, 2005), increasing infiltration rates (Landschoot and McNitt, 1994; Aggelides and Londra, 2000; Curtis et al., 2007), and increasing water holding capacity (Weindorf et al., 2006) along with improving vegetation establishment and decreasing sediment in runoff (Glanville et al., 2004; Harrell and Miller, 2005; Hansen et al., 2012). Furthermore, compost-amended slopes have been shown to reduce runoff volume compared to topsoil alone

(Glanville et al., 2004; Faucette et al., 2005; Muktar et al., 2008). Compost use also has other sustainability benefits including reducing the amount of waste going to landfills and reducing the need for inorganic fertilizers. Nevertheless, compost amendment has also been shown to often leach nutrients (nitrogen and phosphorus) into runoff which can contribute to eutrophication and impair nearby water bodies. Owen et al. (2021) found that biosolids and green waste compost additions on roadside embankments increased nitrogen export by 2.2- to 3.3-fold and increased phosphorous export by 1.5- to 51-fold. The leaching behavior of an amended soil is dependent on the type of compost used and the application rate (Pamuru et al., 2024; Owen et al., 2021).

Tillage, topsoil application, and compost amendment have shown mixed results in improving roadside soils and vegetation. However, the success of these approaches depends on specific local details, such as soil texture, and no specific recommended depths are available for these remedial processes. In particular, compost amendment must be implemented with regard to both the type of compost and the application rate to prevent unacceptable levels of nutrient leaching.

This research project was undertaken at the University of Maryland to assess topsoil application, tillage, and compost amendment as means of restoring roadside soil quality. The objectives of the project were to evaluate the effects of soil quality, topsoil depth, initial soil density, compaction from mowing equipment, and compost amendment on long-term soil density, vegetation establishment, and runoff water quantity and quality. These objectives were addressed through soil characterization, a pot study, and large-scale mesocosm study. A series of recommendations for highway projects to effectively restore roadside soil quality to improve vegetation and stormwater management are provided.

Chapter 2 Materials and Methods

2.1 Soil Characterization

Topsoil and subsoil were collected from U.S. Route 30 in Benton County, Iowa (Figure 2.1) and shipped to the University of Maryland Research Greenhouse Complex in August 2022. Yard waste compost came from Specialized Environmental Technologies, Inc. (Minnetrista, MN USA). The soils and compost were shipped and stored in plastic drums.

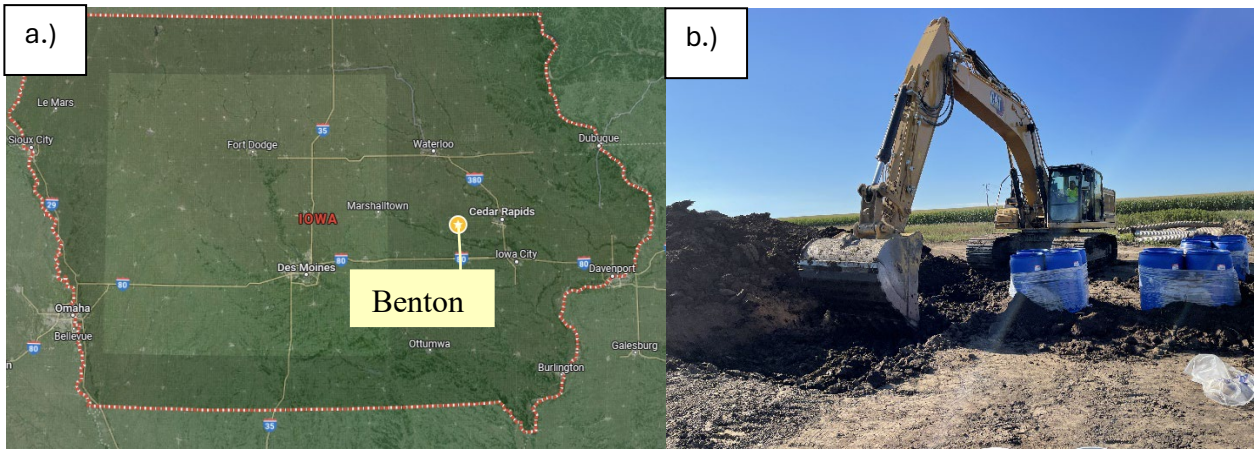

Figure 2.1: a.) Map indicating location of soil collection at 41°57'42.0"N 92°06'19.0"W (Google Maps), and b.) photograph of soil collection.

The particle size distribution of the soils was analyzed following ASTM D6913 for the sieve analysis and ASTM D7928 for hydrometer analysis. The Atterberg Limits of the soils were found in accordance with ASTM D4318. The soils were then classified according to the Unified Soil Classification System (USCS), the American Association of State Highway and Transportation Officials (AASHTO), and the United States Department of Agriculture (USDA) soil texture categories. Soil compaction testing was conducted following the standard Proctor test method (ASTM D698). The optimum moisture contents (w_{opt}) and maximum dry densities

($\rho_{d,max}$) for the soils were derived from the compaction curves. Soil was passed through a 2-mm opening sieve (number 10 sieve) before soil chemical testing. Organic matter (OM) was measured through loss on ignition in accordance with ASTM D2974. Soil pH (EPA Method 9045D) and soil electrical conductivity (EC) were measured in a 1:2 soil to DI water ratio. These results are presented in Table 2.1. This chemical testing was also conducted on the compost. Additionally, compost C and N were measured on the LECO CN628 analyzer using a combustion at 950 ℃ method with infrared detection and thermal conductivity, respectively. Compost P was measured using a Mehlich-3 extraction on a Shimadzu Model ICPE-9820. Compost chemical properties are presented in Table 2.2. Additional nutrient testing of the topsoil and subsoil was completed by the Cornell Soil Health Laboratory, and the results are available in Appendix A.

Table 2.1: Physicochemical properties of the soils

Soil Type	Gravel (%)	Sand (%)	Silt (%)	Clay (%)	w_L	w_P	I_P	USCS	AASHTO	USDA	ρ_{dmax} (g/cm^3)	w_{opt} (%)	OM (%)	pH	EC (µS/cm)
Topsoil	0	9	59	32	45.5	23.3	22.1	CL	A-7-6	Silty Clay Loam	1.60	20.0	5.8 ± 0.3	7.3 ± 0.2	184 ± 24
Subsoil	0	7	64	29	48.3	22.0	26.3	CL	A-7-6	Silty Clay Loam	1.60	20.0	3.8 ± 0.1	7.5 ± 0.1	102 ± 5

Notes: w_L=liquid limit, w_p= plastic limit, I_P= plasticity index, ρ_{dmax}=maximum dry density, w_{opt}=optimum moisture content, OM=organic matter content, EC=electrical conductivity.
OM, pH, and EC were measured on 2 mm sieved samples, and are denoted as the mean ± the standard deviation of three representative samples.

Table 2.2: Chemical properties of the compost

	OM (%)	pH	EC (µS/cm)	C (%)	N (%)	C: N	Mehlich-3 P (mg P/kg)
Compost	33 ± 3	7.52 ± 0.05	3040 ± 219	18.4 ± 0.9	1.39 ± 0.08	13.2	662 ± 49

Notes: All values are denoted as the mean ± the standard deviation of three representative samples. The C:N ratio was calculated using the means of C% and N%, so there is no standard deviation reported.

2.2 Pot Study

The objectives of this 28-week pot study were to evaluate the effects of (1) topsoil depth, (2) initial soil density, and (3) compaction from mowing equipment on long-term soil density, vegetation establishment, and hydraulic properties. The pots were prepared in C2000 (14.55 L/ 3.84 gal) blow molded containers (Nursery Supplies Inc., Chambersburg, PA USA). Given the tapered shape of these pots, the volume of the pot corresponding to relevant depths was determined by filling a pot with water to the desired depth and measuring the weight of the water. A needle-punched staple fiber nonwoven geotextile (Ψ= 0.8 s^{-1}), commonly used in filtration applications, was placed at the bottom to limit soil loss. The soil was air-dried to its optimum moisture content and sieved through a 12.5 mm (½-inch) sieve. The soil was placed on the geotextile and compacted to the desired dry density using a vibratory compaction hammer in five lifts each no more than 5 cm (2") in height. A manual hammer was used to ensure consistent compaction at the edge of the pot.

Experimental Design

Seven configurations of soil layers were selected to represent possible field scenarios of different topsoil and tillage depths. These configurations along with their corresponding labels are represented in Figure 2.2. Each has a total soil depth of 22.9 cm (9 inch) containing one to three layers. High and low density refer to a bulk density of 1.60 g/cm^3 (100 pcf) and of 1.15 g/cm^3 (72 pcf), respectively. The high-density value is the maximum dry density of the soil as determined by a standard Proctor test to represent a highly compacted soil in the field, and it is reported to affect root growth (NRCS Soil Quality Institute, 1999). The low-density value

represents a tilled soil (Mohammadshirazi et al., 2017). The first character for each pot abbreviation is the soil type with "B" to refer to Benton, Iowa. The second character is "L" or "H" to refer to the subsoil as low or high density, respectively, and the third character is "1", "5", or "9" to refer to the subsoil depth. If there is no topsoil, then the fourth character is a "0", otherwise the fourth and fifth characters are a "L" followed by "4" or "8" to signify the depth of low-density topsoil. Only one pot configuration has three layers; this pot is designated "BH1H4L4" to signify Benton soil with a bottom layer of high-density subsoil, a middle layer of high-density topsoil, and a top layer of low-density topsoil. Additionally, two of the configurations were amended with compost in the top 10.2 cm (4 inch) of the pot at the rate required to raise the organic matter to 8%. The letter "C" is used in the amended pot abbreviations to signify compost-amended Benton soil. Other than the compost addition, CH90 is equivalent to BH90 and CH5L4 is equivalent to BH5L4. To account for the lower density of the compost, the amended layer in the CH90 pot was prepared at a density of 1.22 g/cm^3 (76 pcf), and in the CH5L4 pot it had a density of 1.04 g/cm^3 (65 pcf). Each condition was set up in triplicate for a total of 27 pots.

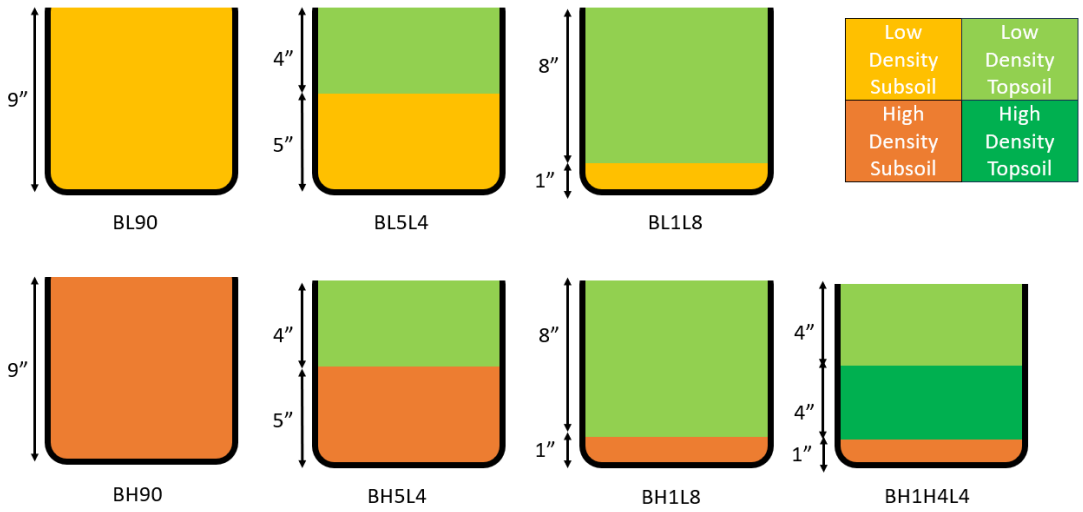

Figure 2.2: Pot configuration diagram with pot abbreviations.

Pot Setup and Environmental Conditions

In accordance with Iowa DOT Article 2601.03, C, 3 (2023), the permanent rural seed mix was applied at a rate of 112 kg/ha (100 lb/ac) tall fescue, 84 kg/ha (75 lb/ac) perennial ryegrass, and 22.4 kg/ha (20 lb/ac) Kentucky bluegrass along with 336 kg/ha (300 lb/ac) of 6-24-24 fertilizer. These values correspond to 1.59 g of seed and 2.45 g of fertilizer per pot. The turfgrass seed mix was from Millborn Seeds (Brookings, SD USA), and the fertilizer was from Des Moines Feed (Des Moines, IA USA). The seeds and fertilizer were applied to the pots on March 6, 2023, by first saturating the soil, then scoring the soil surface to roughen it, and finally pressing the seed and fertilizer into the soil. The pots containing compost did not receive fertilizer.

Each pot received 26.7 mm (1.05 inches) of water per week. This depth was based upon average rainfall across Iowa from April to June from data from the past thirty years (1993-2022) to account for increases due to climate change. The average three-month depth of 348 mm (13.7 inches) was divided evenly into the weekly depth (NOAA, 2023). For the first four weeks after seeding, this weekly volume of water was divided among three applications on Mondays, Wednesdays, and Fridays. Starting week five, watering was reduced to applications on Mondays and Fridays only since the vegetation had become more established and less vulnerable to dry surface soil. The greenhouse room was set at a temperature of 24°C (75°F) during the daytime and 18°C (64°F) during the night. A shade curtain limited direct sunlight from the ceiling. Each week, the placement of the pots within the room was randomly changed to account for any differences in sunlight or temperature across the room. Figure 2.3 shows some of the pots in the greenhouse.

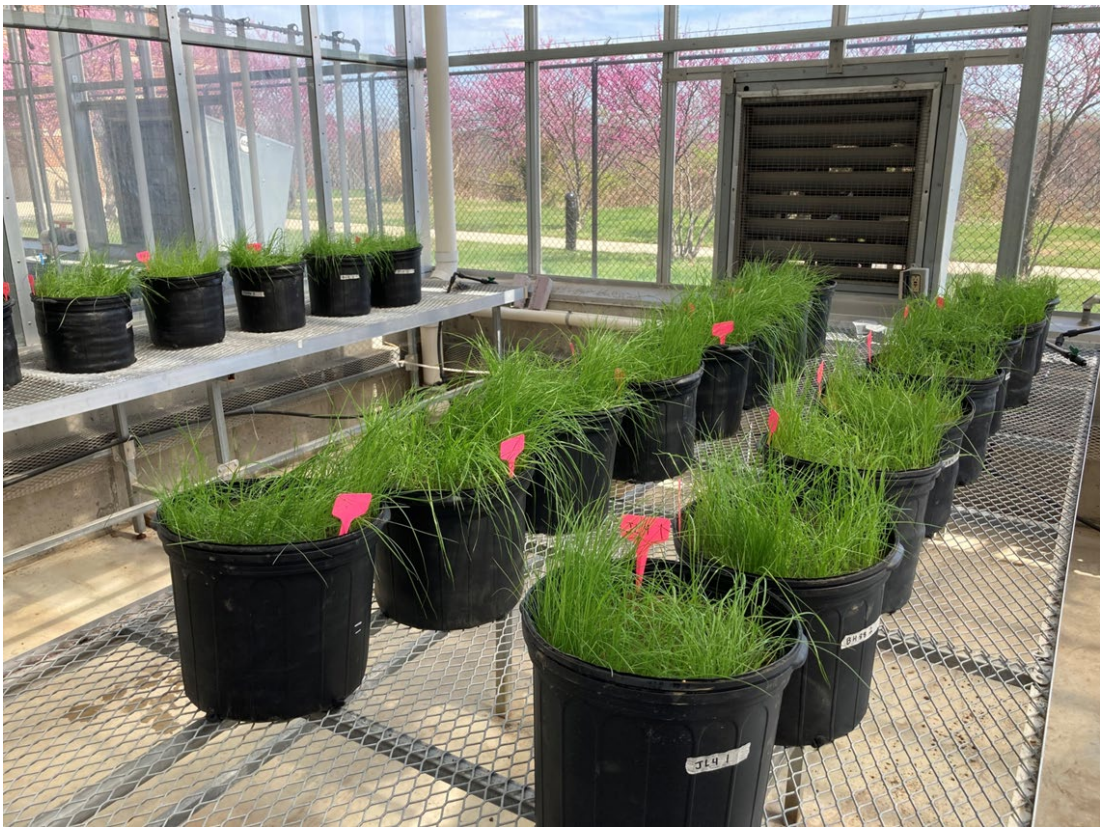

Figure 2.3: Pots in the greenhouse room on April 3, 2023, 4 weeks after seeding.

Vegetation Establishment

Photographs of the pots were taken each week using an iPhone SE 2020 from a height of 0.6 m (2 ft) above the bench top surface. These images were cropped to a circle in *Adobe Photoshop* and analyzed for percent green coverage in the software *Canopeo* using the default settings (Patrignani & Ochsner, 2015). An example captured image is depicted in Figure 2.4a, the image after cropping is shown in Figure 2.4b, and the software output is shown in Figure 2.4c. Pixels contributing to green coverage are depicted as white while the rest of the image is black. A conversion factor of $4/\pi$ was used to account for the circumscribed square input *Canopeo* assumes.

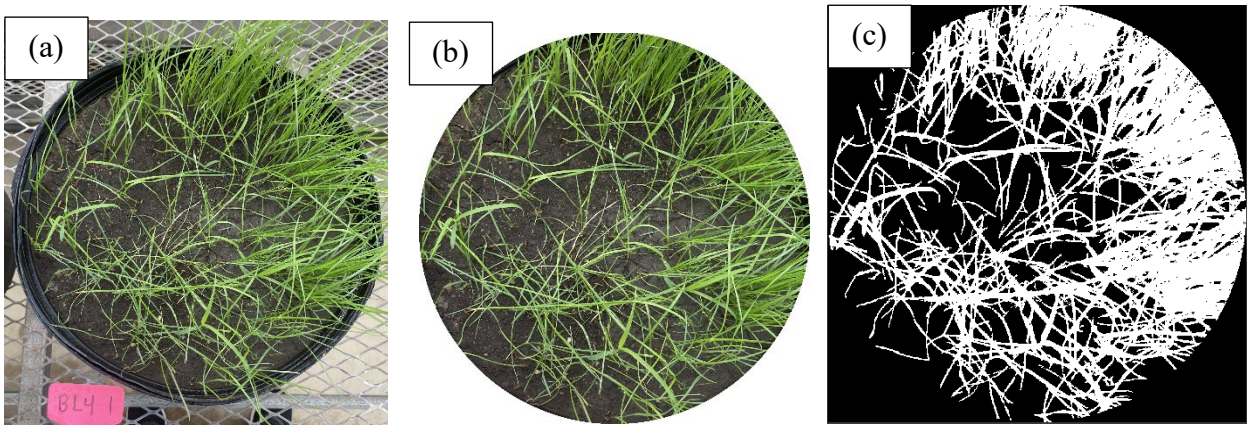

Figure 2.4: (a) Sample captured image of pot vegetation, (b) corresponding cropped image, and (c) corresponding software output.

The grass height for each pot was measured weekly. The pot was split into quadrants and a metal ruler was used to measure the average height from the soil surface for each section. These values were then averaged to find the grass height in a given pot.

Mowing Simulations

The effects of field mowing on vegetation establishment were simulated in the pots through trimming the grass and applying a compaction effort. In weeks 11 and 20 after seeding, grass was trimmed using metal scissors to a height of 15.2 cm (6”) in accordance with Iowa DOT Article 2612.03, A (2023). The specification states to mow when 50% of the vegetation will reach 35.6 cm (14 inches). However, plant growth is reduced when plants are grown in smaller pots (Poorter et al., 2012). Thus, the grasses were trimmed when grass growth had begun to plateau despite the heights being lower than the specification calls for. The trimmed biomass was oven dried at 50°C (122°F) for 48 hours and weighed. Once dried, this biomass was returned to the pots and placed underneath the remaining vegetation (simulating a mowing condition).

Compaction due to mowing was simulated twice on the pots. The representative weight of a tractor mower was assumed to be 2090 kg (4600 lb) based on a WORKMASTER™ 50 2WD tractor (New Holland Agriculture, Turin, Italy) and assuming a 90 kg (200 lb) rider. Assuming an equal distribution of this weight over each of the four tires, then each tire would apply a force of 522 kg (1150 lb). The front tires have a smaller contact area, so these were used to calculate a resultant pressure. For a radius of 18 cm (7 inch), the area is 994 cm^2 (154 in^2). Thus, a pressure of 51.7 kPa (7.5 psi) was calculated which corresponds to a force of 1.5 kN (300 lb) for the 253-cm^2 area of the pot that the compaction effort was applied to. A 12-ton hydraulic benchtop press (Torin Inc., Ontario, CA USA) was used to apply this pressure onto the pots for a duration of 3 seconds after weeks 15 and 20. A semicircular metal plate, as shown in Figure 2.5, was used to ensure uniform application of the pressure. Following this process, grass height, percent green coverage, and biomass data were collected separately for each side of the pots to determine any effects caused by the mowing compaction.

Figure 2.5: Hydraulic press and semi-circular plate applying compaction load to pot.

End of Study Measurements

On September 21, 2023, after 28-weeks of growth, destructive testing of the pots commenced starting with above-ground biomass collection. Metal scissors were used to remove the biomass at the ground surface with biomass separated between the two sides of each pot: the mowing-compacted side and the side with no additional compaction. The collected biomass was oven dried at 50°C (122°F) for 48 hours and weighed.

Four soil cores were collected from each pot to measure bulk density change spatially within the pots. The cores had a diameter of 5 cm (2 inch) and a height of 7.6 cm (3 inch). Upper cores were collected from the soil surface whereas lower cores were collected at mid-depth of the pots from 10.2 to 17.8 cm depth (4 to 7 inch). These lower cores were in the subsoil for pots with a topsoil depth of 10.2 cm (4 inch). These two core depths were collected on both sides of each pot as shown in Figure 2.6. The cores were oven dried at 100°C (212°F) for 24 hours and weighed. Bulk density was calculated by dividing the dry weight by the core's volume.

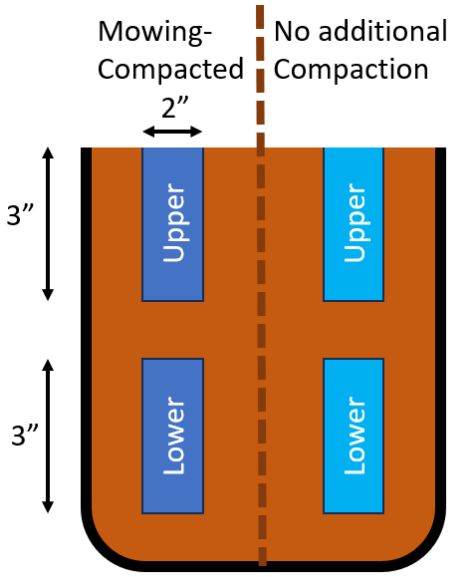

Figure 2.6: Diagram of core locations within pot.

Four additional cores, taken from the same depths as for bulk density, were collected to measure the root density. The cores were soaked in water, and then sieved through a #30 sieve (0.60 mm openings) with a steady water flow until all inorganic matter had been removed. The collected root biomass was oven dried at 50°C (122°F) for 24 hours and weighed (Frasier et al., 2016). This weight was divided by the core volume to calculate the root density.

From select pots, cores were taken to measure hydraulic conductivity. For more permeable soil conditions, 7.6 cm (3 inch) diameter and 7.6 cm (3 inch) height cores were taken, and rigid-walled, constant head tests were conducted using a GEOTAC bubble tube permeameter (Houston, TX USA) with a hydraulic gradient of 0.9. Acrylic tube was cut to length and one end sharpened to allow for cores to be taken directly in a mold compatible with the permeameter. For less permeable soil conditions, 10.2 cm (4 inch) diameter and 7.6 cm (3 inch) height cores were taken, and falling head tests were conducted in a flexible-wall permeameter (GEOTAC). The tests followed the ASTM D5084 test procedure, including saturation criteria of $B > 0.95$. Furthermore, a SATURO dual head infiltrometer (METER Group, München, Germany) with a 5 cm (2 inch) insertion ring was used in select pots to measure saturated hydraulic conductivity directly in the pot for comparison to the laboratory specimen results.

Data Analysis and Statistics

Unless otherwise noted, values are presented as the mean of three replicates plus/minus the standard deviation. A 5% significance level was used to determine whether to accept or reject the null hypothesis. A one-way analysis of variance (ANOVA) was performed to compare soil and vegetation parameters from the different pot conditions. A Tukey's Honest Significant

Difference post hoc test was used to determine pair-wise differences. For hydraulic conductivity, values were log10 transformed prior to statistical analysis. A one-tailed Student's t-test was used to compare parameters from the compost-amended pot groups to the non-amended equivalent pot group.

2.3 Mesocosm Study

Experimental Design

The objectives of this research study were to evaluate the effects of soil density/compaction and soil type on vegetation establishment, and runoff quantity and quality. Six mesocosms were prepared in boxes 1.83 m (6 ft) long and 0.46 m (1.5 ft) wide, depicted in Figure 2.7. The boxes were lined with a textured geomembrane to create a frictional surface to prevent soil from sliding on the steep slope (2H:1V). At the bottom end of the mesocosm, vinyl mesh and metal mesh gutter guard were attached to hold the soil in the box.

The mesocosm soil conditions were selected to represent possible soil scenarios in the field. Three soil types were employed: topsoil (T), subsoil (S), and subsoil amended with yard waste compost (C), using the same soils and compost used in the pot studies. For each soil type, a mesocosm was prepared at high density (H) and at low density (L), referring to a relative compaction of 100% and 72%, respectively. These configurations along with their corresponding abbreviations are represented in Table 2.3.

Figure 2.7: Image of empty mesocosm box.

Table 2.3: Mesocosm Abbreviations and Initial Soil conditions

Mesocosm	**TL**	**TH**	**SL**	**SH**	**CL**	**CH**
Soil Type	Topsoil	Topsoil	Subsoil	Subsoil	Subsoil & Compost	Subsoil & Compost
Density (g/cm^3)	1.15	1.60	1.15	1.60	1.09	1.51
Relative Compaction	72%	100%	72%	100%	72%	100%
Organic Matter (as LOI)	5.8%	5.8%	3.8%	3.8%	5.8%	5.8%

Mesocosm Setup and Environmental Conditions

The compost-amended soil, CL and CH, was prepared with an organic matter content (LOI) of 5.8%. This amendment rate was selected to provide adequate organic matter and nutrients for vegetative growth while minimizing the leaching of nutrients. The resultant C:N ratio of 15:1 is within the recommended range of Pamuru (2024). The soils were air-dried and passed through a 25 mm (1-inch) sieve. For mesocosms CL and CH, dry soil and dry compost were mixed using a shovel on a plastic sheet. The soil was compacted to the desired dry density using a tamper in five lifts of equal depth. The soil was wetted to optimum moisture content to aid in compaction.

In accordance with Iowa DOT Article 2601.03, C, 3, the permanent rural seed mix (Millborn Seeds, Brookings, SD USA) was applied at a rate of 112 kg/ha (100 lb/ac) tall fescue, 84 kg/ha (75 lb/ac) perennial ryegrass, and 22.4 kg/ha (20 lb/ac) Kentucky bluegrass. In mesocosms TL, TH, SL, and SH, 336 kg/ha (300 lb/ac) of 6-24-24 fertilizer (Des Moines Feed (Des Moines, IA USA) was also applied. These values correspond to 18.3 g of seed and 28.1 g of fertilizer per mesocosm. The seeds and fertilizer were applied to the mesocosms on January 18, 2024, by first wetting the soil, then scoring the soil surface to roughen it, and finally pressing the seed and fertilizer, if applicable, into the soil. To ensure more even coverage, each mesocosm was split into five sections with each section seeded separately. Finally, a double-layered erosion control blanket (AEC Premier Straw® Double Net FibreNet™ from American Excelsior) was placed upon the soil surface to limit erosion from the steep slope.

TEROS 12 soil sensors (METER Group, München, Germany) were placed at mid-depth of the soil. Three sensors were placed per mesocosm in the locations depicted in Figure 2.8. Soil

temperature, water content, and bulk electrical conductivity were recorded at 15-minute intervals for the duration of the study.

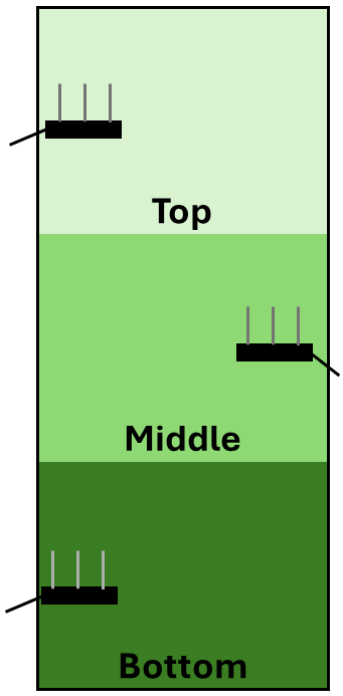

Figure 2.8: Soil sensor locations in each mesocosm.

On January 22, 2024, a 15-minute rainfall event was simulated at an intensity of 10.2 cm/hr (4 in/hr) for a total depth of 2.54 cm (1 inch). The rainfall simulator was composed of a 1.27-cm (0.5-inch) HH-30 W SQ Fulljet® nozzle connected to a tap water faucet. The simulator was situated 2.75 m (9 ft) above the ground and centered overtop of two mesocosms at a time. SL & CH, TH & CL, and SH & TL were paired together. These rainfall events occurred every week for a total of 12 rainfall events. The greenhouse room was set at a temperature of 24°C (75°F) during the daytime and 18°C (64°F) during the nighttime. Figure 2.9 shows two of the mesocosms and the rainfall simulator in the greenhouse during a rainfall event.

Figure 2.9: Mesocosms TH and CL with rainfall simulator (circled) during rainfall event 12.

Vegetation Establishment

Photographs of the mesocosms were taken each week using an iPhone SE 2020. A ladder was used so that the image would be perpendicular to the soil surface. Matching the pot study, these images were analyzed for percent green coverage in the software *Canopeo* (Patrignani & Ochsner, 2015).

The grass height for each mesocosm was measured weekly. The mesocosm was split into five sections from the top to the bottom of the box. A metal ruler was used to measure the average height from the soil surface at a random location in each section. The mean of these values was calculated to find the representative grass height for that mesocosm. Once the average height of a mesocosm was approximately 30 cm (12 inches), grass was trimmed (to simulate field mowing) using metal scissors to a height of 15.2 cm (6 inches) in accordance with Iowa DOT Article 2612.03, A. This maximum height of 30 cm (12 inches) was selected to match the tallest grasses grown in the pot study. Biomass was collected separately for the top, middle, and bottom of each mesocosm. The trimmed biomass was oven dried at 50°C (122°F) for 48 hours and weighed. Once dried, this biomass was returned to the mesocosms and placed underneath the remaining vegetation to better match in the field where grass clippings are not collected.

Water Quality Analysis

Plastic collection bins were placed underneath the bottom end of each mesocosm to collect the runoff as shown in Figure 2.10a. The plastic collection bins were washed with Alconox Liquinox™ Detergent and DI water prior to each rainfall event. Plastic sheets were used to cover the collection bins (Figure 2.9) to prevent rainwater from directly entering the collection bin. After the rainfall simulation ended, runoff drained for two hours before 1 L samples were collected in acid-washed HDPE bottles as shown in Figure 2.10b. The collection bins were well-mixed prior to sample collection. Total effluent volumes were measured using a graduated cylinder the following morning after a rainfall event, and 1 L was added to each volume to

account for the sample already removed. This time delay allowed for all runoff to drain and be measured.

Within four hours of sample collection, pH and electrical conductivity (EC) were measured by directly immersing a pH and EC probe in the sample bottles according to EPA Method 9040C and EPA Method 120.1, respectively. Total suspended solids (TSS) were measured using 0.7-µm glass fiber filters in accordance with EPA Method 160.2.

Figure 2.10: a.) Runoff collection bin and b.) runoff samples collected following rainfall event number 3.

Runoff samples were digested for total phosphorous (TP) following EPA persulfate method 365.1, and a SEAL AQ300 instrument was used to analyze the digested samples. Unfiltered samples were measured for total nitrogen (TN) and total organic carbon (TOC) using a 720°C thermal decomposition- chemiluminescence method on a Shimadzu SSM-5000A Total Organic Carbon/Total Nitrogen Analyzer. Standards made with glycine were used to create the calibration for both TN and TOC. For dissolved species, samples were filtered through a 0.22-μm membrane. Orthophosphate (PO_4-P) was measured for all rainfall events using the SEAL AQ300. For rainfall events 1, 6, 10, and 12, nitrate/nitrite (NO_x-N), ammonium (NH_4-N), and total dissolved phosphorous (TDP) were also measured using the SEAL AQ300. Likewise, for these four select rainfall events, filtered samples were measured for total dissolved nitrogen (TDN) and dissolved organic carbon (DOC) on the Shimadzu SSM-5000A Total Organic Carbon/Total Nitrogen Analyzer.

Particulate phosphorous (PP), dissolved organic phosphorous (DOP), particulate nitrogen (PN), dissolved organic nitrogen (DON), and particulate organic carbon (POC) were calculated using equations 1-5, respectively. Due to limitations in detection precision, if any calculated concentrations were below zero, then they were assumed to be zero.

$$TP = TDP + PP \quad (1)$$

$$TDP = PO_4\text{-}P + DOP \quad (2)$$

$$TN = TDN + PN \quad (3)$$

$$TDN = NO_x\text{-}N + NH_4\text{-}N + DON \quad (4)$$

$$TOC = POC + DOC \quad (5)$$

End of Study Measurements

On April 10, 2024, after 12 simulated rainfall events, destructive testing of the mesocosms commenced, starting with above-ground biomass collection. Metal scissors were used to remove the biomass at the ground surface. Biomass was collected separately for the top, middle, and bottom of each mesocosm. The collected biomass was oven dried at 50°C (122°F) for 48 hours and weighed. Soil samples were collected from the top, middle, and bottom of each mesocosm to measure the final organic matter through loss on ignition in accordance with ASTM D2974.

A SATURO dual head infiltrometer (METER Group, München, Germany) with a 5-cm (2-inch) insertion ring was used to measure saturated hydraulic conductivity directly in the mesocosms. A measurement was taken for the top, middle, and bottom sections of each mesocosm. An 8-cm (3.15-inch) diameter and 5-cm (1.97-inch) height HYPROP mold core (volume of 250 mL) was used to collect core samples from the middle of each mesocosm to create a soil moisture characteristic curve and determine the unsaturated hydraulic conductivity of the soil using HYPROP (METER Group, München, Germany).

Soil cores were also collected, using the 250-mL HYPROP molds, from the top, middle, and bottom of each mesocosm, to measure the final bulk density. The cores were oven dried at 100°C (212°F) for 24 hours and weighed. Bulk density was calculated by dividing this dry weight by the core's volume. Additional cores were collected, again using the 250-mL HYPROP molds, from the top, middle, and bottom of each mesocosm to measure root density. The cores were soaked in water, and then sieved through a #30 sieve (0.60 mm openings) with a steady water flow until all inorganic matter and compost, if applicable, had been removed. The collected root biomass was oven dried at 50°C (122°F) for 24 hours and weighed (Frasier et al., 2016).

This weight was divided by the core volume to calculate the root density. A diagram of the end-of-study soil testing samples is shown in Figure 2.11.

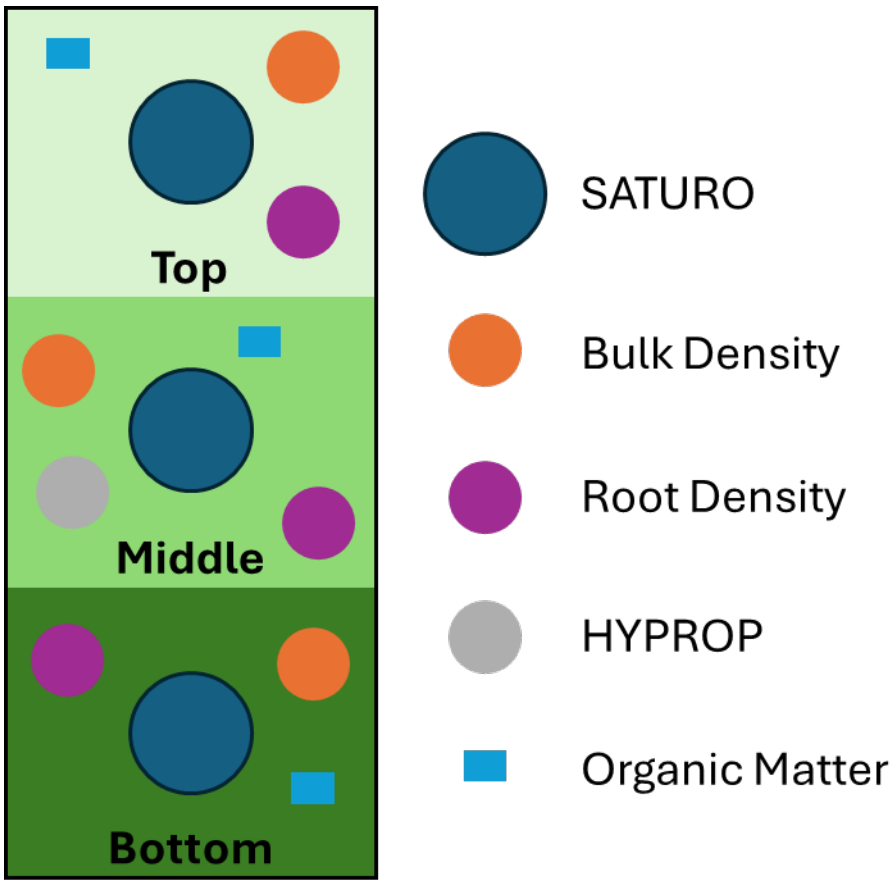

Figure 2.11: Diagram of end-of-study soil testing samples within a mesocosm.

Data Analysis and Sample Collection QA/QC

Given the lack of experimental replicates, many measurements were repeated for the top, middle, and bottom of each mesocosm. Likewise, many water quality parameters were repeated in triplicate from the same sample to account for analytical variation. Unless otherwise noted, values are presented as the mean of the replicate measurements plus/minus the standard deviation.

A separate runoff sample was collected for mesocosms TL and SH for rainfall event 8. EC, pH, TSS, TP, and PO_4-P were all measured on the duplicate sample as well as the main sample to confirm that the runoff samples were representative of the entire volume of runoff. Furthermore, the tap water sample from this storm underwent a digestion to measure TP to ensure that all phosphorous present was in the form of orthophosphate as assumed. All measurements agreed within 5%.

Chapter 3 Results and Discussion

3.1 Pot Study Results

Vegetation Establishment

No differences in the vegetation parameters were found between the two halves of each pot, so mean values for the entire pot are considered in this section. A comparison between the two halves for grass heights, biomass, and root density can be found in Appendix B.

Green coverage in the pots over time is shown in Figure 3.1, and final green coverage is shown in Figure 3.2. Except for pots BH90 and BHL0, all pots surpassed 90% coverage within 6 weeks after seeding. When grasses were first trimmed in week 11, green coverage dropped by approximately 12% for all pots. Green coverage continued to generally decline in all pots until the second trimming, in week 20, because of yellow discoloration of dead and dormant grass blades. After the second trimming, green coverage generally increased for all pots other than BH90. BH90 had a significantly lower final green coverage of 47 ± 8% compared to all other pots. CH90 had the highest final green coverage at 91 ± 2%.

Mean grass height over time is shown in Figure 3.3. Before the first trimming, the grass heights began to plateau with most pots having an average height of 28 ± 1 cm. However, pots BH90, BL90, and CH90 had an average height of 24 ± 1 cm. At the time of the second trimming, the pot with the tallest grass, BL1L8, had a height of 23.2 ± 0.6 cm while the pot with the shortest grass, BH90, had a height of 18.0 ± 0.4 cm. Final grass heights are depicted in Figure 3.4. BH90 and BL90 had the lowest final grass heights and were significantly different at a 95% confidence level from all other pots. BH1L8 and BL1L8 had the highest final grass heights and were significantly different from all other pots.

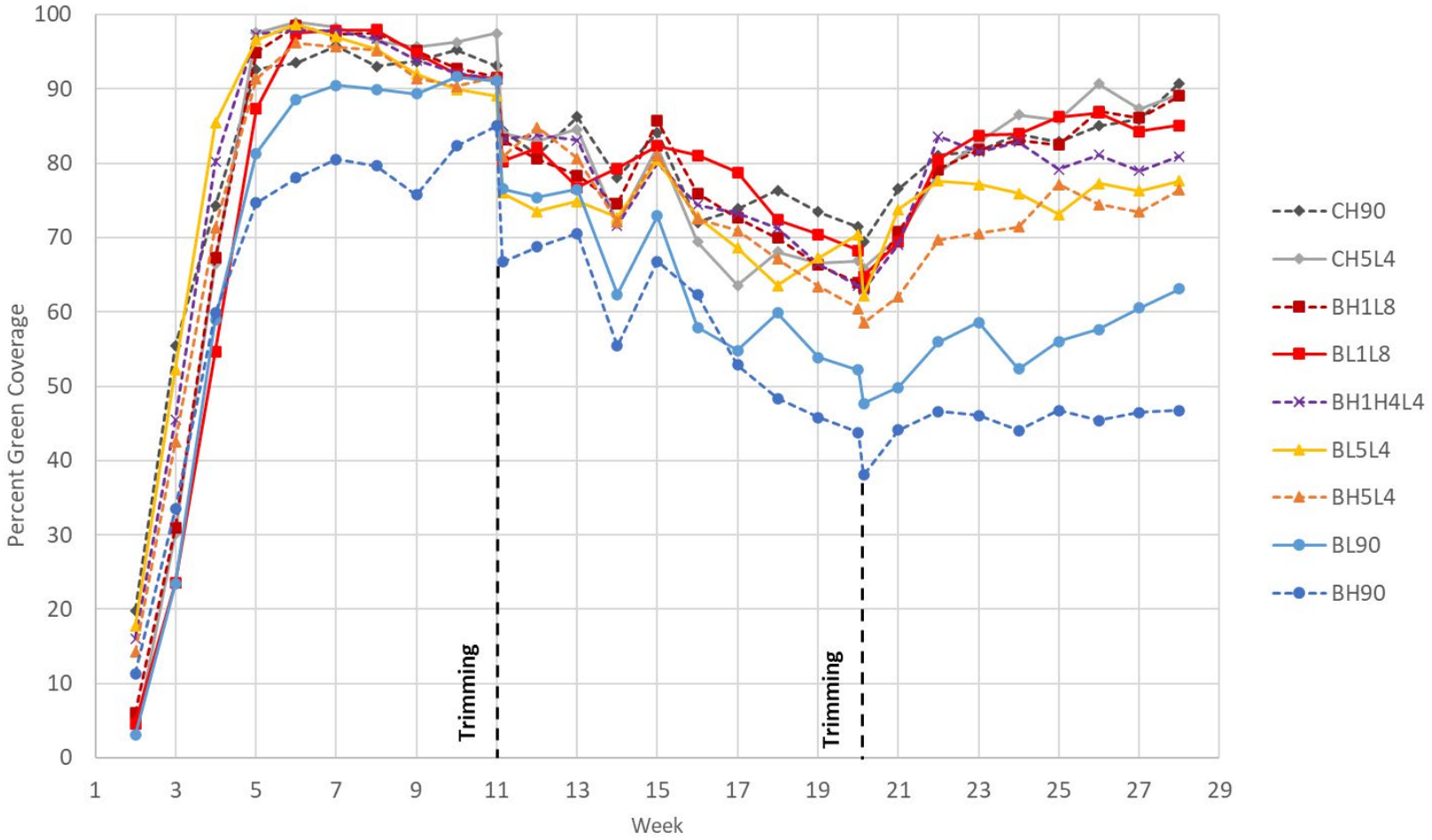

Figure 3.1: Green coverage of pots throughout the study. Note: the drops in green coverage during week 11 and week 20 are due to trimming of the grasses at these times. Values are the mean of the three replicate pots.

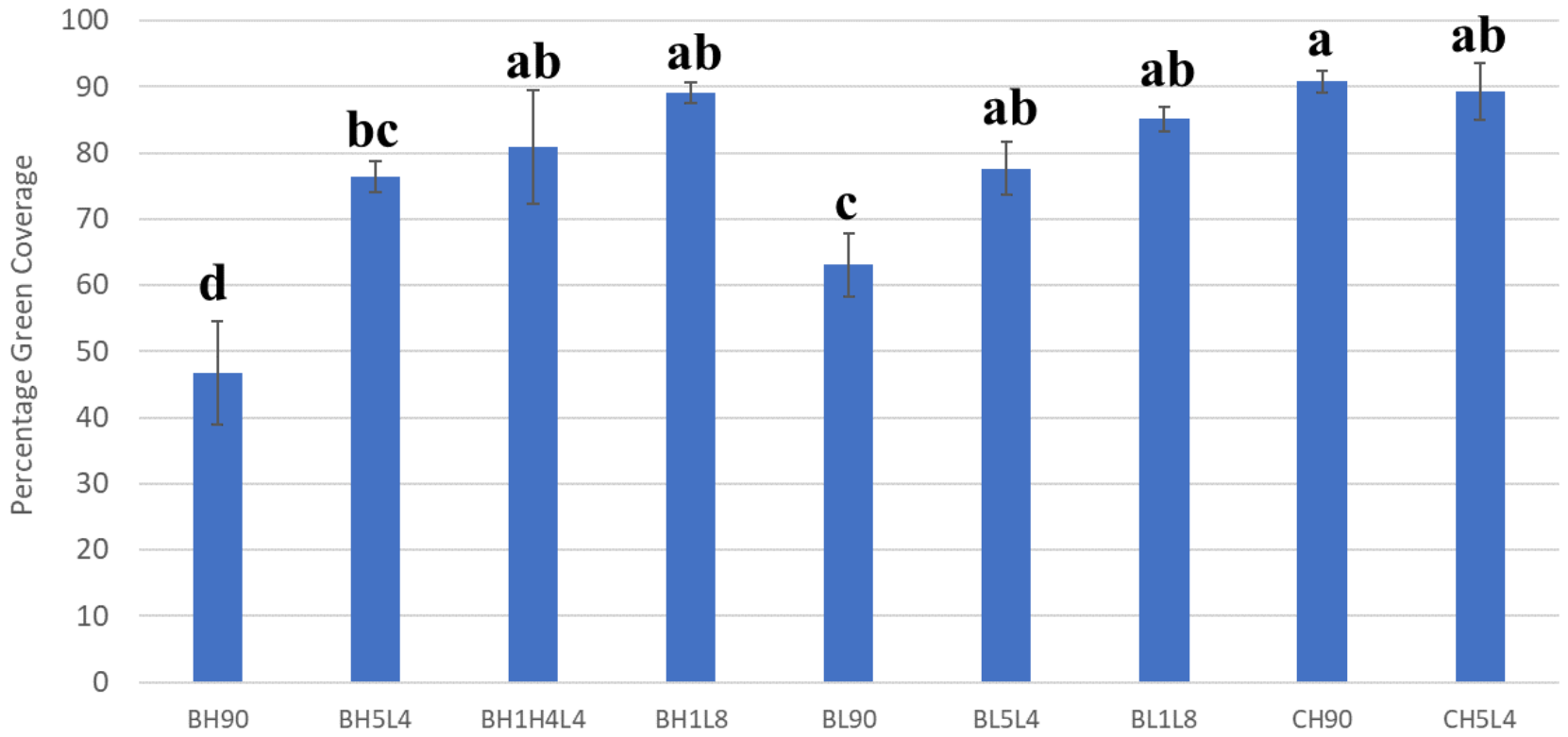

Figure 3.2: Final green coverage of pots. Note: error bars represent the standard deviation among the replicates and mean heights with the same letters indicate no significant differences at a 95% confidence level according to a Tukey test.

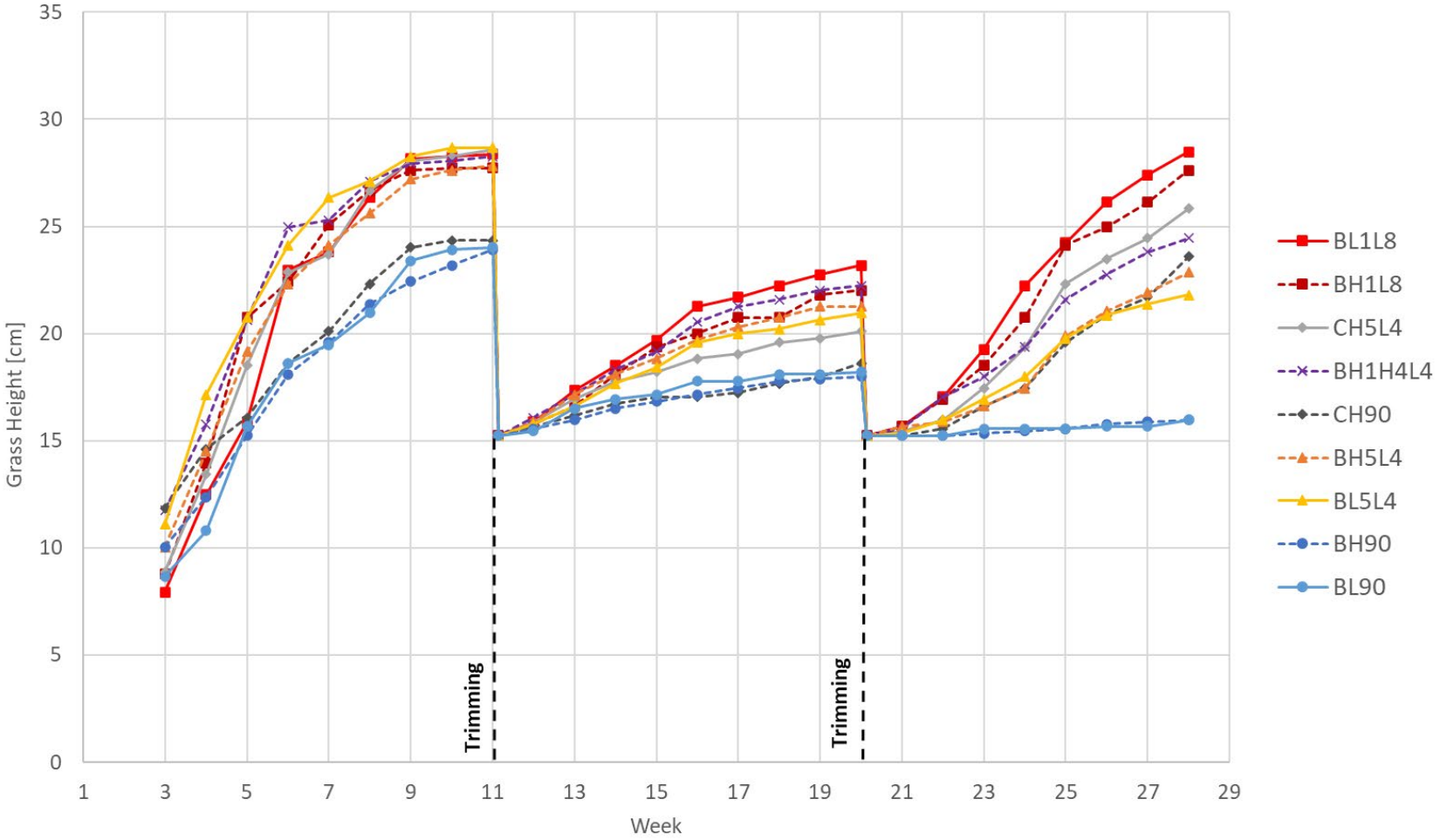

Figure 3.3: Mean grass heights of pots throughout the study. Note: the drops in heights during week 11 and week 20 are due to trimming of the grasses at these times. Values are the mean of the three replicate pots.

The dry biomass from the two rounds of trimming and the final collection are shown in Figure 3.5. BL1L8 had the highest average biomass with a total of 44 ± 2 g across the two trimmings and the final collection. This was followed by 39 ± 3 g for BH1L8, 35 ± 5 g for BH1H4L4, 31 ± 3 g for BH5L4, 29 ± 4 g for CH5L4, 26 ± 1 g for BL5L4, 19 ± 1 g for CH90, 16 ± 2 g for BH90, and 15 ± 2 g for BL90. For pots BH1H4L4, BH1L8, BL1L8, and CH90, the second trimming removed more biomass than the first trimming. For pots, BH90, BL90, BH5L4, BL5L4, and CH5L4, the first trimming removed more biomass than the second trimming. Hence, the pots with no topsoil or a shallower layer of topsoil had comparatively more growth earlier in the study whereas the pots with a deeper topsoil layer had comparatively more growth later in the study.

The root densities found in the upper cores and the lower cores are depicted in Figure 3.6a and 3.6b, respectively. In the upper cores, a range of root densities was found, with BL1L8 having the highest value of 4.6 ± 0.8 mg/cm^3 and BL90 the lowest value of 1.9 ± 0.5 mg/cm^3. In the lower cores, the pots with low density topsoil at the depth of the core, BH1L8 and BL1L8, had significantly higher root densities than all the other pots which had either high density soil and/or subsoil at this depth.

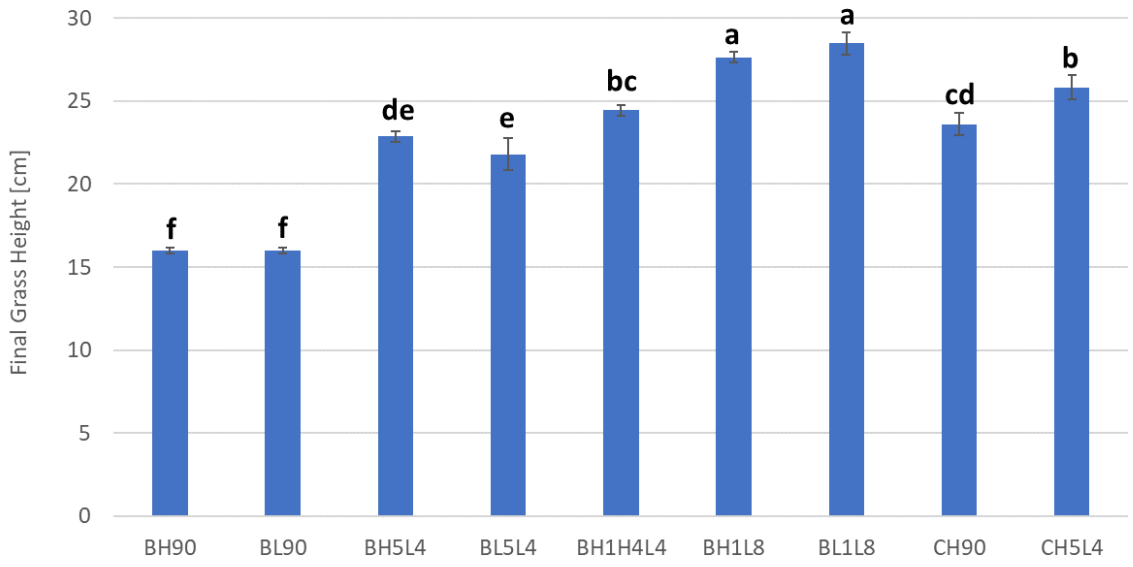

Figure 3.4: Final grass heights. Note: error bars represent the standard deviation among the replicates and mean heights with the same letters indicate no significant differences at a 95% confidence level according to a Tukey test.

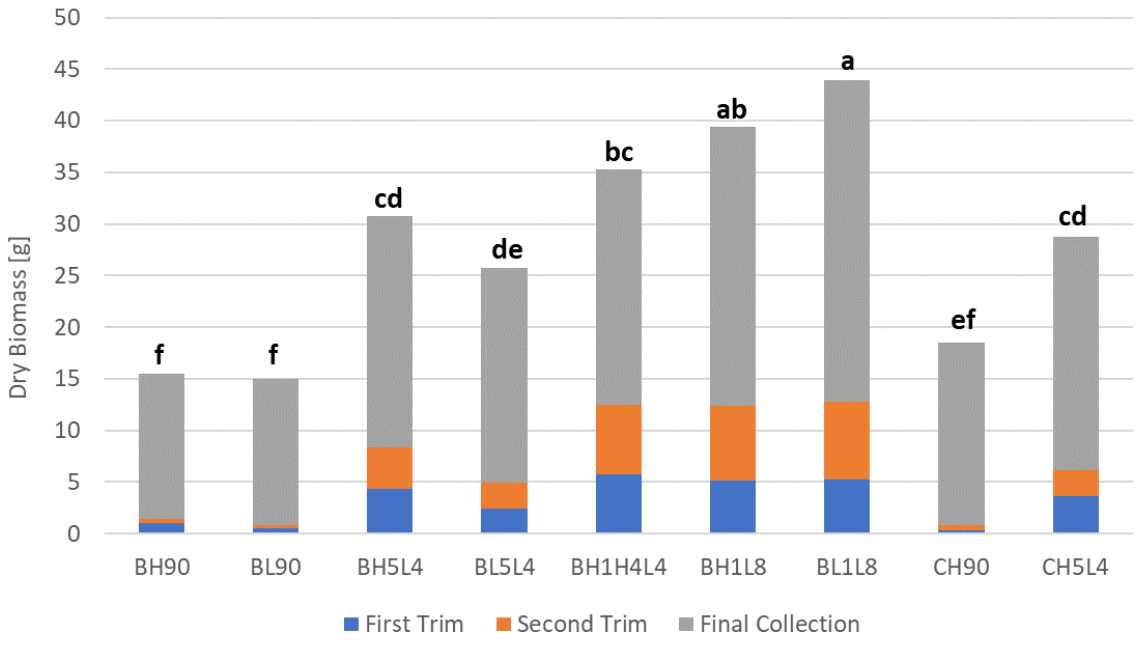

Figure 3.5: Total dry biomass from the first and second trimmings and the final collection. Note: mean heights with the same letters indicate no significant differences at a 95% confidence level according to a Tukey test.

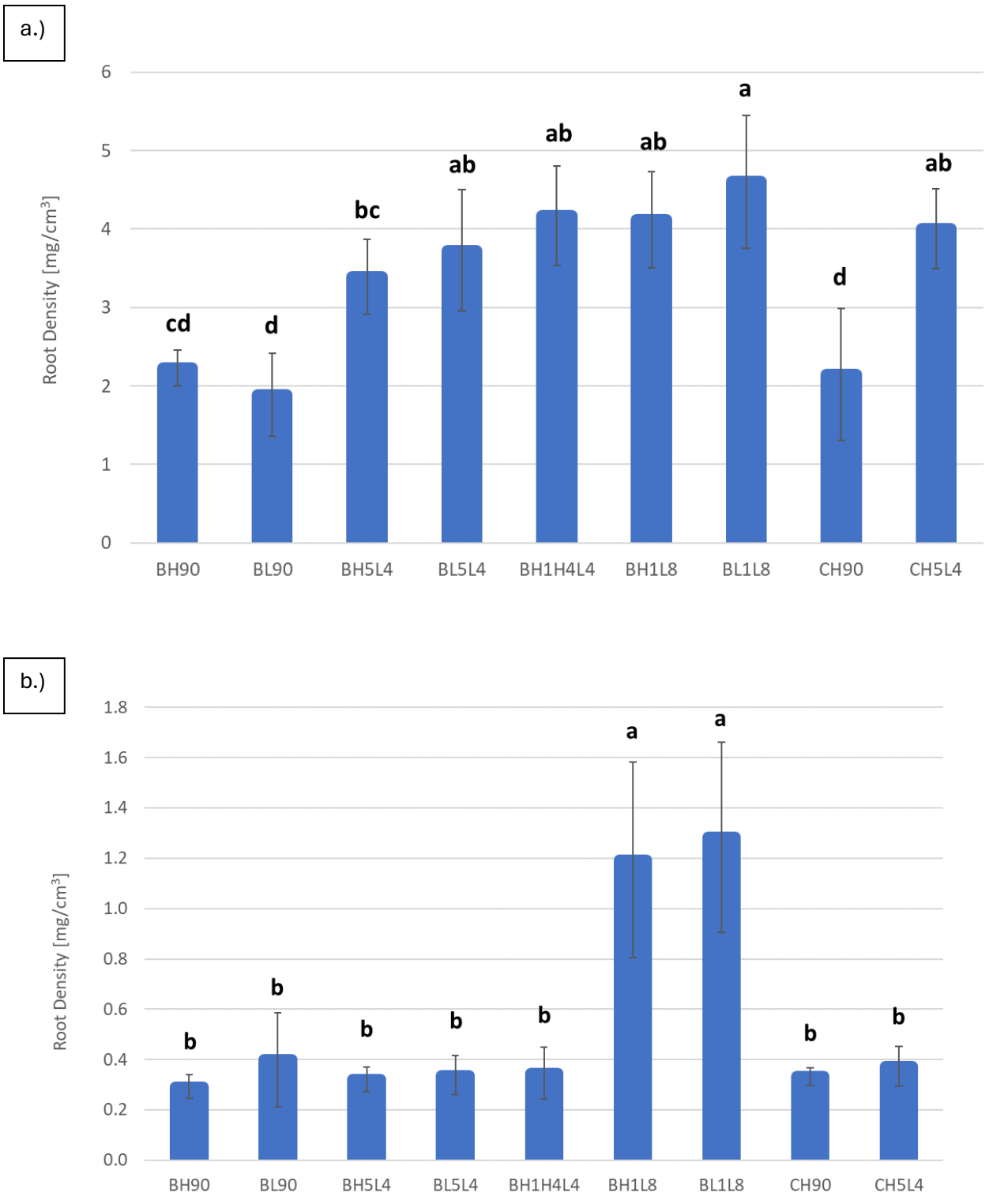

Figure 3.6: a.) Root densities in upper cores, and b.) root densities in lower cores. Note: error bars represent the standard deviation between the replicates and mean densities with the same letters indicate no significant differences at a 95% confidence level according to a Tukey test.

Final Soil Conditions

Final soil bulk density along with the initial density for upper and lower cores are shown in Figures 3.7a and 3.7b, respectively. In the upper cores, the bulk densities on the sides of the pots that did not receive additional compaction were all within 0.03 g/cm^3 of the initial densities. In contrast, on the sides of the pots that received mowing compaction, the densities increased above the initial value by up to 0.08 g/cm^3. BH90 did not increase from the initial density. In the lower cores, there was no difference between the two sides of each pot. For the high-density lower cores, the densities all matched the initial density within ± 0.02 g/cm^3. However, for the low-density lower cores, the densities ranged from 0.03 to 0.07 g/cm^3 higher than the initial densities.

Saturated hydraulic conductivity values for select pots are presented in Figure 3.8. For the high-density subsoil cores, BH90 and lower cores from BH5L4, the conductivity was significantly lower than all other pots with values of $3 \times 10^{-5} \pm 2 \times 10^{-5}$ cm/s and $4 \times 10^{-5} \pm 2 \times 10^{-5}$ cm/s, respectively. For BL1L8, the conductivity was $1.4 \times 10^{-2} \pm 5 \times 10^{-3}$ cm/s for both sides of the pots. For BL90 and upper cores from BH5L4, the conductivity on the side that did not receive additional compaction was $8 \times 10^{-3} \pm 1 \times 10^{-3}$ cm/s and $4 \times 10^{-3} \pm 6 \times 10^{-4}$ cm/s, respectively, whereas it was significantly lower at $5 \times 10^{-4} \pm 9 \times 10^{-5}$ cm/s and $6 \times 10^{-4} \pm 2 \times 10^{-4}$ cm/s, respectively, on the side that did receive mowing compaction. For all other pots, no significant difference was found between the two pot sides. CH90 had a hydraulic conductivity of $3 \times 10^{-3} \pm 1 \times 10^{-3}$ cm/s on both sides while the value for CH5L4 was $7 \times 10^{-3} \pm 2 \times 10^{-3}$ cm/s on both sides. Overall, the hydraulic conductivity of the cores varied by three orders of magnitude.

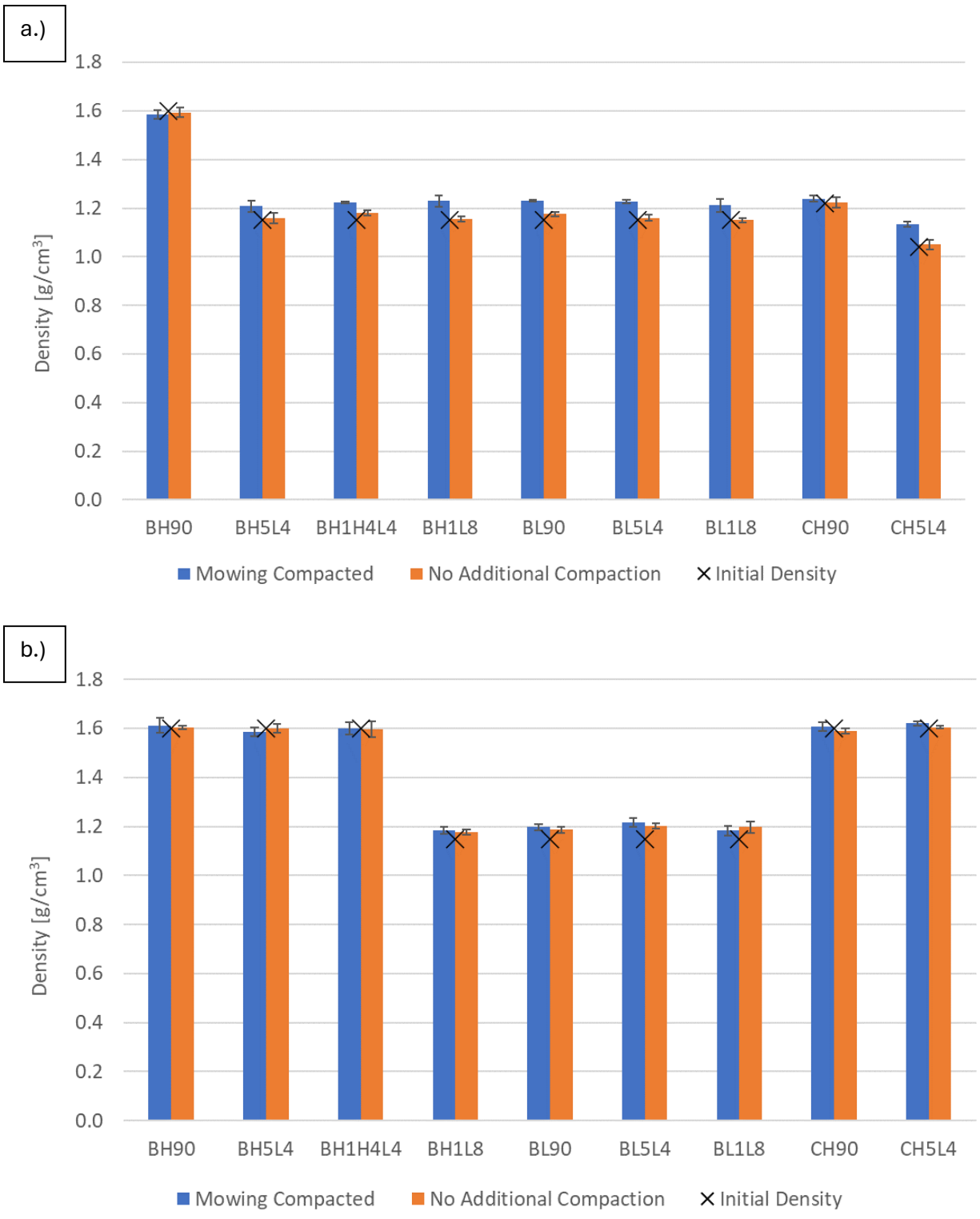

Figure 3.7: Soil bulk densities in a.) upper cores and b.) lower cores with the initial target density represented by an "X". Note: error bars represent the standard deviation between the replicates.

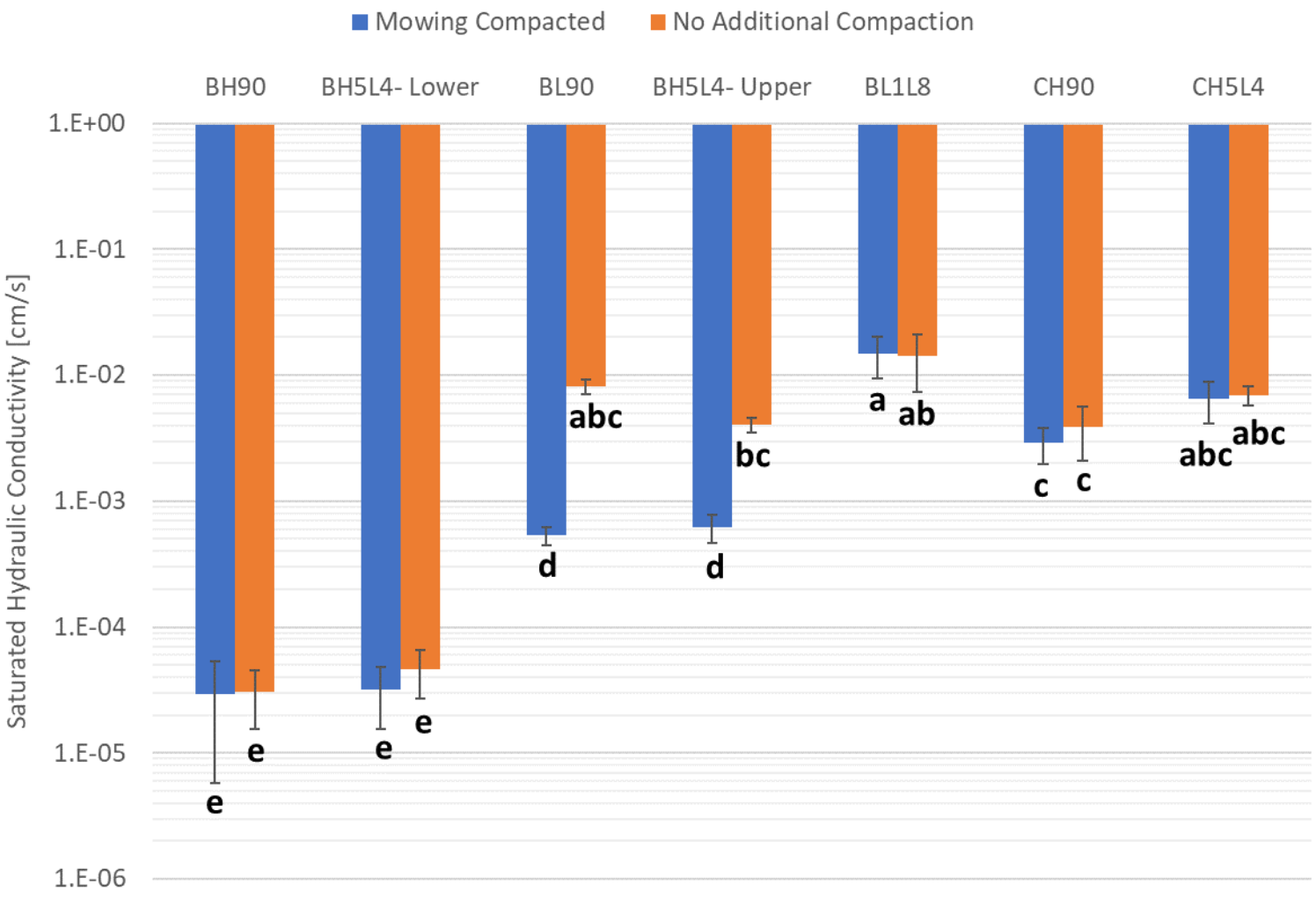

Figure 3.8: Saturated hydraulic conductivity of cores taken from select pot types. Note: error bars represent the standard deviation between the replicates. and mean densities with the same letters indicate no significant differences at a 95% confidence level according to a Tukey test.

3.2 Mesocosm Results

Soil Sensors

As an example, the soil sensor readings for mesocosm TL are presented in Figure 3.9a for water content, 3.9b for soil temperature, and 3.9c soil bulk electrical conductivity (EC). Results for all mesocosms are presented in Appendix E. For both water content and bulk EC, the twelve peaks correspond to the twelve storm events. The bottom of the mesocosm has the highest water content while the top has the lowest water content. The spatial pattern is similar for bulk EC, except the middle sensor has greater variation. Bulk EC generally declined over the course of the study. Soil temperature is consistent spatially within the mesocosm, but it has a daily cycle of being lower at night and higher during the day. The other mesocosms have comparable results.

The mean water content for each mesocosm was calculated using all measurements throughout the study from all three sensors within the mesocosm. The mean water content for SL was 0.23 m^3/m^3 and SH was 0.22 m^3/m^3 whereas it was higher for the other soil types at 0.28 m^3/m^3 for TL and TH, 0.29 m^3/m^3 for CL, and 0.27 m^3/m^3 for CH.

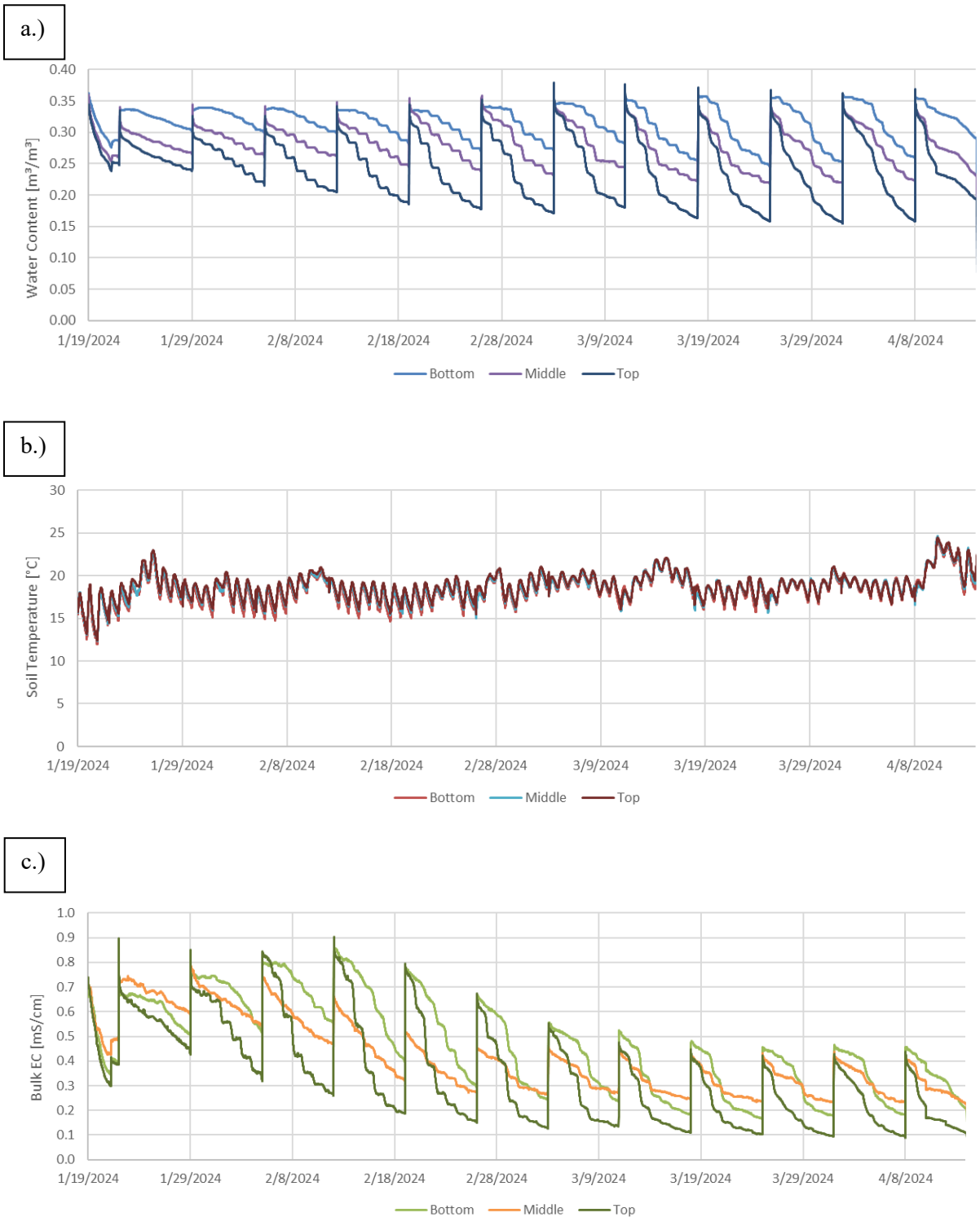

Figure 3.9: Soil sensor readings for TL. a.) water content, b.) soil temperature, and c.) soil bulk electrical conductivity (EC).

Vegetation Establishment

Grass heights are presented in Figure 3.10. Trimmings occurred twice in mesocosms TL and TH, following rainfall events 7 and 11, once in mesocosms CL and CH following rainfall event 7, and once in mesocosms SL and SH following rainfall event 9. The order of grass height growth is TH > TL > CH > CL > SL ≈ SH. The three soil types resulted in differences in grass heights with topsoil the most productive and subsoil the least. However, soil density had no clear impact on grass heights.

Green coverage results are presented in Figure 3.11. All mesocosms, except SL, reached at least 90% green coverage by rain event 6. At the end of the study, all mesocosms had a green coverage of at least 99%. The trimmings did not result in a significant change in green coverage. Mesocosms SL and CH had lower grass heights and green coverage initially due to a ventilation fan in the greenhouse room that was drying out the soil and delayed germination. The fan was turned off 10 days after seeding. Also, aphids were observed on the grasses in all mesocosms following rain event 11. The infestation is not believed to have had any impact on the results of the study because of how late in the study it occurred.

The dry biomass results from the trimmings and the final collection are presented in Figure 3.12. The order of the greatest total dry biomass is TH (152 g) > TL (119 g) > CH (86 g) > CL (83 g) > SH (72 g) > SL (68 g). Hence, the biomass matches the grass height results with topsoil mesocosms being the most productive and subsoil mesocosms being the least productive. For all three soil types, the high density mesocosm had greater biomass than the low density mesocosm. However, generally, the difference in biomass between the three different soil types is much greater than the difference based on soil density.

The root density results are presented in Figure 3.13. The order of root density is TL > CL > CH > SL > TH > SH. For all three soil types, the low density mesocosm had higher root density than its high-density counterpart. However, it should be recognized that the variation in the replicate measurements was large, with standard deviations among replicates as high as 0.3 mg/cm^3. Biomass and root density results based on position within the mesocosm are provided in Appendix D; however, no spatial trend was observed despite the differences in water content of the soil.

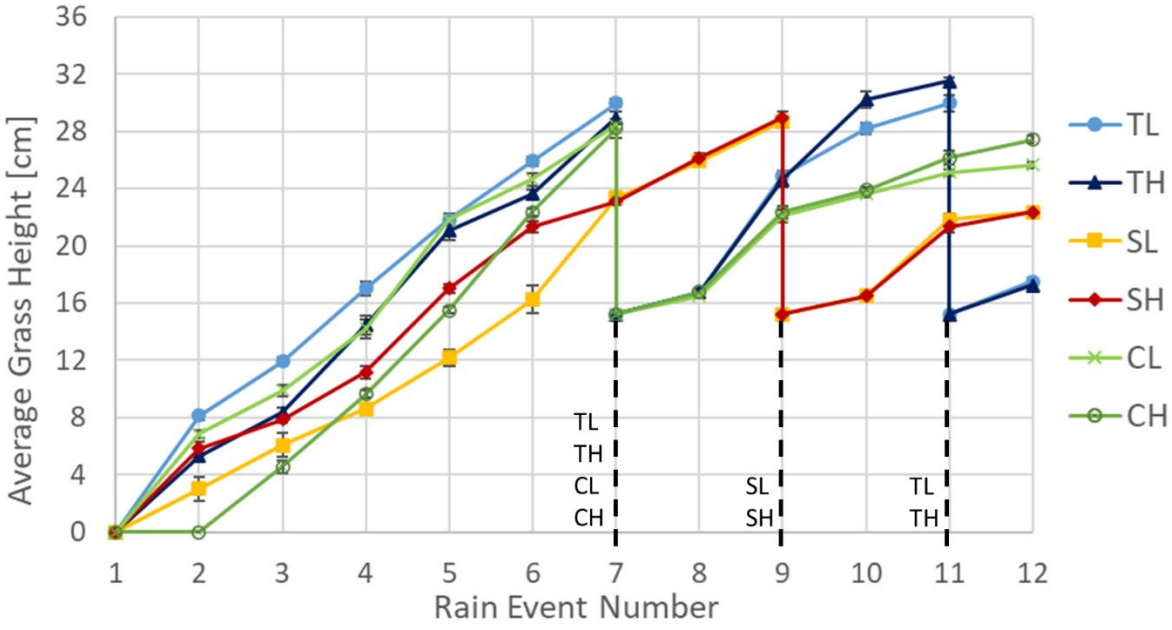

Figure 3.10: Average grass heights of mesocosms with trimming events marked. Note: mesocosms TL, TH, CL, and CH were trimmed after rain event 7, mesocosms SL and SH after rain event 9, and mesocosms TL and TH again after rain event 11. Error bars represent the standard deviation of the five measurements per mesocosm.

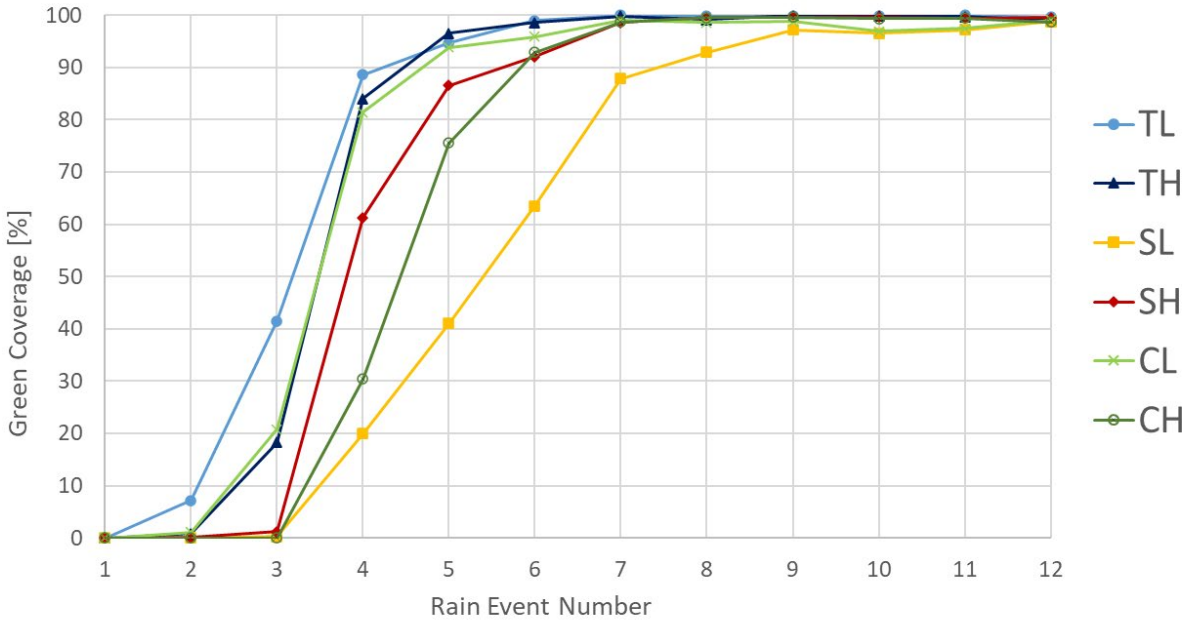

Figure 3.11: Green coverage of mesocosms throughout the study.

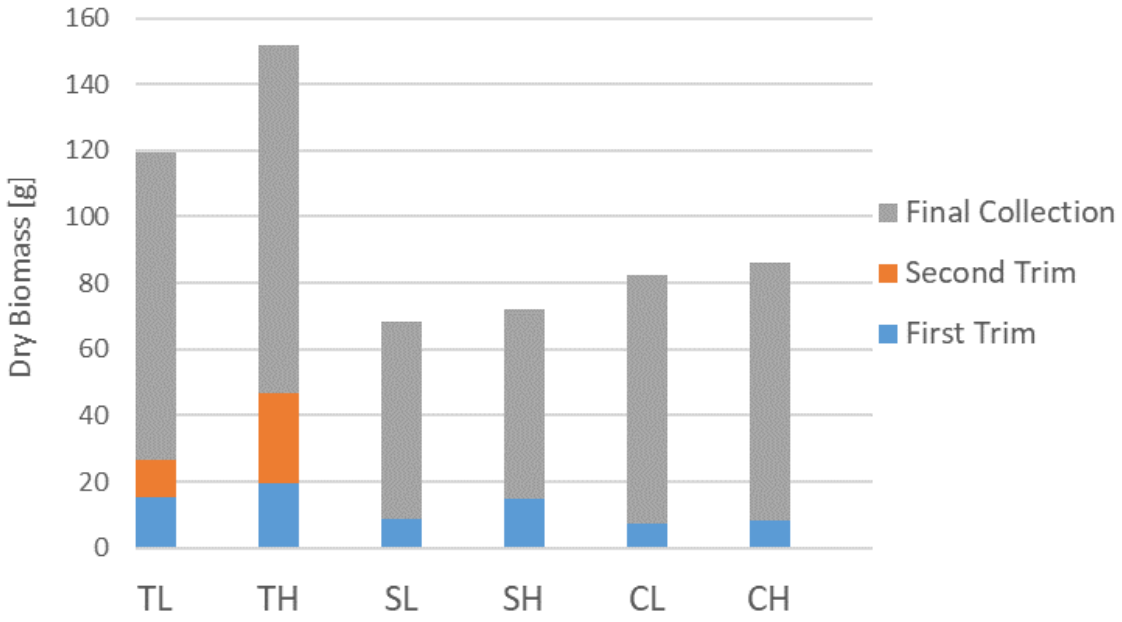

Figure 3.12: Dry biomass from trimmings and final collection. Note: first trim occurred after rain event 7 for mesocosms TL, TH, CL, and CH, and after rain event 9 for mesocosms SL and SH. Only mesocosms TL and TH received a second trim, and it occurred after rain event 11. Final collection was all biomass down to ground surface after rain event 12.

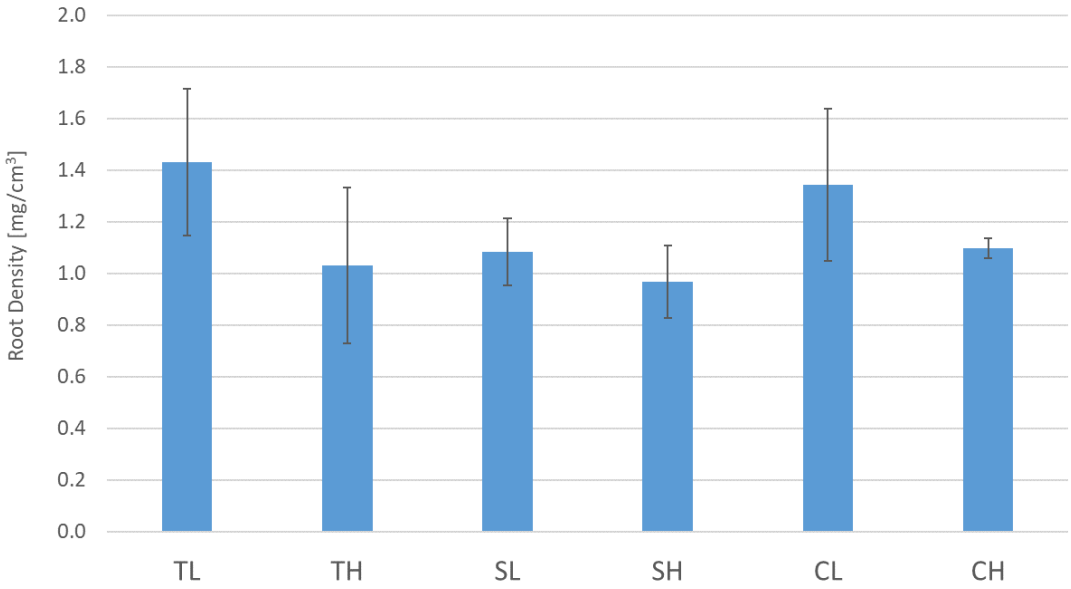

Figure 3.13: Root density results for each mesocosm. Note: error bars represent the standard deviation among the measurements for the top, middle, and bottom of each mesocosm.

Runoff Water Quality Analysis

Runoff volumes are depicted in Figure 3.14. The volumes ranged from 35% to 83% of the stormwater applied. Volumes varied among mesocosms and rain events, but neither soil type nor density had a clear influence on the volumes. For TL, TH, CL, and CH, runoff volume increased following trimming of the grass. These increases ranged from 5% to 16% of the stormwater applied. However, this effect was not observed in the subsoil mesocosms.

During rain event 5, orange and black flakes were observed in the influent sample. Upon further investigation, a layer of presumably predominantly iron had formed on the inside of the PVC section of the rainfall simulator. In all following rain events, the rainfall simulator was flushed at high pressure for two minutes prior to use which considerably minimized any visible contamination of the influent water. This defect is not believed to have influenced any results from the study.

The pH of the runoff samples and influent tap water are shown in Figure 3.15. The runoff samples were slightly alkaline of neutral with values ranging from 7.2 to 8.2. Runoff pH increased over the course of the study with CL and CH having the highest values. In Figure 3.16, the electrical conductivity (EC) of the runoff samples and influent tap water are presented. Runoff EC decreased over the course of the study, and the subsoil mesocosms had the lowest EC. The total suspended solids (TSS) of the runoff samples are depicted in Figure 3.17. The topsoil mesocosms had the highest TSS with TSS decreasing over the course of the study.

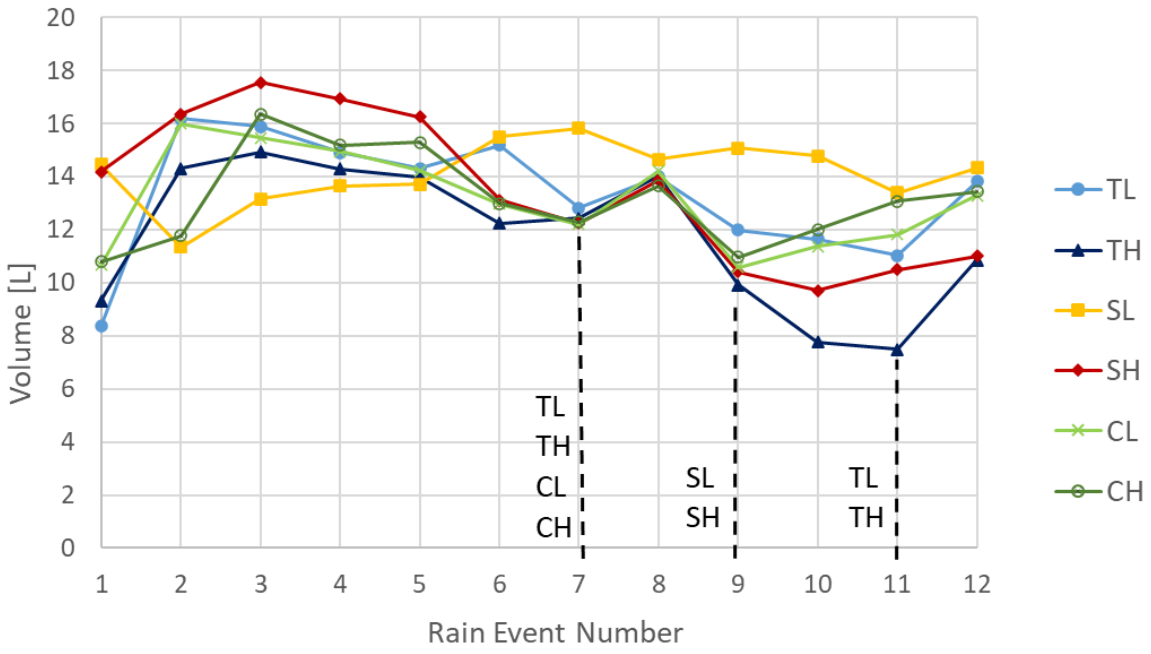

Figure 3.14: Runoff volumes from each rain event with trimming events marked. Note: mesocosms TL, TH, CL, and CH were trimmed after rain event 7, mesocosms SL and SH after rain event 9, and mesocosms TL and TH again after rain event 11

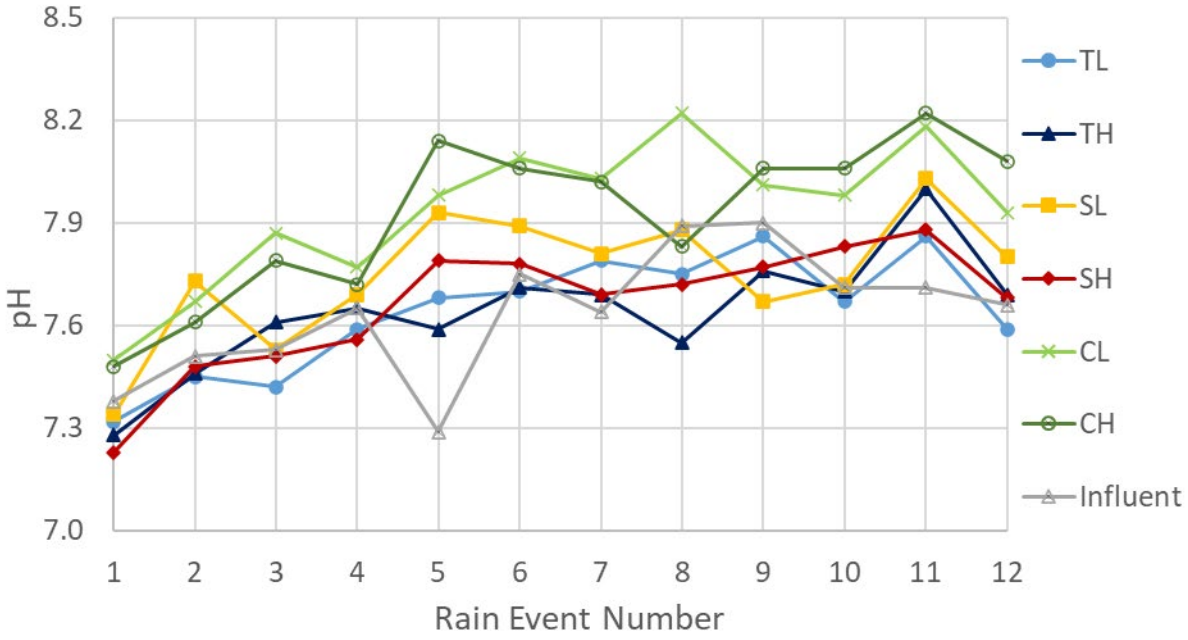

Figure 3.15: Runoff and influent pH measurements from each rain event.

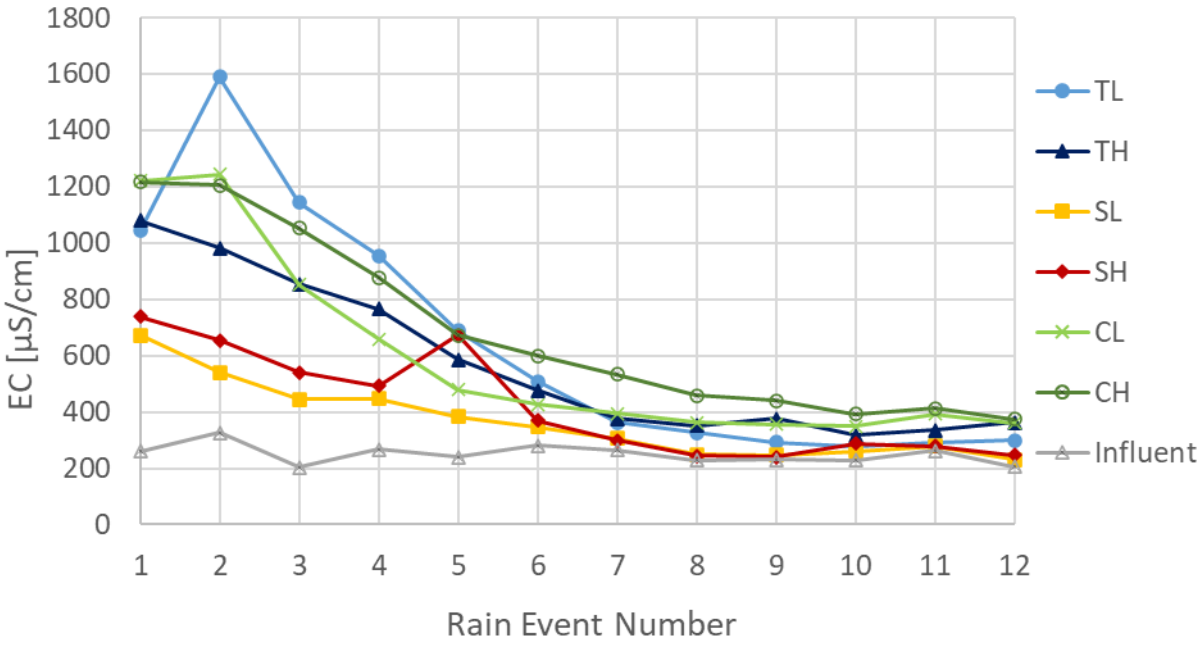

Figure 3.16: Runoff and influent EC measurements from each rain event.

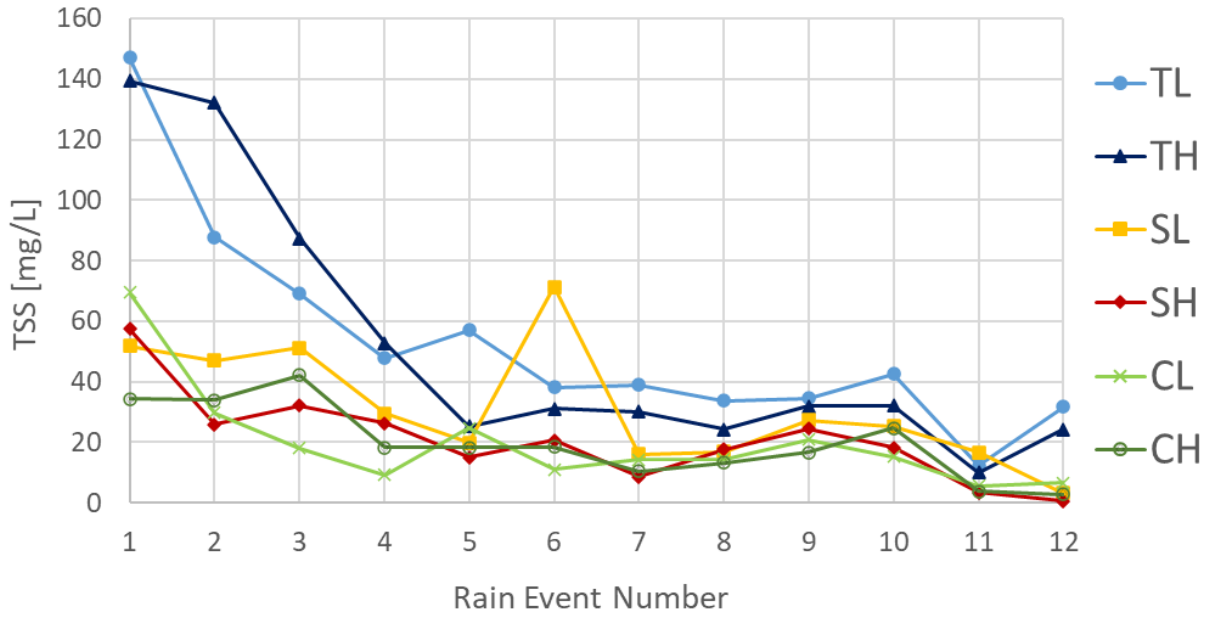

Figure 3.17: Runoff TSS measurements from each rain event.

The total organic carbon (TOC) concentrations from the runoff and influent tap water samples are presented in Figure 3.18. Dissolved organic carbon (DOC) and particulate organic carbon (POC) for select rain events are shown in Figure 3.19. TOC was highest in CH and CL. Initially, TOC concentrations decreased, before plateauing. For mesocosms SL and SH, TOC started to increase at rain event 10, the first event after grass trimmings were returned to the mesocosms. Likewise, TOC increased for TL and TH following the second trimming. The percentage of TOC in the form of POC was higher for the first event than the other events considered.

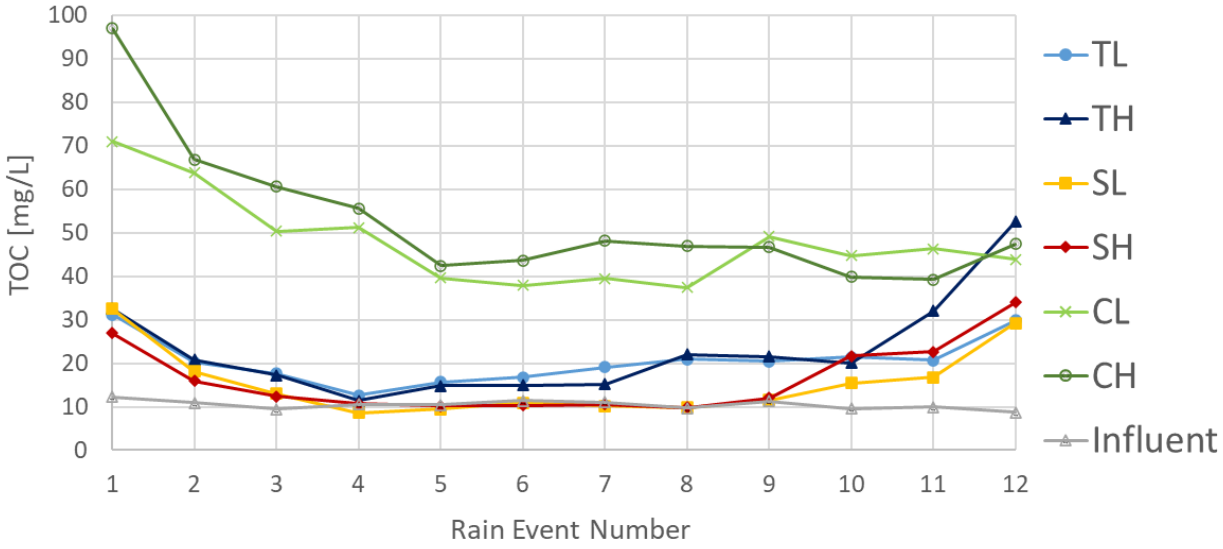

Figure 3.18: Runoff and influent TOC measurements from each rain event.

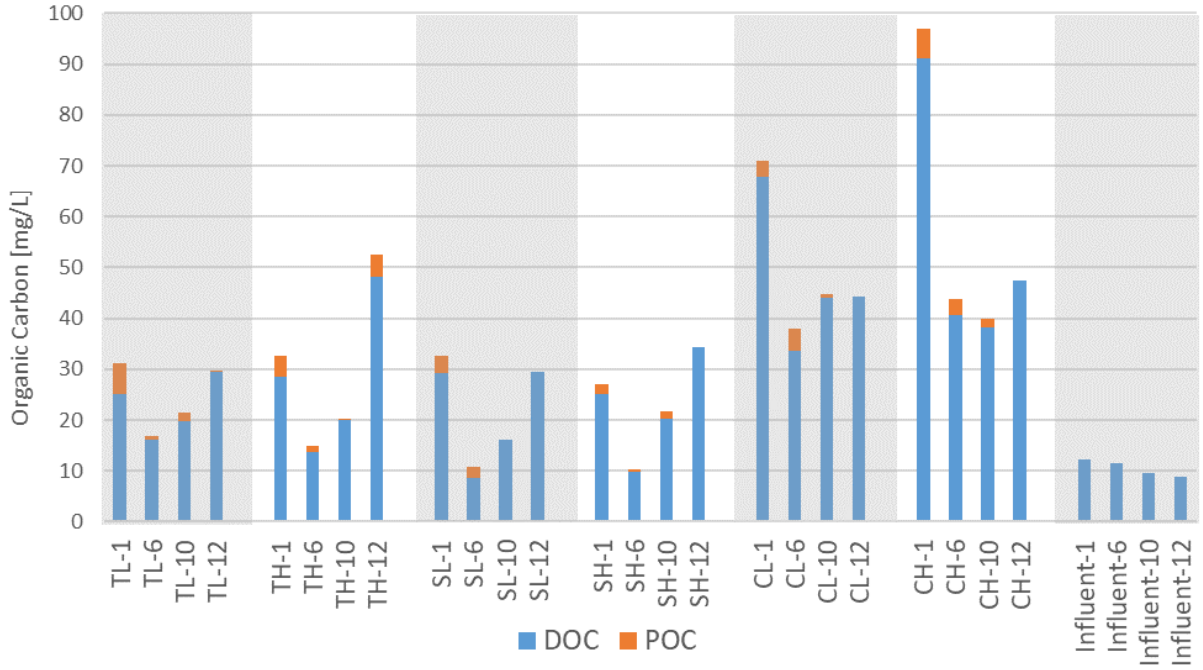

Figure 3.19: TOC speciation measurements from rain events 1, 6, 10, and 12.

The total phosphorous (TP) concentrations from the runoff and influent tap water samples are presented in Figure 3.20. Orthophosphate (OP), particulate phosphorous (PP), and dissolved organic phosphorous (DOP) for select rain events are shown in Figure 3.21. The subsoil and topsoil mesocosms had very high TP for rain event 1; TP was 11.1 mg/L and 3.4 mg/L for SL and SH, respectively, and 0.8 mg/L and 2.7 mg/L for TL and TH, respectively. SH, SL, and CL had phosphorous removal from the influent in rain event 5 and all following events. For rain event 1, the percentage of TP in the form of orthophosphate was 43% for CH and 64% for CL whereas, for all other mesocosms, at least 90% of TP was OP. In contrast, CH and CL had higher amounts of DOP in the first rain event compared to the other mesocosms.

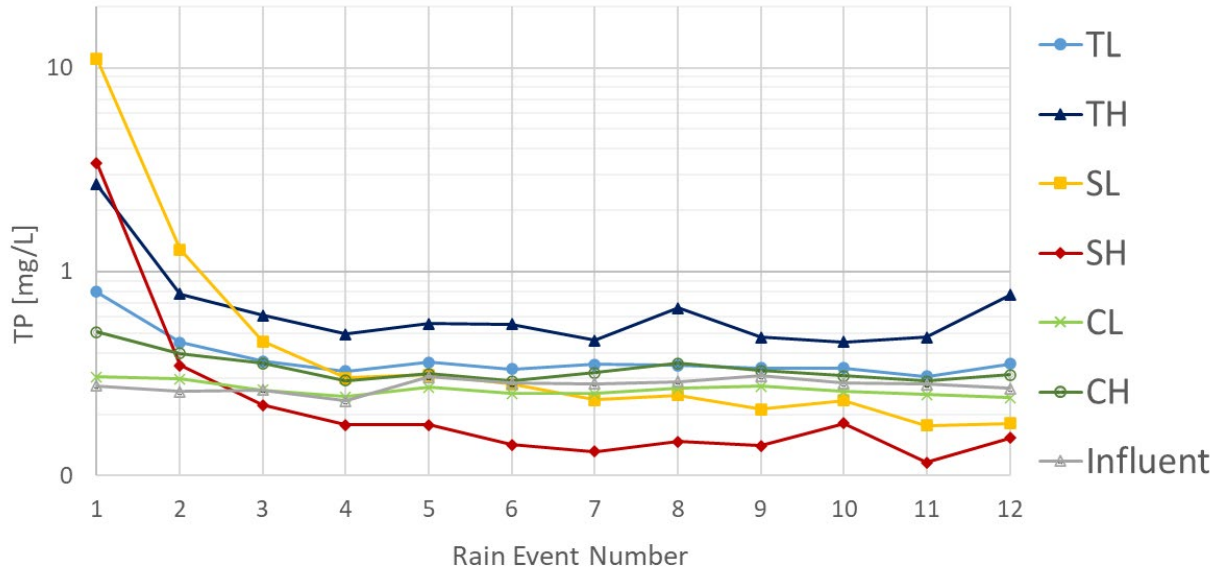

Figure 3.20: Runoff and influent TP measurements from each rain event.

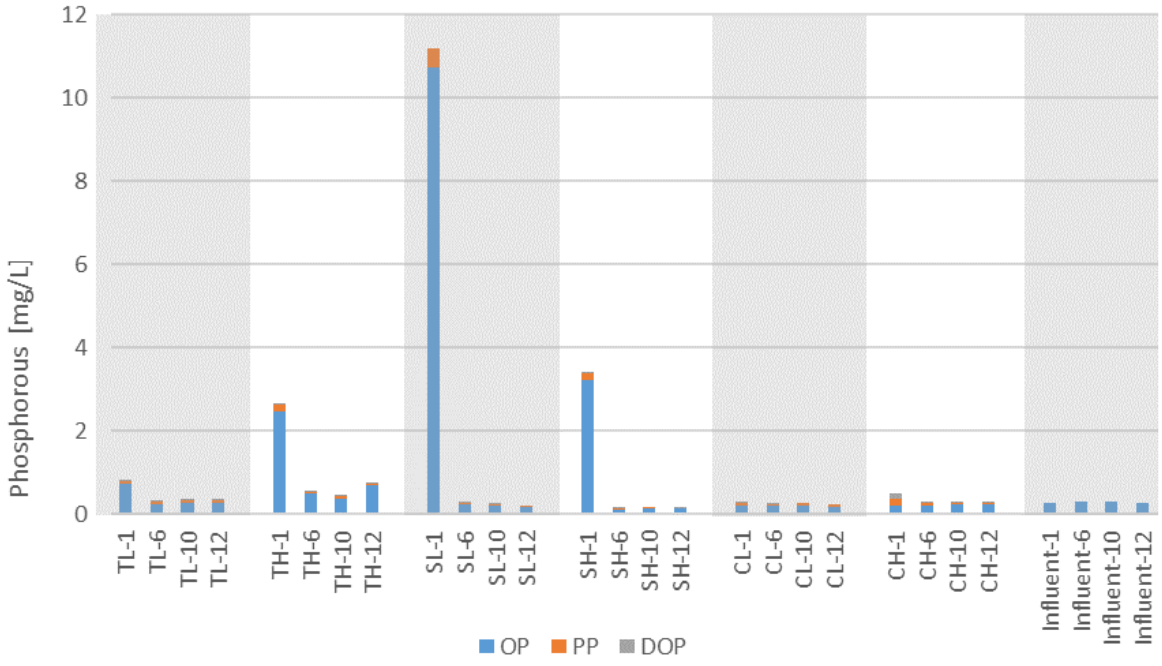

Figure 3.21: TP speciation measurements from rain events 1, 6, 10, and 12.

The total nitrogen (TN) concentrations from the runoff and influent tap water samples are presented in Figure 3.22. Nitrate/nitrite (NO_X-N), ammonium (NH_4-N), dissolved organic nitrogen (DON), and particulate nitrogen (PN) for select rain events are shown in Figure 3.23. TN concentrations decreased throughout the study. In rain event 1, the order of TN was TL > TH > CH > CL > SH > SL. For mesocosms SL and SH, TN started to increase at rain event 10, the first event after grass trimmings were returned to the mesocosms. Likewise, TN increased for TL and TH following the second trimming. These increases in TN also correspond to increases in TOC. NO_X-N was generally the dominant form of nitrogen in the runoff, particularly for earlier rain events.

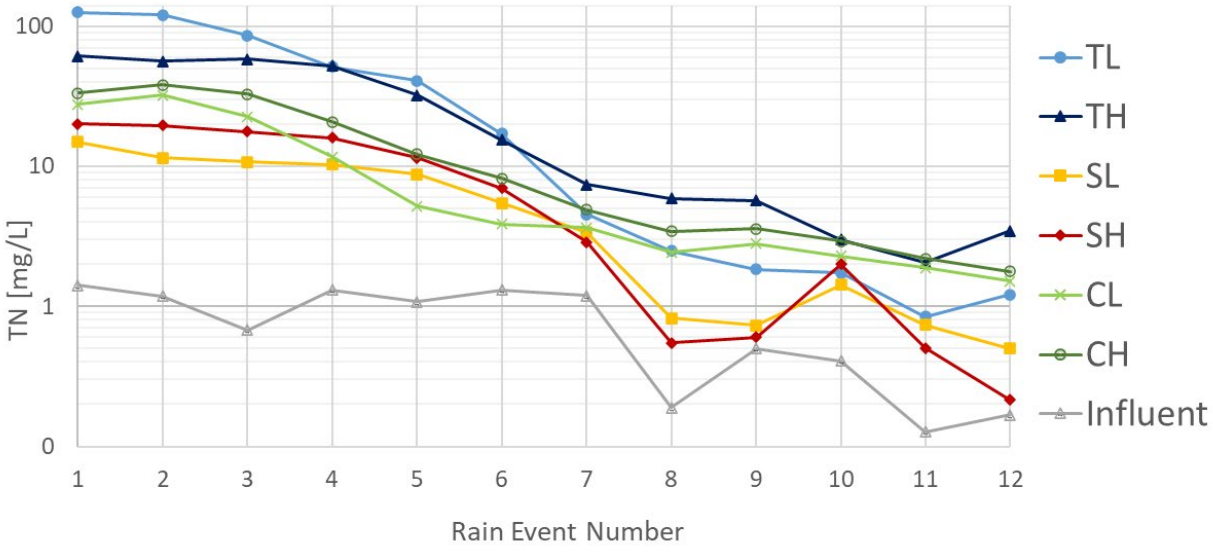

Figure 3.22: Runoff and influent TN measurements from each rain event.

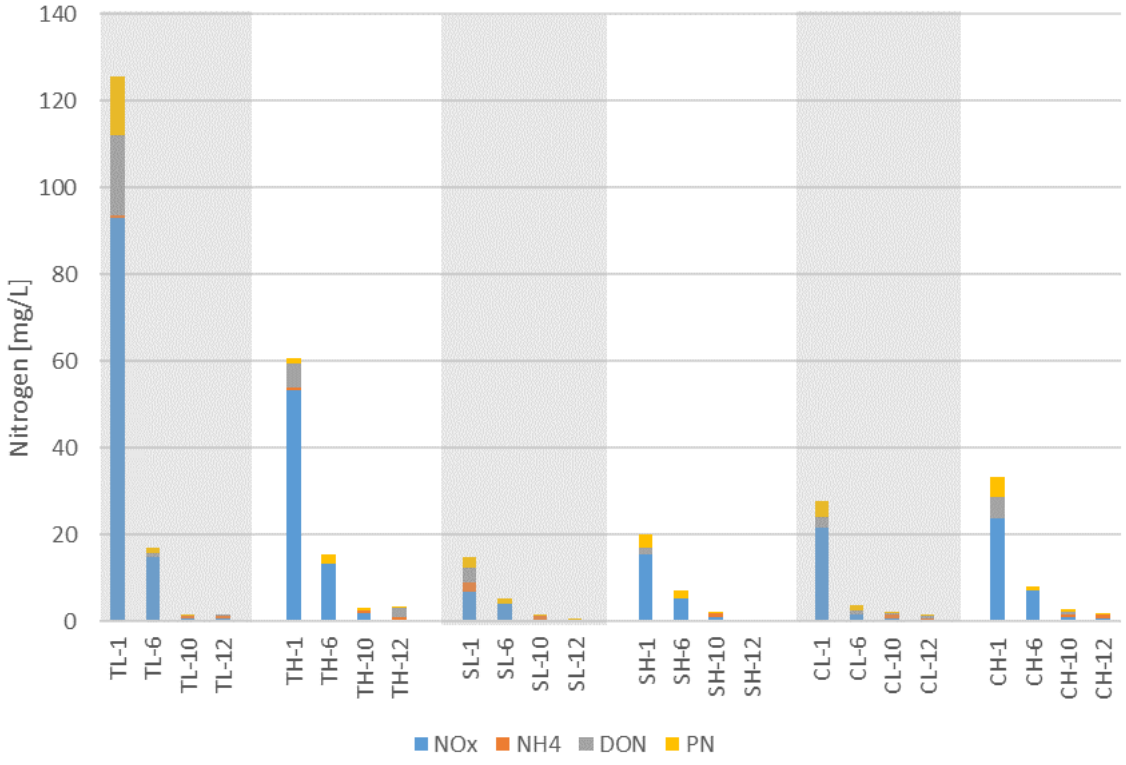

Figure 3.23: TN speciation measurements from rain events 1, 6, 10, and 12.

Final Soil Conditions

The final bulk density results are presented in Figure 3.24. SL and CL had densities of 1.15 ± 0.09 g/cm^3 and 1.09 ± 0.05 g/cm^3, respectively, which matched their target densities. TL had a final density of 1.17 ± 0.02 g/cm^3 which was slightly higher than its target density of 1.15 g/cm^3. All three high density mesocosms were slightly below the target densities with final and target values of 1.59 ± 0.02 g/cm^3 and 1.60 g/cm^3 for TH, 1.57 ± 0.06 g/cm^3 and 1.60 g/cm^3 for SH, and 1.48 ± 0.11 g/cm^3 and 1.51 g/cm^3 for CH.

The saturated hydraulic conductivity results are shown in Figure 3.25. CL had the highest hydraulic conductivity at $1.4 \times 10^{-2} \pm 8 \times 10^{-3}$ cm/s, followed by $7.3 \times 10^{-3} \pm 3 \times 10^{-3}$ cm/s for TL, and $2.7 \times 10^{-3} \pm 7 \times 10^{-4}$ cm/s for SL. The high density mesocosms had hydraulic conductivities of about an order of magnitude smaller than their low-density counterparts. For the high density mesocosms, CH had the highest hydraulic conductivity at $9.6 \times 10^{-4} \pm 5 \times 10^{-5}$ cm/s, followed by $2.9 \times 10^{-4} \pm 2 \times 10^{-5}$ cm/s for TH, and $1.2 \times 10^{-4} \pm 5 \times 10^{-5}$ cm/s for SH. Hence, for the same relative compaction, compost-amended subsoil had the highest hydraulic conductivity, followed by topsoil, and subsoil had the lowest value.

The final organic matter contents of the mesocosm soils are presented in Figure 3.26. All final values were slightly higher than the initial ones, but the magnitude of the difference varied by soil type. For TL and TH, the OM increase was 0.6%, for SL and SH, the increase was 0.2%, and for CL and CH, the increase was 0.3% and 0.4%, respectively.

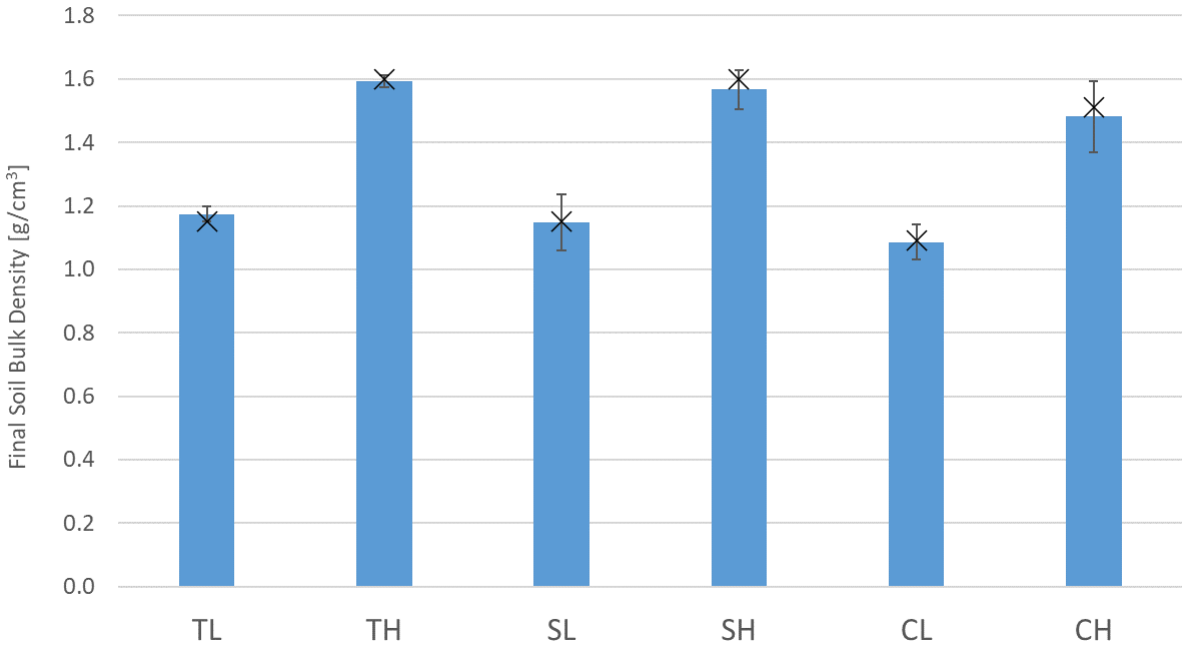

Figure 3.24: Final soil bulk density with the initial target density represented by an "X". Note: error bars represent the standard deviation of measurements taken from the top, middle, and bottom of each mesocosm.

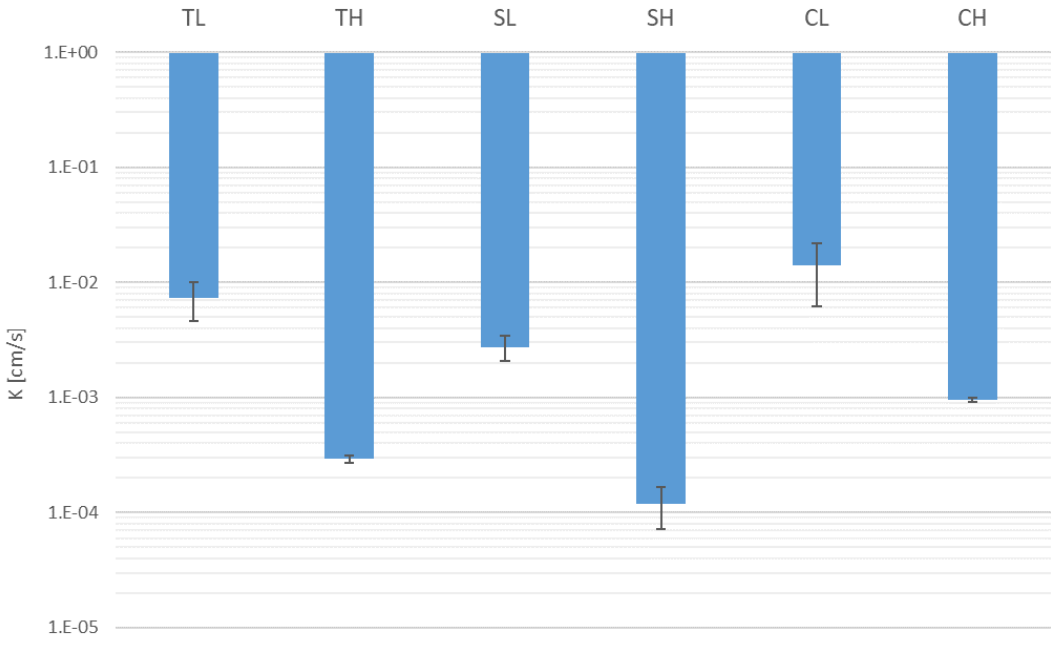

Figure 3.25: Saturated hydraulic conductivity of each mesocosm. Note: error bars represent the standard deviation of measurements taken from the top, middle, and bottom of each mesocosm.

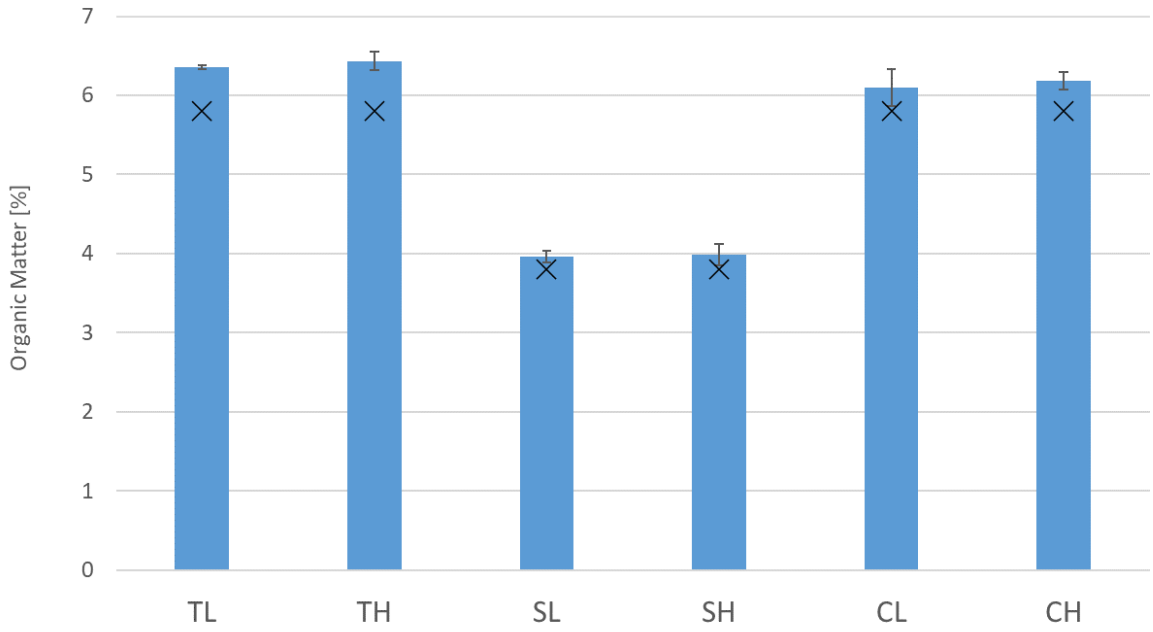

Figure 3.26: Final organic matter (LOI) of soil from each mesocosm with the initial soil organic matter represented by an "X". Note: error bars represent the standard deviation of a measurement taken from the top, middle, and bottom of each mesocosm.

3.3 Discussion

Vegetation Establishment

The pots with no topsoil (BH90 and BL90) had the lowest final green coverage, significantly lower final grass heights, and significantly lower total biomass than all the other pots (the biomass for CH90 was greater, but not statistically significant). The pots with 20.3 cm of topsoil (BH1L8, BL1L8, and BH1H4L4) had significantly higher final grass heights and significantly higher total biomass (the biomass for BH1H4L4 was greater than BH5L4, but not statistically significant). Thus, soil quality at depths greater than 10 cm was found to be important for better vegetation formation. Nevertheless, shallower topsoil still resulted in higher green coverage, grass heights, and biomass than the complete absence of topsoil. Tall fescue

grass roots can grow over 90-cm deep, so it follows that soil at these greater depths would impact its growth (Qian et al., 1997).

Final grass heights, biomass, and root densities were not significantly different between pots BH90 and BL90, despite the difference in soil density. Furthermore, the mesocosms of the same soil type had similar vegetation outcomes regardless of density; grass heights, green coverage, and biomass (except for topsoil mesocosms biomasses) were all within 5%. Therefore, from these two studies, the soil type/mix appears to have a greater effect on vegetation than the soil bulk density. However, BH1H4L4 had lower biomass, significantly lower final grass height, and significantly lower root density in the deeper layer than BH1L8 and BL1L8. Furthermore, the high density mesocosms had lower root density compared to the low density mesocosms of the same soil type. Thus, soil density did reduce root development as expected for a soil of this texture at this density (NRCS Soil Quality Institute, 1999). Both water and nitrogen stresses have been shown to increase the root/shoot ratio of grasses with water stress increasing the proportion of deep roots (Skinner & Comas, 2010). If the mesocosms were operated so that they were drought stressed, then it is possible that the soil density would have had a measurable impact on the vegetation. Additionally, response to drought stress and response to compaction are dependent on grass species (Braun et al., 2022; Carrow 1980). Further testing, particularly with more varied soil water contents and different plant species, is needed to better understand the relationship of tillage and soil density on roadside vegetation.

Compost amendment resulted in significantly higher final green coverage for both CH90 (91 ± 2%) and CH5L4 (89 ± 4%), compared to the non-amended controls, BH90 (47 ± 8%) and BH5L4 (76 ± 2%), with p-values of 0.004 and 0.009, respectively. The difference in final dry biomass was not significant for CH5L4, but it was almost significant for CH90 ($p = 0.052$). The

compost-amended mesocosms had greater grass heights and biomass than the subsoil mesocosms although statistical analysis cannot be performed due to the lack of replicates. These results further support that compost amendment can improve vegetation establishment in poor soils, which is well documented (Kranz et al., 2020).

Effects of Simulated Mowing

Tractor wheel traffic during mowing has been noted to contribute to soil compaction and reduced infiltration (Oliveira & Merwin, 2001). The simulated mowing compaction in the pot study resulted in higher soil density on the side of all pots, except for BH90, that received the additional compaction. However, this increased density had no observable effects on the vegetation and impact on hydraulic conductivity varied. The study may not have been long enough to allow for mowing compaction effects on vegetation to fully develop, and as noted above, may be more noticeable under vegetative stress.

In the later mesocosm rain events, TOC and TN sometimes increased followed trimming the grasses. Since the grass clippings were returned to the mesocosms, these clippings are the likely source of these increases. Jani et al. (2020) found that about one third of the PON in stormwater runoff from an urban residential catchment area came from grass clippings. Grass clippings can increase soil carbon and soil nitrogen and minimize the need for nitrogen fertilizer, particularly over longer periods of time (Qian et al., 2003).

Water Quality

Prior studies have shown that compost amendment can leach greater nutrient concentrations than unamended soil, particularly during the first flush (Owen et al., 2023; Puppala et al., 2011). Nutrient leaching from compost and chemical fertilizer is of concern since it can contribute to eutrophication of downstream waters or contaminate groundwater. Based on the recommendations of Pamuru (2024), yard waste compost was selected at the desired rate of increasing organic matter by 2% to minimize the risk of nutrient leaching while still improving soil nutrients and organic matter for vegetation. To evaluate the performance of the compost mix, Table 3.1 presents the amounts of nitrogen in the mesocosms initially and in the runoff from rain event 1; Table 3.2 shows the same information for phosphorous.

Table 3.1: Nitrogen initially in mesocosms and in runoff from rain event 1.

Mesocosm	Soil N [%]	Fertilizer N [g]	Runoff TN [mg/L]	Runoff Volume [L]	Total Nitrogen in Runoff [g]
TL	0.23	1.69	126	8	1.05
TH	0.23	1.69	61	9	0.57
SL	0.08	1.69	15	14	0.22
SH	0.08	1.69	20	14	0.28
CL	0.17	0	28	11	0.30
CH	0.17	0	33	11	0.36

Note: measurements are provided as single values since there was only one mesocosm of each type.

Table 3.2: Phosphorous initially in mesocosms and in runoff from rain event 1.

Mesocosm	Soil P [mg/L]	Fertilizer P [g]	Runoff TP [mg/L]	Runoff Volume [L]	Total Phosphorous in Runoff [mg]
TL	6.3	6.74	0.8	8	6.7
TH	6.3	6.74	2.7	9	25
SL	1.1	6.74	11.1	14	160
SH	1.1	6.74	3.4	14	48
CL	41.1	0	0.3	11	3.2
CH	41.1	0	0.5	11	5.5

Note: measurements are provided as single values since there was only one mesocosm of each type.

Mesocosms TL and TH had the highest initial nitrogen concentration in the soil in addition to receiving nitrogen from the fertilizer application. TL and TH also had the most nitrogen leach during the first rain event. Although CL and CH leached slightly more nitrogen than SL and SH, the compost amendment did not result in a substantial release of nitrogen. TL had 3.5 times more nitrogen leach than CL and 2.9 times more than CH. Throughout the study, NO_X-N was generally the dominant form of nitrogen in all mesocosms. In the later rain events, there was more NH_4-N leached for all mesocosms. NO_X-N and NH_4-N are bioavailable forms of nitrogen. Pamuru et al. (2024) found nitrate as the dominant nitrogen species in runoff from soil and compost-amended soils during a tub study. The study structure of weekly rain events caused the soil to remain wet throughout the study. Jani et al. (2020) found that longer periods without rainfall and higher rainfall depths were positively correlated with NO_x-N, NH_4-N, and particulate organic nitrogen in urban residential stormwater runoff. Hence, a more varied and realistic rainfall pattern may result in different nitrogen speciation than observed.

Mesocosms SL and SH had the most phosphorous leach during rain event 1 despite having the lowest concentration of phosphorous in the soil. CL and CH had less release of

phosphorus than the other four mesocosms. SL had 50 times more phosphorus leach than CL and 29 times more than CH. There was also a difference in the speciation of the phosphorus between the compost-amended and fertilized mesocosms during the first rain event. Figure 3.27 shows the phosphorus speciation from select rain events with the y-axis over a smaller range for easier comparison of smaller concentrations. In rain event 1, 64% of the total phosphorus was orthophosphate for CL and, for CH, it was 43%. In contrast, for the fertilized mesocosms, at least 90% of the total phosphorus was orthophosphate. Further, dissolved organic phosphorus was higher for the compost-amended mesocosms. Hence, there was a clear difference in the phosphorus leached from compost compared to inorganic fertilizer. This difference in the runoff speciation corresponds to differences in the phosphorus in the mesocosm; in the fertilizer, phosphorous is in the form of phosphate ions whereas compost contains organic phosphorus. Orthophosphate is the most bioavailable form of phosphorus whereas organic phosphorus must be transformed before it is used by microorganisms or plants. The tap water applied throughout the study contained orthophosphate, and, for rain events 9 through 12, at least 70% of runoff TP was orthophosphate for all mesocosms. Pamuru et al. (2024) also saw orthophosphate as the dominant phosphorus species in runoff after multiple simulated rain events using tap water.

Overall, chemical fertilizer application resulted in greater leaching of nutrients than compost amendment. The type of compost (yard waste) and the application rate (organic matter raised by 2%) were successful at minimizing nutrient leaching. The results support the recommendations of Pamuru (2024). Nevertheless, further testing would provide greater insight into if the fertilizer was needed for sufficient vegetation establishment or if it was predominantly washed out during the rain event.

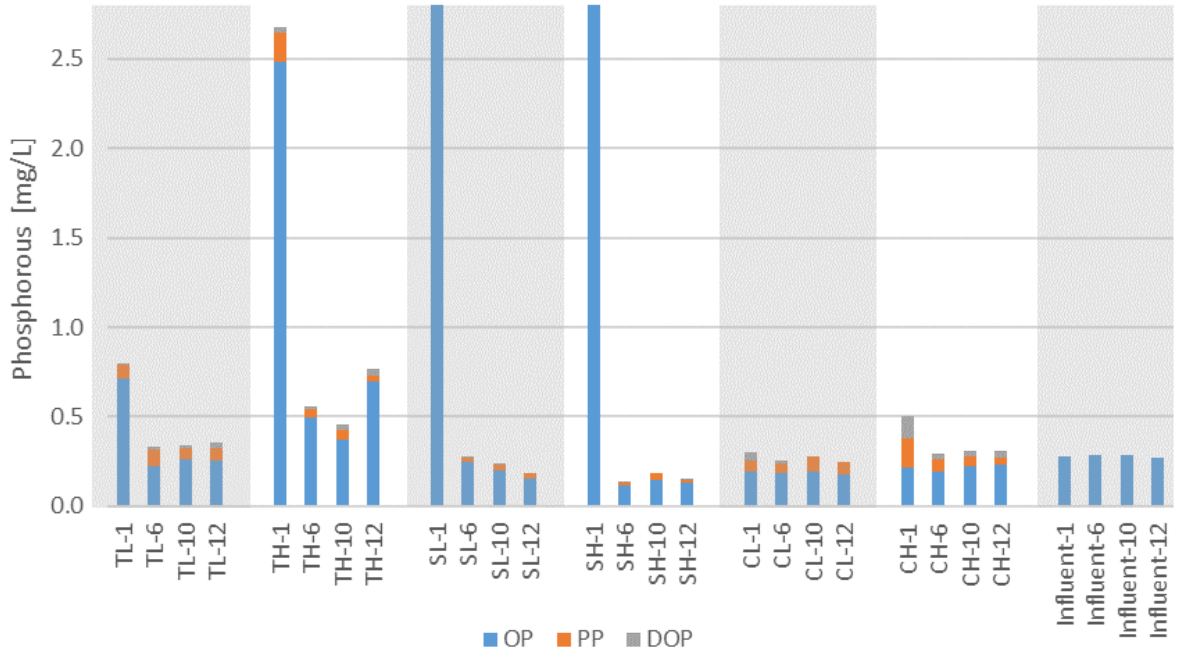

Figure 3.27: TP speciation measurements from rain events 1, 6, 10, and 12. Note: y-axis is over a smaller range than the data to allow for better comparison.

Hydraulic Conductivity

Saturated hydraulic conductivity at different densities is presented in Figure 3.28 with results from both the pot study and the mesocosm study. For all soil types, hydraulic conductivity decreased with increasing bulk density. When examining the effects of tillage, Kool et al. (2019) found a decrease in hydraulic conductivity by over an order of magnitude with increasing bulk density from 1.06 g/cm^3 to 1.4 g/cm^3. The initial tilled soil layer was 30 cm, but, for soil at depths greater than 10 cm, as the soil structure stabilized over time following tillage, the bulk density increased. In turn, for bulk densities above 1.06 g/cm^3, there was a clear correlation between bulk density and hydraulic conductivity (Kool et al., 2019).

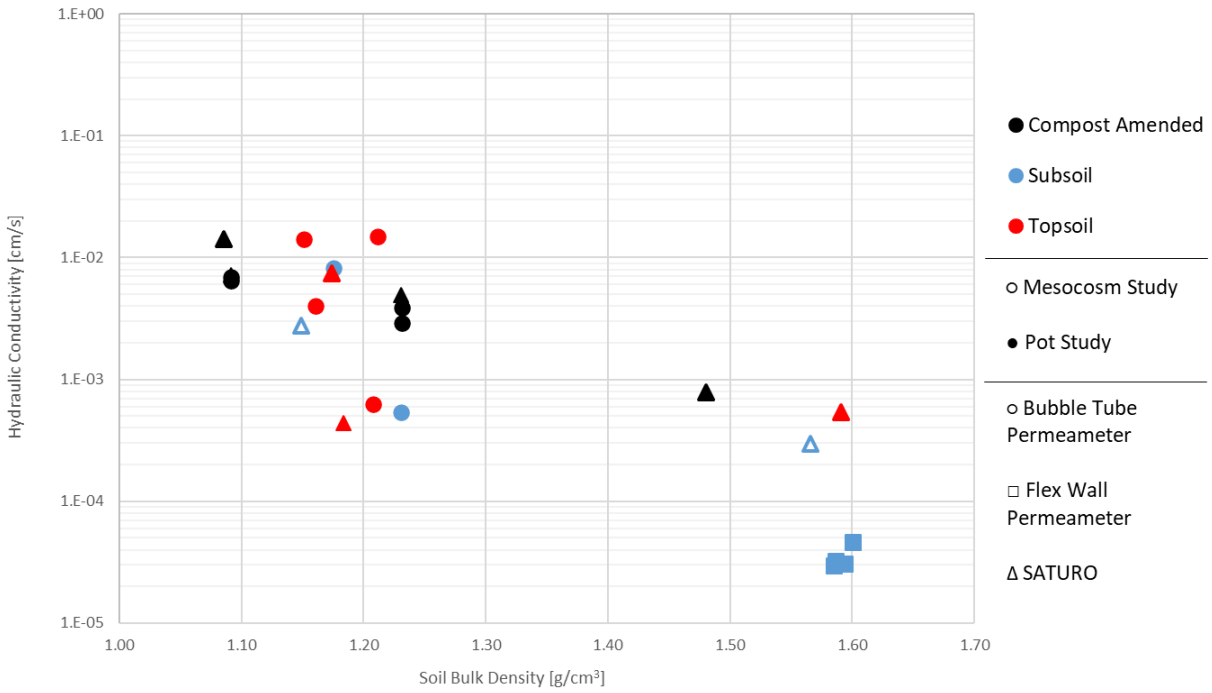

Figure 3.28: Hydraulic conductivity results sorted by soil type (black markers for compost amended subsoil, blue for subsoil, and red for topsoil), pot or mesocosm study (filled and empty markers, respectively), and testing method (circle markers for bubble tube permeameter, square for flex wall permeameter, and triangle for SATURO). Note: density and hydraulic conductivity values are the mean of three replicate measurements.

Compost amendment resulted in significantly higher hydraulic conductivity for both CH90 ($3 \times 10^{-3} \pm 1 \times 10^{-3}$ cm/s) and CH5L4 ($7 \times 10^{-3} \pm 2 \times 10^{-3}$ cm/s) compared to the non-amended controls, BH90 ($3 \times 10^{-5} \pm 2 \times 10^{-5}$ cm/s) and BH5L4 ($2 \times 10^{-3} \pm 2 \times 10^{-3}$ cm/s) with p-values of 0.005 and 0.015, respectively. For the mesocosms, compost amendment increased hydraulic conductivity at both low and high density with CL ($1.4 \times 10^{-2} \pm 8 \times 10^{-3}$ cm/s) larger than SL ($2.7 \times 10^{-3} \pm 7 \times 10^{-4}$ cm/s), and CH ($9.6 \times 10^{-4} \pm 2 \times 10^{-4}$ cm/s) larger than SH ($1.2 \times 10^{-4} \pm 5 \times 10^{-5}$ cm/s). These results match many other results where compost amendment has increased hydraulic conductivity (Olson et al., 2013; Cannavo et al., 2014; Duzgun et al., 2021; Pamuru et al., 2024). This increased hydraulic conductivity generally allows for greater

stormwater infiltration and reduced runoff volumes. In a greenhouse study, Owen et al. (2022) found that compared to the standard topsoil practice, compost amendment generally lowered runoff volume by 13%–64%.

Compost amendment also increased the mean water content of the mesocosms (SL 0.23 m^3/m^3 and SH 0.22 m^3/m^3 compared to CL 0.29 m^3/m^3 and CH 0.27 m^3/m^3). Weindorf et al. (2006) found that for some soils, increased compost amendment significantly increased soil water content because of the attraction between water and organic matter. Duzgun et al. (2021) found that a mixture of 85% topsoil and 15% leaf compost had an available water content of 16.7% compared to only 10.9% for unamended topsoil. Vegetation establishment and drought resistance benefit from compost amendment and the corresponding increased available water content (Kirchoff et al. 2003).

Chapter 4 Conclusions

4.1 Conclusions and Recommendations

Good soil quality is critical in roadside soils to allow for sufficient vegetation establishment, stormwater infiltration, and runoff quality, yet cost effective methods to improve roadside soil quality need to be better understood. A pot study and a mesocosm study were conducted to evaluate the effects of soil quality, topsoil depth, compost amendment, initial soil density, and compaction from mowing equipment on vegetation establishment, soil hydraulic characteristics, and runoff water quantity and quality.

In the pot study, the grass heights and total biomass amounts increased with increasing topsoil depths. For pots with 20.3 cm (8 inches) of topsoil, the mean final grass height was 1.7 times higher, and the mean total dry biomass was 2.6 times higher than for pots with no topsoil. In the mesocosm study, topsoil had the greatest grass heights and total biomass. The mean total dry biomass was 1.9 times higher in the topsoil mesocosms than in the subsoil ones. A deep, low-density layer of topsoil, ideally at least 20 cm, was shown to be most effective for vegetation establishment and growth, although shallower layers of topsoil still performed better than no topsoil. However, quality topsoil is not always available at a construction site. Yard waste compost, when applied at the correct rate (maximum 2% increase in soil organic matter), is an effective amendment for soil of poor quality to improve vegetation without unacceptable leaching of nutrients. In the mesocosm study, compost-amended subsoil actually leached less nitrogen initially compared to topsoil with inorganic fertilizer applied and less phosphorous compared to topsoil and subsoil with inorganic fertilizer applied. The topsoil mesocosm TL had a

nitrogen load 3.5 times more than CL and 2.9 times more than CH, and the subsoil mesocosm SL had a phosphorus load 50 times more than CL and 29 times more than CH.

Although soil density had limited effects on grass heights and biomass in this work, higher density soil reduced root density in both studies. In the mesocosm study, root density was on average 25% higher in the low-density mesocosm compared to the high-density mesocosm of the same soil type. A greater impact may have been noted if the grasses were water stressed. Hydraulic conductivity was also reduced by two orders of magnitude in soil at higher densities. Thus, reduced soil density is also critical for roadside soil performance as vegetated stormwater control measures because adequate stormwater infiltration is required. For some soil conditions in the pot study, it was seen that the use of routine mowing equipment can recompact soil enough to significantly affect hydraulic conductivity. Hence, possible re-compaction will need to be considered for the long-term performance of these soils. Overall, the soil type (topsoil, subsoil, or compost-amended subsoil) seemed most critical for successful vegetation establishment, but soil density also needs to be considered and further examined.

4.2 Limitations and Future Work

This work was limited to topsoil and subsoil from one site and a single yard waste compost. Other soils and composts may have differences in their behavior and performance. Yard waste compost feedstock may vary geographically and seasonally which could affect the performance of the final compost. Moreover, in urbanized areas topsoil can be degraded, so it should not be assumed that the topsoil present at a site will always be sufficient as is for vegetation establishment. More work is required to produce recommendations for determining if

a soil is of “high quality” or if it needs amendment. Furthermore, only one turfgrass seed mix was used. A future study is planned that will repeat the mesocosm study with a native seed mix to examine the effects of plant type on the performance of these systems. Native species have many ecological benefits and can be more resilient to disturbance than non-native turfgrasses, but natives can also have slower growth rates (Simmons et al., 2011). It is also possible that if the rainfall on the mesocosms was more variable, including times of drought stress, then there would have been greater differences in the outcomes, particularly on the above-ground vegetation at different soil densities. With climate change making weather patterns more extreme and less predictable, this potential source of deviation is of timely consideration.

In the field, tillage is used on compacted soil to reduce its density. In the greenhouse, disturbed soil was already present, so it was assumed that by placing the soil at a low density this could simulate tillage compared to a highly compacted control pot or mesocosm. However, actual tillage is more complex than simply altering the soil density. Tillage disrupts the soil which can reduce soil aggregation, increase soil erosion, decrease soil organic matter, reduce microbial biomass, and alter soil microbial community composition (Helgason et al., 2010). Tillage can also increase nutrient loads in runoff, particularly nutrients in particulate phase (Melland et al., 2016). Thus, there could be impacts of tillage missed in these smaller-scale, greenhouse experiments. A field study is also a future next step to see the effects of these soil restoration processes under less controlled and more realistic conditions. In particular, actual stormwater will be used rather than the tap water used in the greenhouse studies. Fieldwork will also help to better understand the re-compaction of soil over time, and if compost amendment can be used to reduce this phenomenon. The pot study was limited to two compaction events that used a hydraulic press, which is a different motion than a tractor wheel.

The hydraulic conductivity of these soils was shown to vary significantly, particularly based on soil density. However, there was no clear pattern to runoff volume measurements in the mesocosm study to connect to soil storage capacity or hydraulic conductivity. Further, heavy compaction of deeper soil can have significant effects on the hydrology of a site and its ability to infiltrate stormwater, regardless of the hydraulic conductivity of the uppermost soil layer. Additional testing could be done to better link these changes in hydraulic conductivity to impacts on the performance of vegetated stormwater control measures.

Overall, more work is needed to examine these practices on a larger scale with different soils, plants, composts, and rainfall conditions. Cost-benefit analysis should also be conducted on different restoration techniques. Ultimately, the goal is to develop a flow chart to guide roadside soil quality restoration based on local soil properties and conditions.

Appendices

APPENDIX A: Soil Nutrient Characterization

Table A.1: Topsoil and subsoil nutrient characterization from the Cornell Soil Health Laboratory

Nutrient	Topsoil	Subsoil
Total Carbon (%)	2.48	0.80
Total Nitrogen (%)	0.23	0.08
Extractable Phosphorus (ppm)	6.3	1.1
Extractable Potassium (ppm)	268.9	100.7
Magnesium (ppm)	626.0	804.6
Iron (ppm)	17.3	0.4
Manganese (ppm)	5.6	1.0
Zinc (ppm)	0.8	0.1
Aluminum (ppm)	17.4	18.2
Calcium (ppm)	4355.3	3897.4
Copper (ppm)	0.16	0.11
Sulfur (ppm)	26.2	5.4
Boron (ppm)	0.23	0.16

APPENDIX B: Pot Study Additional Compaction Effects on Vegetation

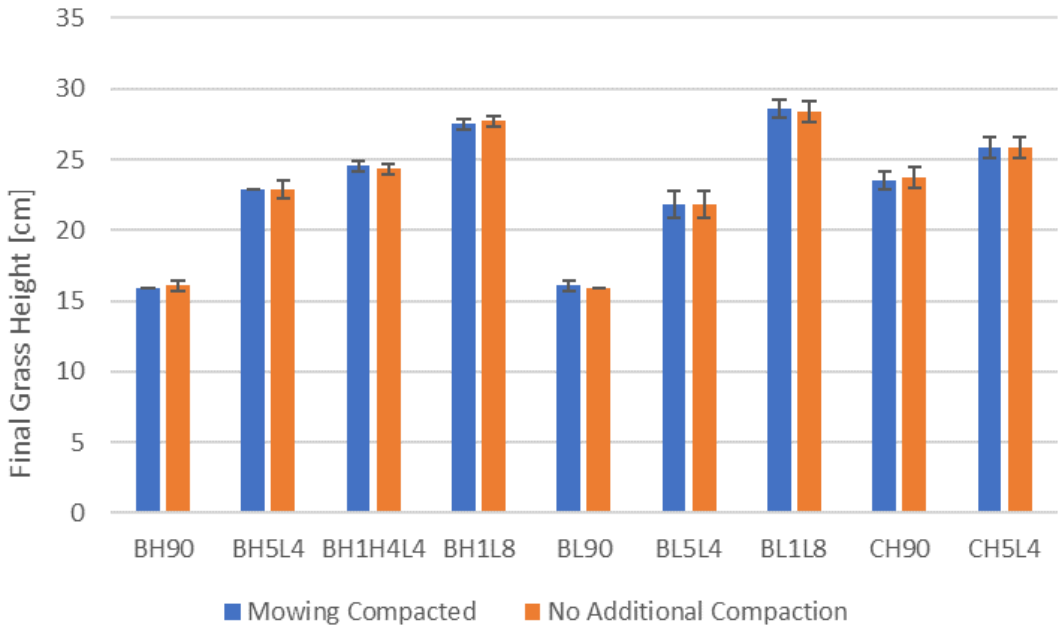

Figure B.1: Comparison of final grass heights on the mowing compacted and no additional compaction sides of individual pots. Note: error bars represent the standard deviation among the replicates.

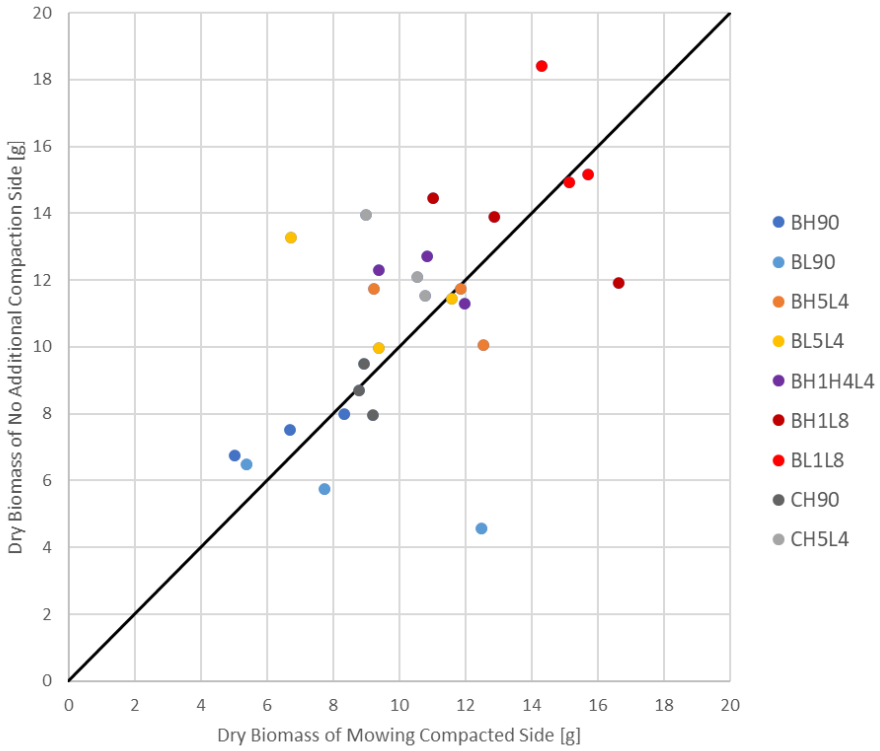

Figure B.2: Comparison of dry biomass in the final collection on the mowing compacted and no additional compaction sides of individual pots.

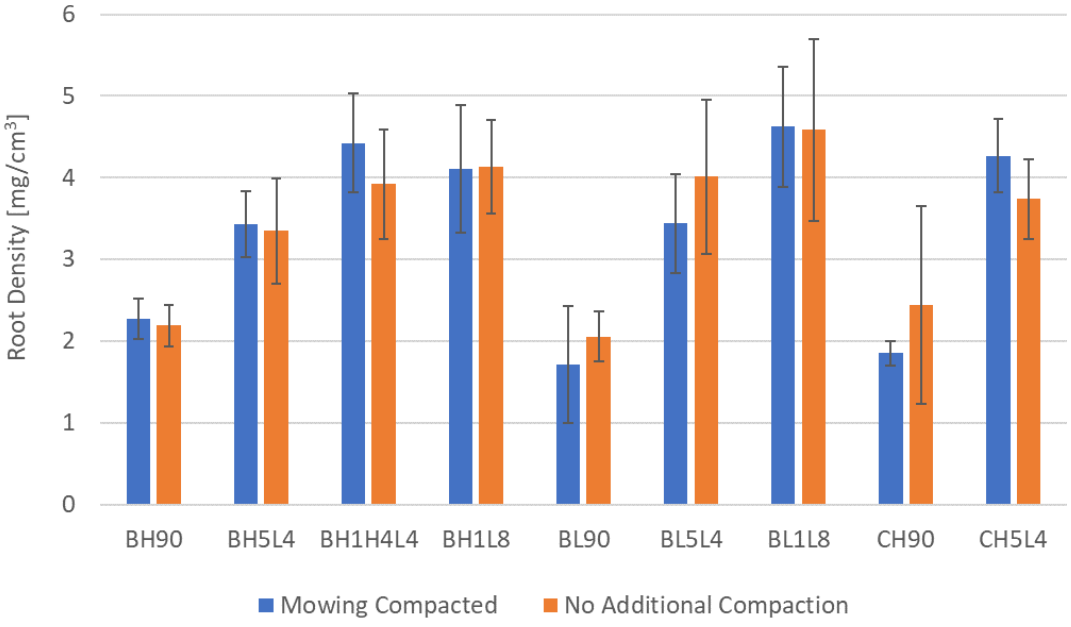

Figure B.3: Root density in upper cores. Note: error bars represent the standard deviation among the replicates.

APPENDIX C: Select Photos for Green Coverage Analysis

Figure C.1: Select photos from the pot with the highest vegetative growth, BL1L8, and the lowest vegetative growth, BH90.

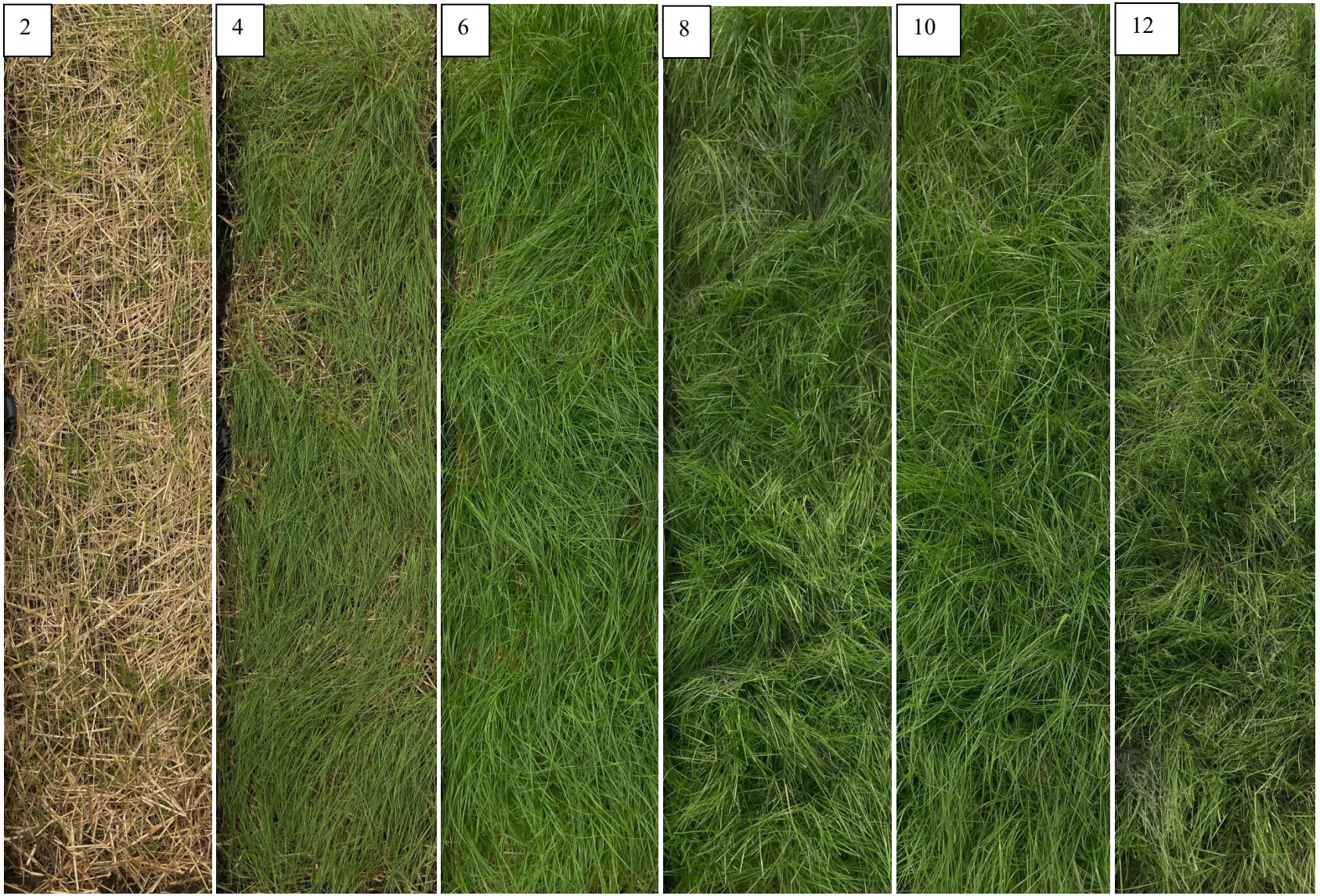

Figure C.2: TL mesocosm after rain events 2, 4, 6, 8, 10, and 12.

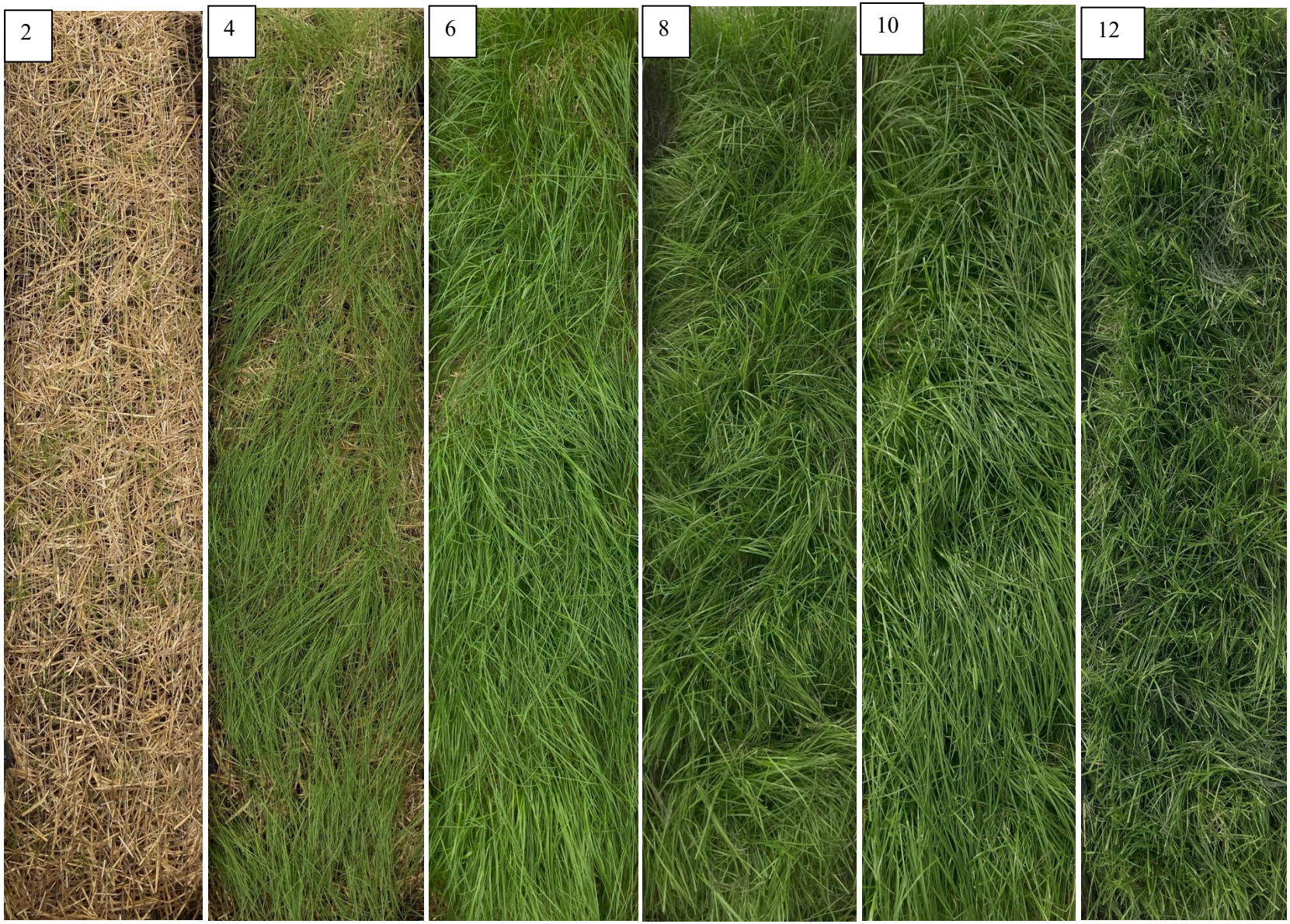

Figure C.3: TH mesocosm after rain events 2, 4, 6, 8, 10, and 12.

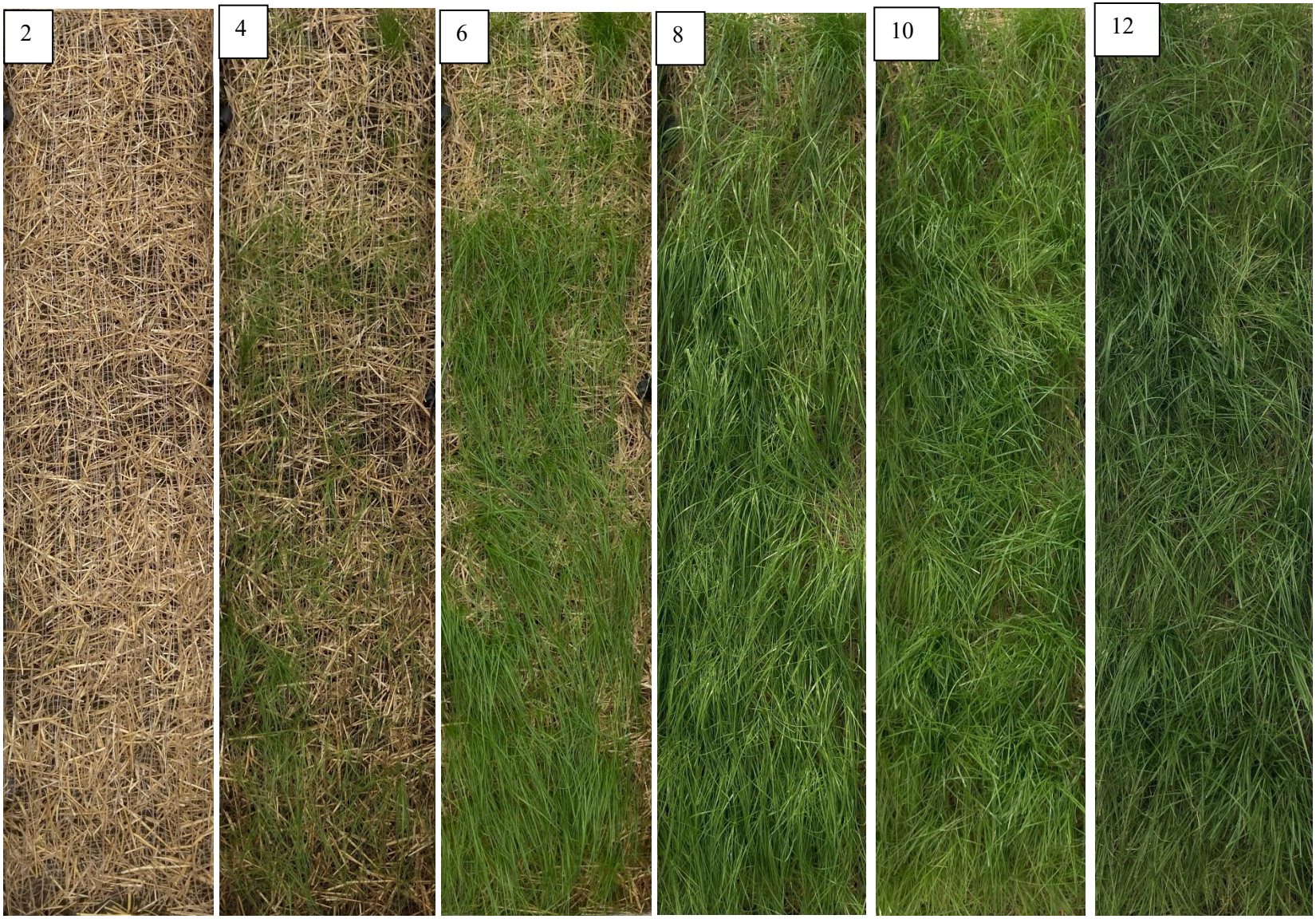

Figure C.4: SL mesocosm after rain events 2, 4, 6, 8, 10, and 12.

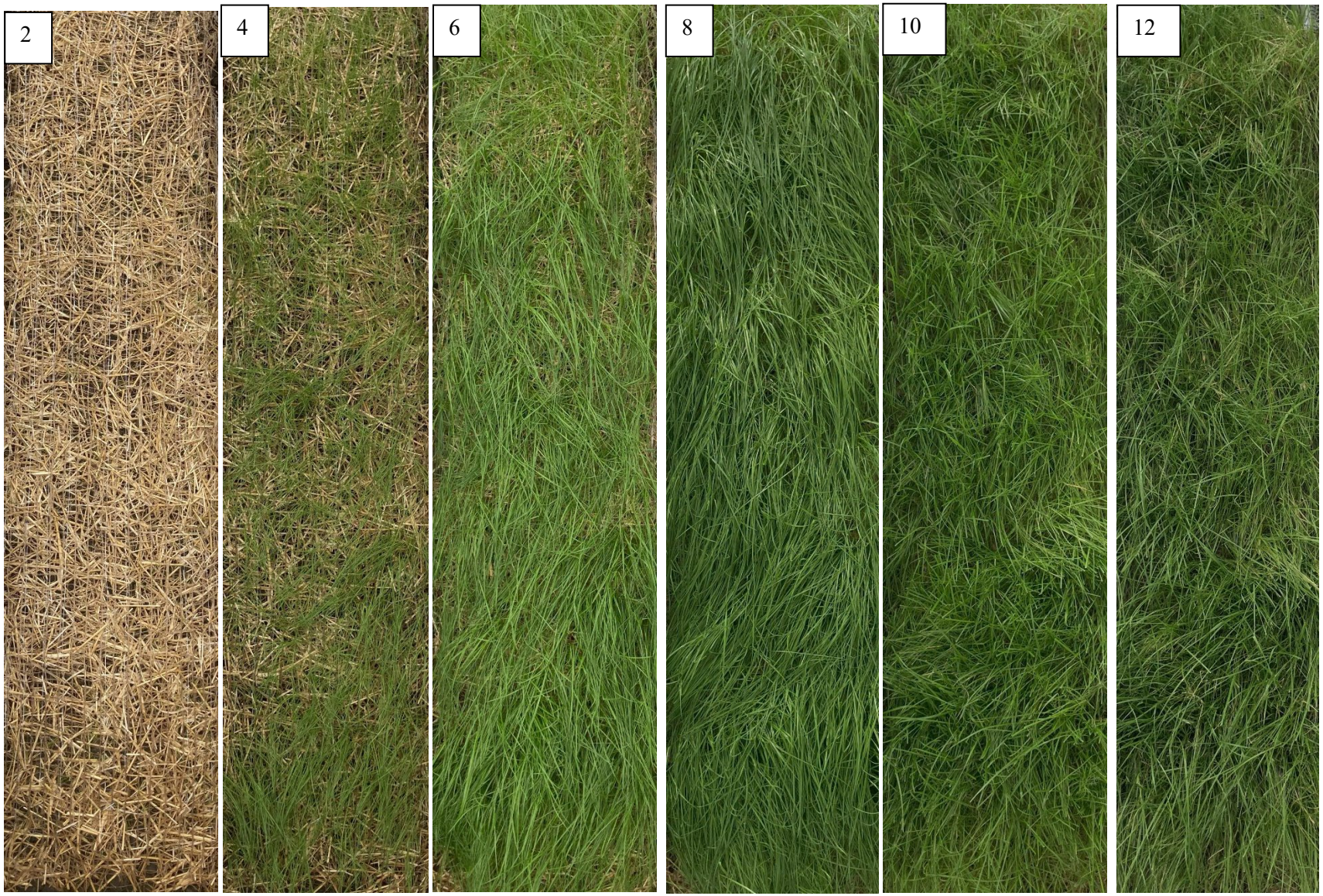

Figure C.5: SH mesocosm after rain events 2, 4, 6, 8, 10, and 12.

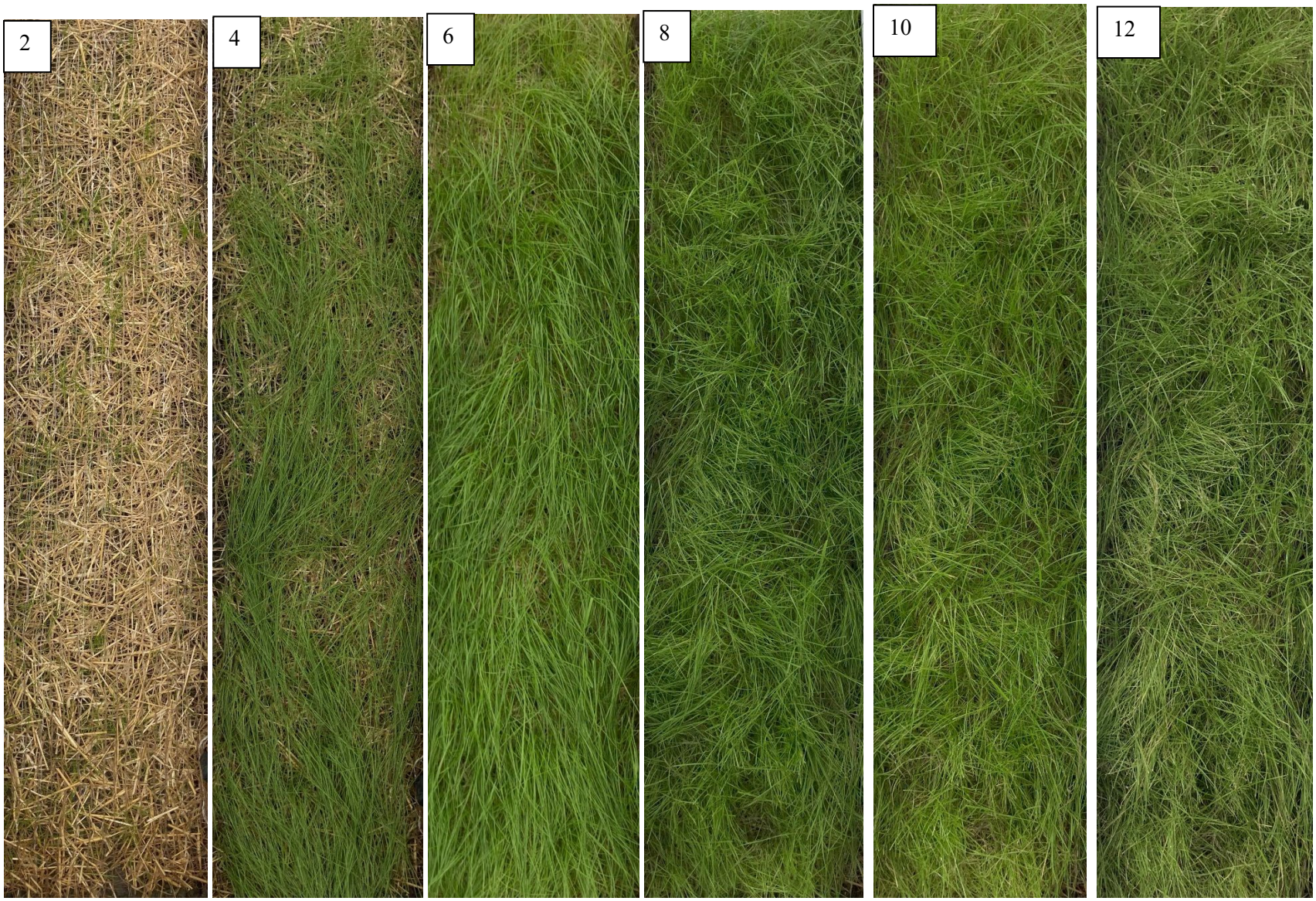

Figure C.6: CL mesocosm after rain events 2, 4, 6, 8, 10, and 12.

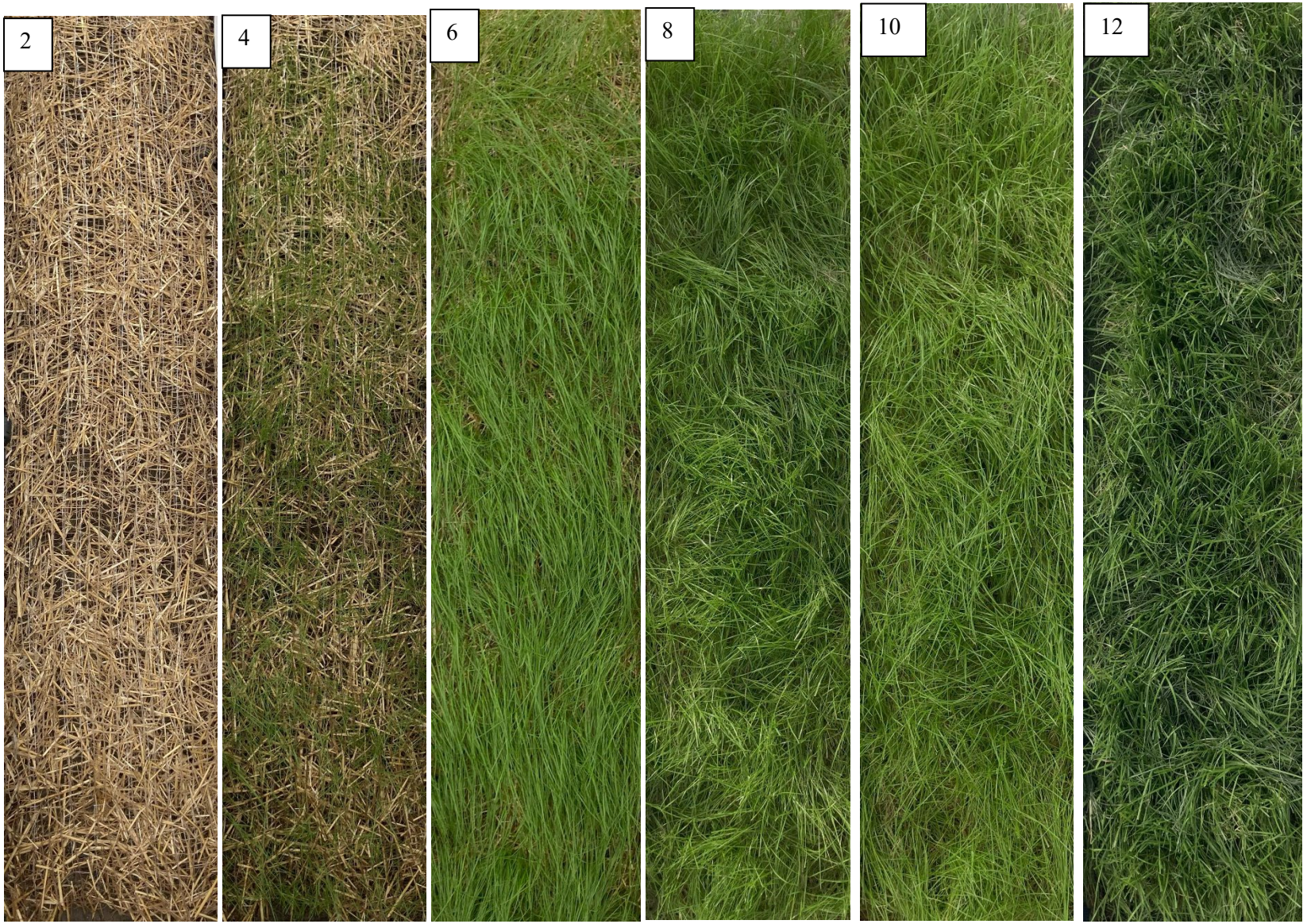

Figure C.7: CH mesocosm after rain events 2, 4, 6, 8, 10, and 12.

APPENDIX D: Mesocosm Study Measurement Location Comparison

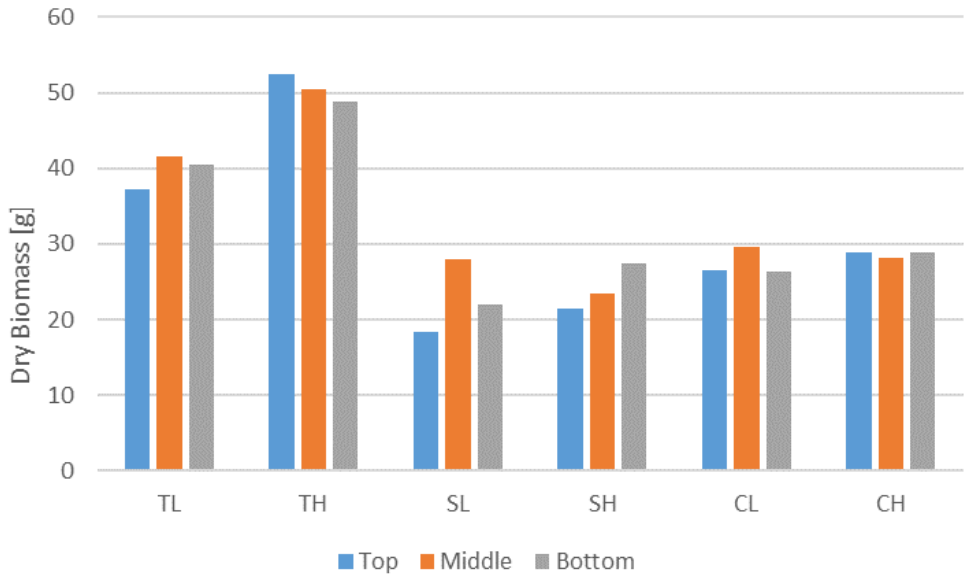

Figure D.1: Biomass from trimmings and final collection separated by top, middle, and bottom of each mesocosm.

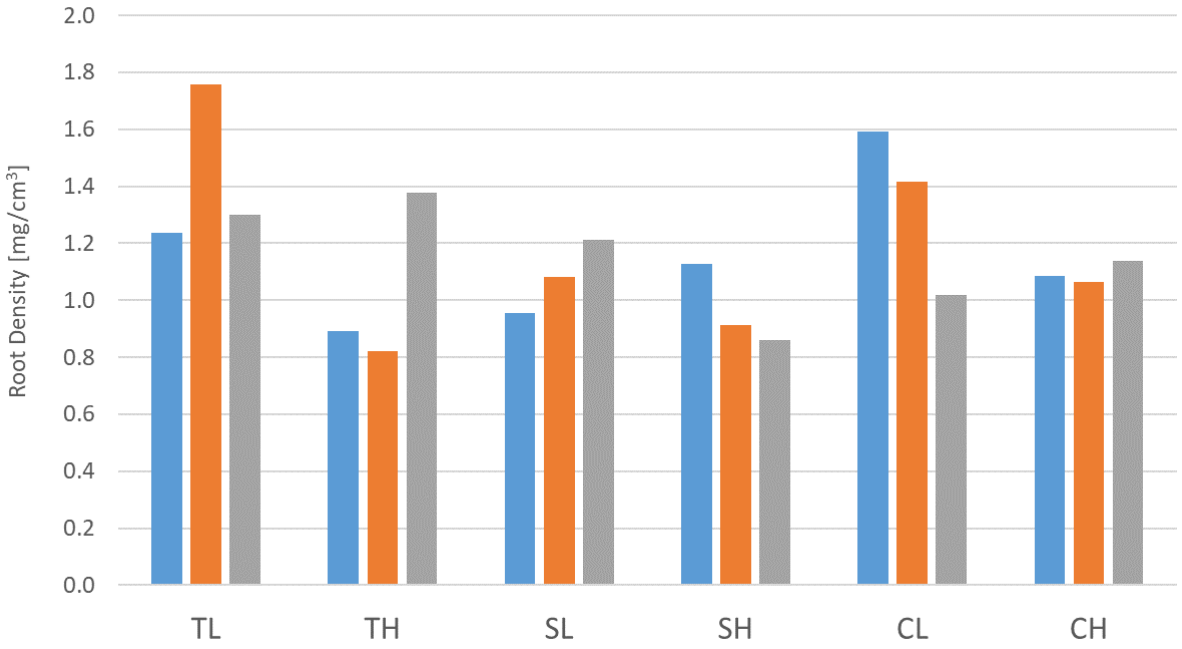

Figure D.2: Root density measurements by location within mesocosm.

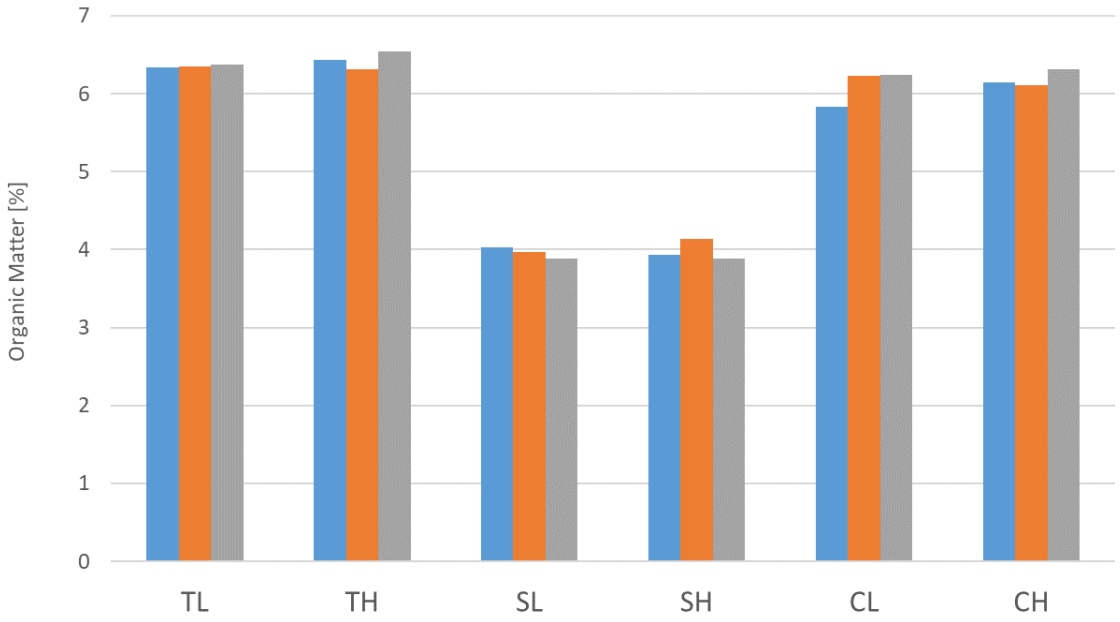

Figure D.3: Organic matter content measurements by location within mesocosm.

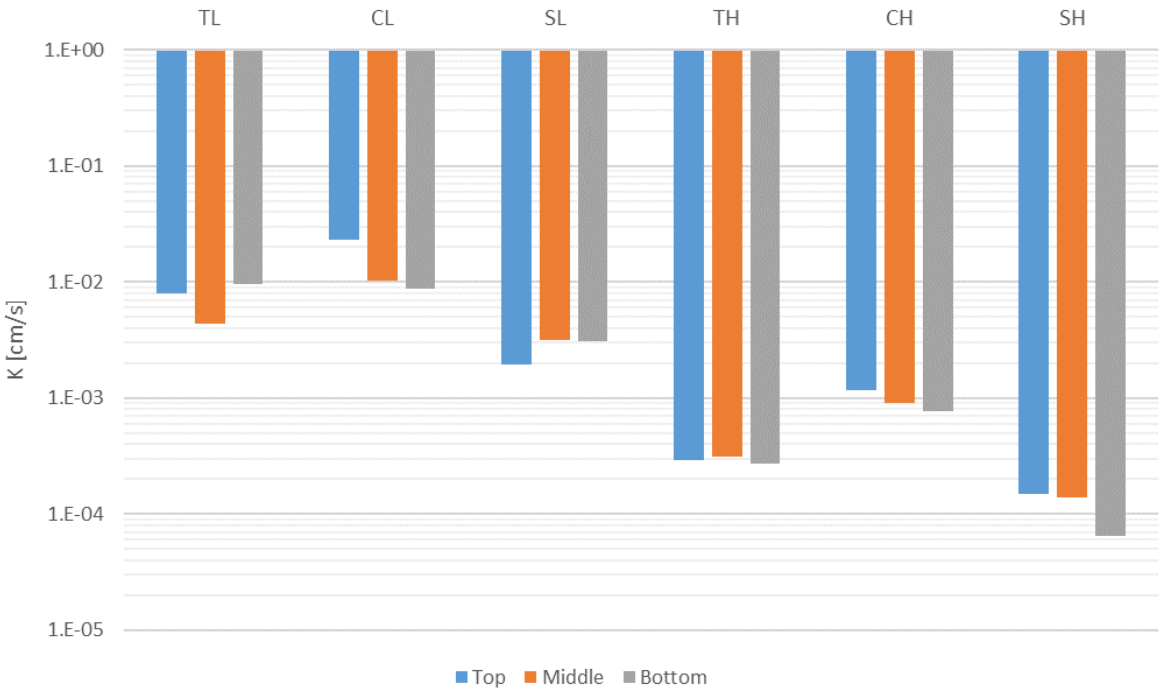

Figure D.4: Saturated hydraulic conductivity measurements by location within mesocosm.

APPENDIX E: Mesocosm Study Soil Sensor Data

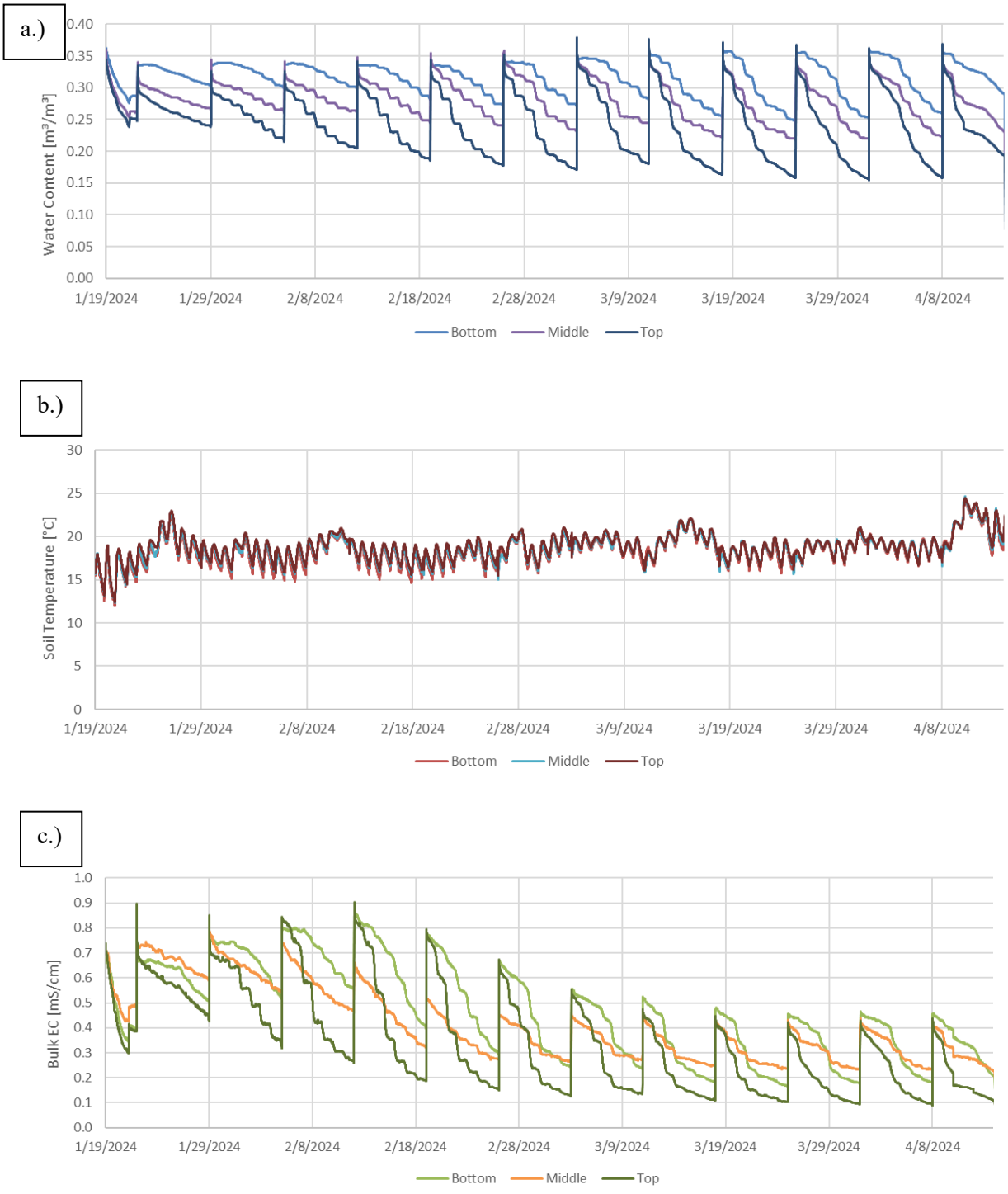

Figure E.1: Soil sensor readings for TL. a.) water content, b.) soil temperature, and c.) soil bulk electrical conductivity (EC).

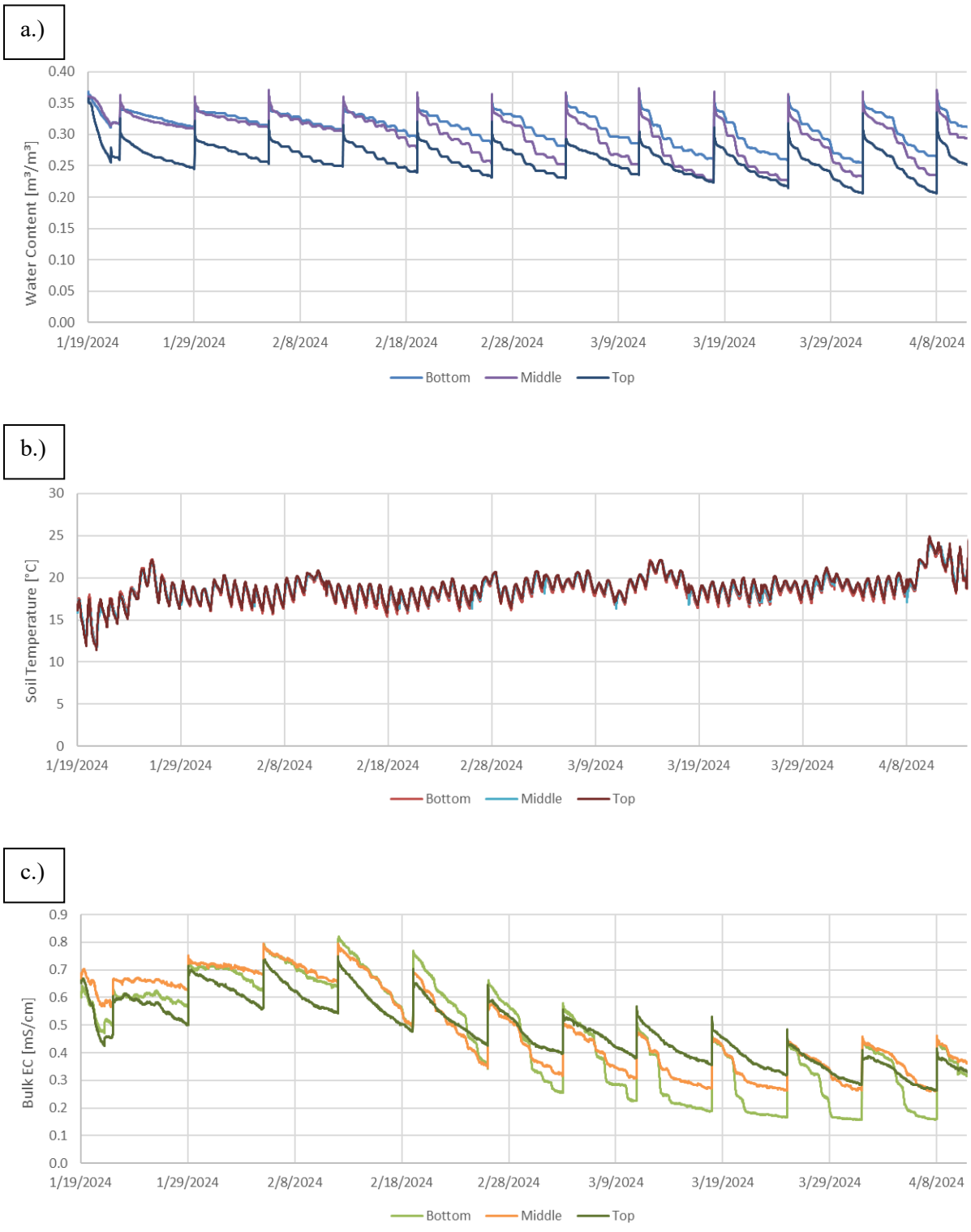

Figure E.2: Soil sensor readings for TH. a.) water content, b.) soil temperature, and c.) soil bulk electrical conductivity (EC).

Figure E.3: Soil sensor readings for SL. a.) water content, b.) soil temperature, and c.) soil bulk electrical conductivity (EC).

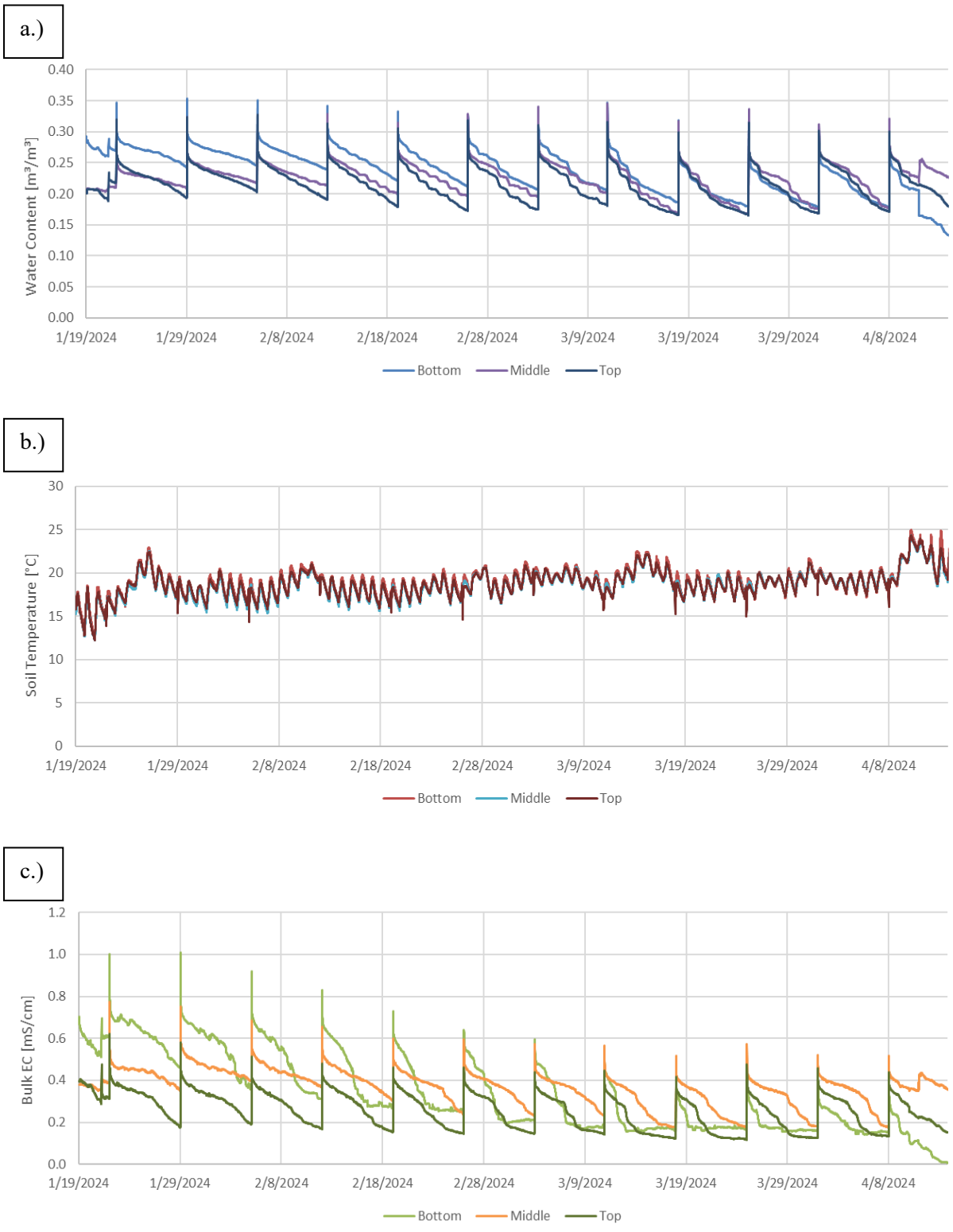

Figure E.4: Soil sensor readings for SH. a.) water content, b.) soil temperature, and c.) soil bulk electrical conductivity (EC).

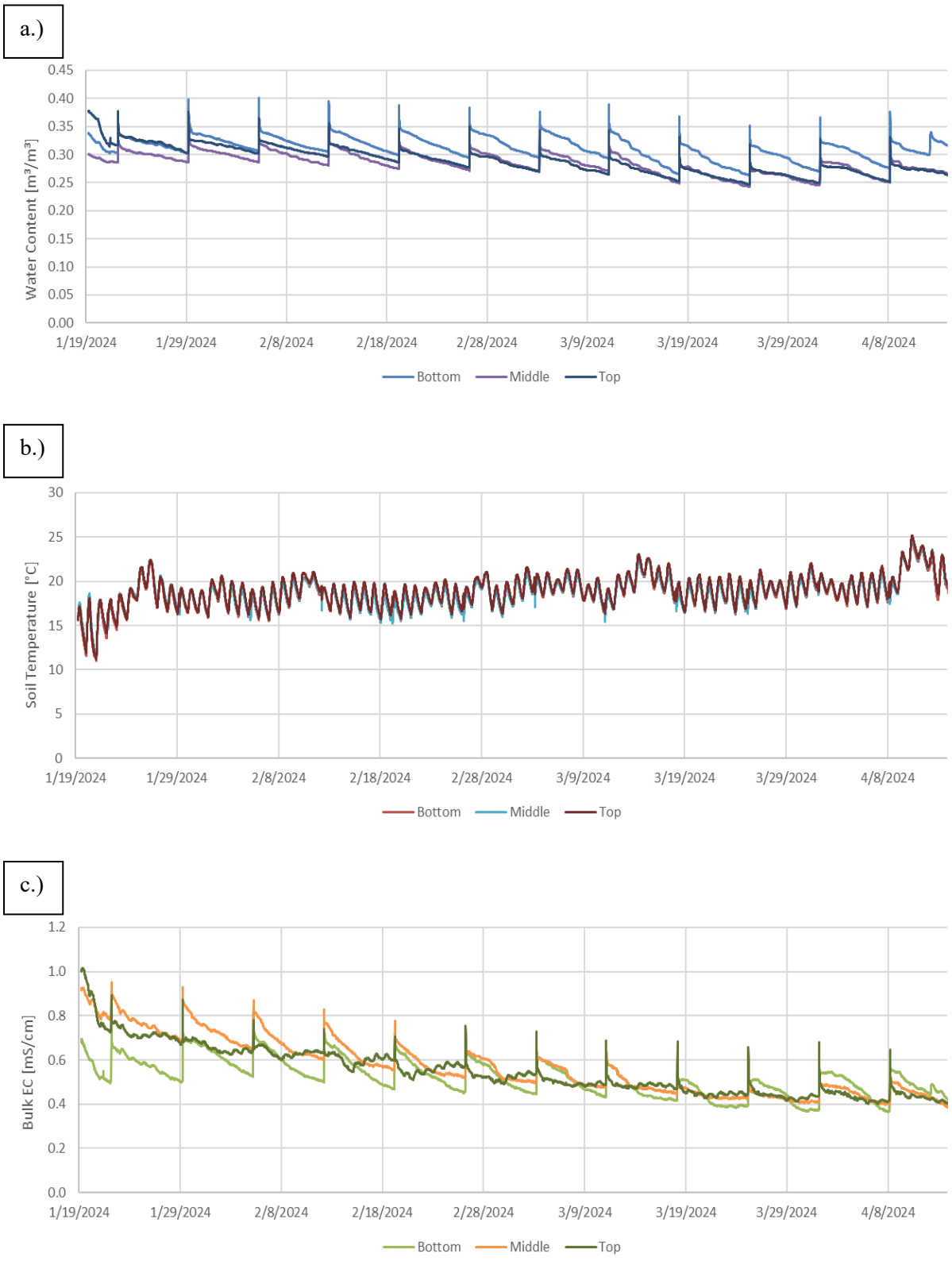

Figure E.5: Soil sensor readings for CL. a.) water content, b.) soil temperature, and c.) soil bulk electrical conductivity (EC).

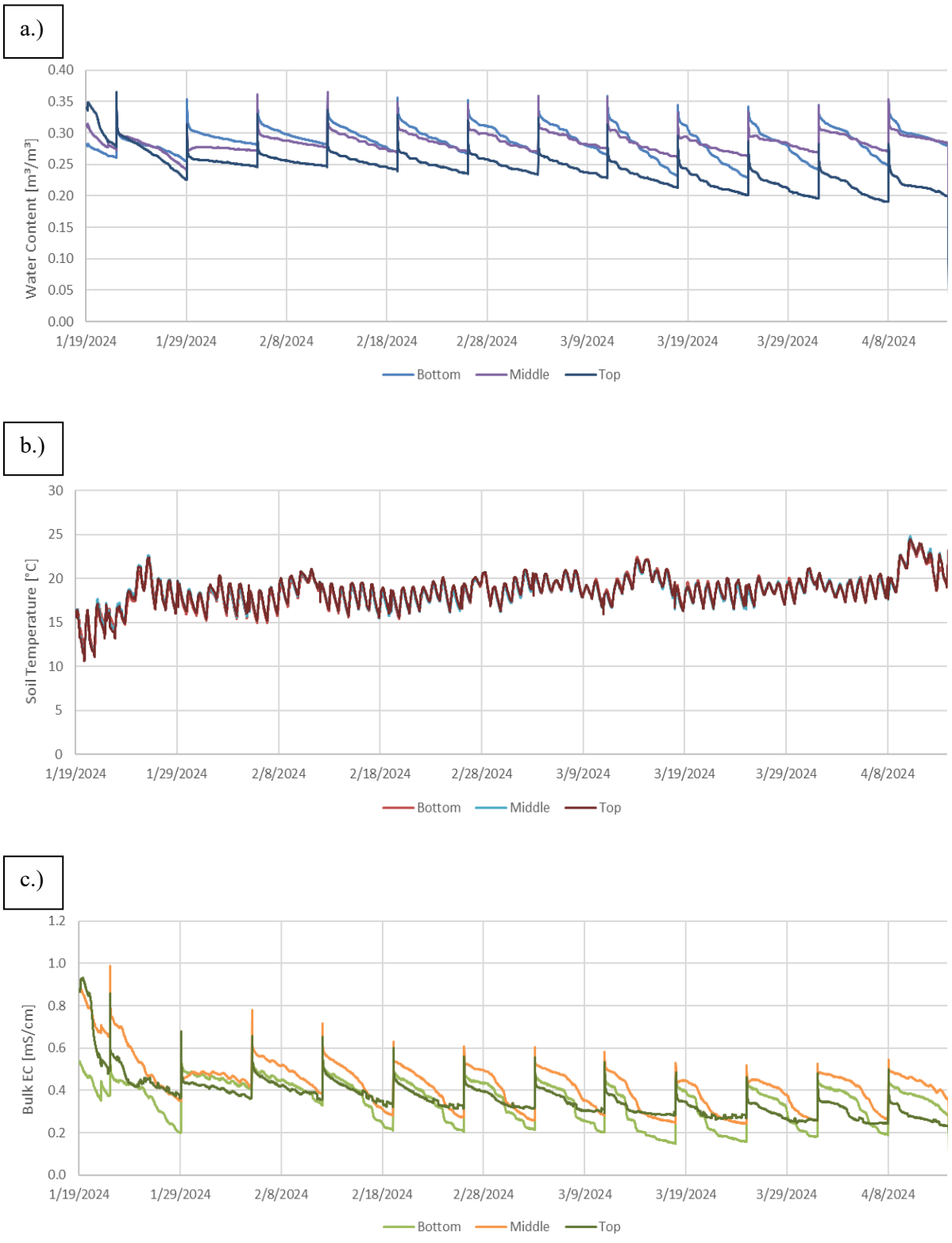

Figure E.6: Soil sensor readings for CH. a.) water content, b.) soil temperature, and c.) soil bulk electrical conductivity (EC).

References

Aggelides, S. M., and Londra, P. A. (2000). Effects of compost produced from town wastes and sewage sludge on the physical properties of a loamy and a clay soil, *Bioresource Technology*, 71(3), 253–259.

Bochet, E. and Garcia Fayos, P. (2004). Factors Controlling Vegetation Establishment and Water Erosion on Motorway Slopes in Valencia, Spain. *Restoration Ecology*, 12, 166-174.

Braun, R. C., Bremer, D. J., Ebdon, J. S., Fry, J. D., & Patton, A. J. (2022). Review of cool-season turfgrass water use and requirements: II. Responses to drought stress. *Crop Science*, *62*(5), 1685–1701. https://doi.org/10.1002/csc2.20790

Cannavo, P., Vidal-Beaudet, L., & Grosbellet, C. (2014). Prediction of long-term sustainability of constructed urban soil: Impact of high amounts of organic matter on soil physical properties and water transfer. *Soil Use and Management*, *30*(2), 272–284. https://doi.org/10.1111/sum.12112

Carrow, R. N. (1980). Influence of Soil Compaction on Three Turfgrass Species. *Agronomy Journal*, *72*(6), 1038–1042. https://doi.org/10.2134/agronj1980.00021962007200060041x

Cogger, C. G. (2005). Potential compost benefits for restoration of soils disturbed by urban development, *Compost Science & Utilization*, 13(4), 243–251.

Curtis, M. J., Grismer, M. E., and Classen, V. P. (2007). Effect of compost incorporation on infiltration capacity and erosion from a decomposed granite road cut, *Journal of Soil and Water Conservation*, 62(5), 338–344.

Duzgun, A. O., Hatipoglu, M., & Aydilek, A. H. (2021). Shear and Hydraulic Properties of Compost-Amended Topsoils for Use on Highway Slopes. *Journal of Materials in Civil Engineering*, *33*(8), 04021192. https://doi.org/10.1061/(ASCE)MT.1943-5533.0003797

Faucette, L.B., Jordan, C.F., Risse, L.M., Cabrera, M.L., Coleman, D.C., and West L.T. (2005). Evaluation of Stormwater from Compost and Conventional Erosion Control Practices in Construction Activities, *Journal of Soil and Water Conservation*, 60(6), 288-297.

Frasier, I., Noellemeyer, E., Fernández, R., & Quiroga, A. (2016). Direct field method for root biomass quantification in agroecosystems. *MethodsX*, *3*, 513–519. https://doi.org/10.1016/j.mex.2016.08.002

Glanville, T. D., Persyn, R.A., Richard, T.L., Laflen, J.M., and Dixon, P. M. (2004). Environmental effects of applying composted organics to new highway embankments: Part 2. Water quality, *Transactions of the American Society of Agricultural Engineers*, 471-478

Hansen, N.E., Vietor, D.M., Munster, C.L., White, R.H., and Provin, T.L. (2012). Runoff and nutrient losses from constructed soils amended with compost, *Applied and Environmental Soil Science*, article no. 542873.

Harrell, M. and Miller, G. (2005). Composted yard waste affects soil displacement and roadside vegetation, *HortScience*, 40 (7), 2157-2163.

Haynes, M.A., McLaughlin, R.A., Heitman, J.L., (2013). Comparison of methods to remediate compacted soils for infiltration and vegetative establishment. *Open Journal of Open Science*, 3, 225–234. https://doi.org/10.4236/ojss.2013.35027.

Helgason, B. L., Walley, F. L., & Germida, J. J. (2010). No-till soil management increases microbial biomass and alters community profiles in soil aggregates. *Applied Soil Ecology*, *46*(3), 390–397. https://doi.org/10.1016/j.apsoil.2010.10.002

Hino, M., Fujita, K., & Shutto, H. (1987). A laboratory experiment on the role of grass for infiltration and runoff processes. *Journal of Hydrology*, *90*(3–4), 303–325. https://doi.org/10.1016/0022-1694(87)90073-4

Hunt, W. F., Davis, A. P., & Traver, R. G. (2012). Meeting Hydrologic and Water Quality Goals through Targeted Bioretention Design. *Journal of Environmental Engineering*, *138*(6), 698–707. https://doi.org/10.1061/(ASCE)EE.1943-7870.0000504

Iowa DOT. (2023). "GS-Section 2601. Erosion Control." https://iowadot.gov/erl/current/GS/content/2601.htm

Iowa DOT. (2023). "GS-Section 2612. Mowing." https://iowadot.gov/erl/current/GS/content/2612.htm

Jani, J., Yang, Y.-Y., Lusk, M. G., & Toor, G. S. (2020). Composition of nitrogen in urban residential stormwater runoff: Concentrations, loads, and source characterization of nitrate and organic nitrogen. *PLOS ONE*, *15*(2), e0229715. https://doi.org/10.1371/journal.pone.0229715

Kirchoff, C. J., Malina, J. F., & Barrett, M. E. (2003). *Characteristics of composts: Moisture holding and water quality improvement*. Center for Research in Water Resources, University of Texas at Austin.

Kool, D., Tong, B., Tian, Z., Heitman, J. L., Sauer, T. J., & Horton, R. (2019). Soil water retention and hydraulic conductivity dynamics following tillage. *Soil and Tillage Research*, *193*, 95–100. https://doi.org/10.1016/j.still.2019.05.020

Kranz, C. N., McLaughlin, R. A., Johnson, A., Miller, G., & Heitman, J. L. (2020). The effects of compost incorporation on soil physical properties in urban soils – A concise review. *Journal of Environmental Management*, *261*, 110209. https://doi.org/10.1016/j.jenvman.2020.110209

Landschoot, P. and McNitt, A. (1994). Improving turf with compost, *BioCycle*, 35(10), 54–57.

Lipiec, J., Kuś, J., Słowińska-Jurkiewicz, A., & Nosalewicz, A. (2006). Soil porosity and water infiltration as influenced by tillage methods. *Soil and Tillage Research*, *89*(2), 210–220. https://doi.org/10.1016/j.still.2005.07.012

Melland, A. R., Antille, D. L., & Dang, Y. P. (2017). Effects of strategic tillage on short-term erosion, nutrient loss in runoff and greenhouse gas emissions. *Soil Research*, *55*(3), 201. https://doi.org/10.1071/SR16136

Mohammadshirazi, F., McLaughlin, R. A., Heitman, J. L., & Brown, V. K. (2017). A multi-year study of tillage and amendment effects on compacted soils. *Journal of Environmental Management*, *203*, 533–541. https://doi.org/10.1016/j.jenvman.2017.07.031

Mukhtar, S, McFarland, M.L., and Wagner, C.A. (2008). Runoff and water quality from inorganic fertilizer and erosion control compost treatments on roadway sideslopes, *Transactions of the ASABE*, 51(3), 927-936.

NOAA National Centers for Environmental information, Climate at a Glance: Statewide Time Series, published February 2023, retrieved on February 27, 2023 from https://www.ncei.noaa.gov/access/monitoring/climate-at-a-glance/statewide/time-series

NRCS Soil Quality Institute. (1999). Soil quality test kit guide. United States Department of Agriculture, Agricultural Research Service and Natural Resource Conservation Service. Kit guide can be obtained at http://www.statlab.iastate.edu/survey/SQI

Oliveira, M. T., & Merwin, I. A. (2001). Soil physical conditions in a New York orchard after eight years under different groundcover management systems. *Plant and Soil*, *234*(2), 233–237. https://doi.org/10.1023/A:1017992810626

Olson, N. C., Gulliver, J. S., Nieber, J. L., & Kayhanian, M. (2013). Remediation to improve infiltration into compact soils. *Journal of Environmental Management*, *117*, 85–95. https://doi.org/10.1016/j.jenvman.2012.10.057

Owen, D. C., Davis, A. P., & Aydilek, A. H. (2021). Compost for Permanent Vegetation Establishment and Erosion Control along Highway Embankments. *Journal of Irrigation and Drainage Engineering*, *147*(8), 04021031. https://doi.org/10.1061/(ASCE)IR.1943-4774.0001587

Owen, D. C., Davis, A. P., & Aydilek, A. H. (2022). Effects of Straw Mulching, Compost Percentage, and Slope Ratio on Green Vegetation Establishment and Runoff Quality Control. *Journal of Irrigation and Drainage Engineering*, *148*(1), 04021067. https://doi.org/10.1061/(ASCE)IR.1943-4774.0001641

Owen, D. C., Gardina, C., Ostrom, T. K., & Davis, A. P. (2023). Understanding Nitrogen and Phosphorus Leaching from Compost Addition to Bioretention Media. *Journal of Sustainable Water in the Built Environment*, *9*(2), 04023003. https://doi.org/10.1061/JSWBAY.SWENG-472

Pamuru, S. T. (2024). "Assessing the Impacts of Organic Amendments on Disturbed Soil Properties, Water Quality and Vegetation Growth." Doctor of Philosophy Thesis. College Park, MD: University of Maryland.

Pamuru, S. T., Morash, J., Lea-Cox, J. D., Ristvey, A. G., Davis, A. P., & Aydilek, A. H. (2024). Nutrient transport, shear strength and hydraulic characteristics of topsoils amended with mulch, compost and biosolids. *Science of The Total Environment*, *918*, 170649. https://doi.org/10.1016/j.scitotenv.2024.170649

Patrignani, A. and Ochsner, T.E. (2015), Canopeo: A Powerful New Tool for Measuring Fractional Green Canopy Cover. Agronomy Journal, 107: 2312-2320. https://doi.org/10.2134/agronj15.0150

Poorter, H., Bühler, J., Van Dusschoten, D., Climent, J., & Postma, J. A. (2012). Pot size matters: A meta-analysis of the effects of rooting volume on plant growth. *Functional Plant Biology*, *39*(11), 839. https://doi.org/10.1071/FP12049

Puppala, A. J., Hoyos, L. R., Qasim, S. R., & Intharasombat, N. (2011). Quality of Runoff Leachate Collected from Biosolids and Dairy-Manure Compost-Amended Topsoils. *Journal of Hazardous, Toxic, and Radioactive Waste*, *15*(2), 80–88. https://doi.org/10.1061/(ASCE)HZ.1944-8376.0000069

Qian, Y. L., Bandaranayake, W., Parton, W. J., Mecham, B., Harivandi, M. A., & Mosier, A. R. (2003). Long-Term Effects of Clipping and Nitrogen Management in Turfgrass on Soil Organic Carbon and Nitrogen Dynamics: The CENTURY Model Simulation. *Journal of Environmental Quality*, *32*(5), 1694–1700. https://doi.org/10.2134/jeq2003.1694

Qian, Y. L., Fry, J. D., & Upham, W. S. (1997). Rooting and Drought Avoidance of Warm-Season Turfgrasses and Tall Fescue in Kansas. *Crop Science*, *37*(3), 905–910. https://doi.org/10.2135/cropsci1997.0011183X003700030034x

Richard, G., Cousin, I., Sillon, J. F., Bruand, A., & Guérif, J. (2001). Effect of compaction on the porosity of a silty soil: Influence on unsaturated hydraulic properties: Soil compaction, pore geometry and hydraulic properties. *European Journal of Soil Science*, *52*(1), 49–58. https://doi.org/10.1046/j.1365-2389.2001.00357.x

Rivers, E. N., Heitman, J. L., McLaughlin, R. A., & Howard, A. M. (2021). Reducing roadside runoff: Tillage and compost improve stormwater mitigation in urban soils. *Journal of Environmental Management*, *280*, 111732. https://doi.org/10.1016/j.jenvman.2020.111732

Schmid, C. J., Murphy, J. A., & Murphy, S. (2017). Effect of tillage and compost amendment on turfgrass establishment on a compacted sandy loam. *Journal of Soil and Water Conservation*, *72*(1), 55–64. https://doi.org/10.2489/jswc.72.1.55

Simmons, M., Bertelsen, M., Windhager, S., & Zafian, H. (2011). The performance of native and non-native turfgrass monocultures and native turfgrass polycultures: An ecological approach to sustainable lawns. *Ecological Engineering*, *37*(8), 1095–1103. https://doi.org/10.1016/j.ecoleng.2011.03.004

Skinner, R. H., & Comas, L. H. (2010). Root Distribution of Temperate Forage Species Subjected to Water and Nitrogen Stress. *Crop Science*, *50*(5), 2178–2185. https://doi.org/10.2135/cropsci2009.08.0461

Vogel, J. R., Moore, T. L., Coffman, R. R., Rodie, S. N., Hutchinson, S. L., McDonough, K. R., McLemore, A. J., & McMaine, J. T. (2015). Critical Review of Technical Questions Facing Low Impact Development and Green Infrastructure: A Perspective from the Great Plains. *Water Environment Research*, *87*(9), 849–862. https://doi.org/10.2175/106143015X14362865226392

Wang, M., Zhang, D. Q., Su, J., Trzcinski, A. P., Dong, J. W., & Tan, S. K. (2017). Future Scenarios Modeling of Urban Stormwater Management Response to Impacts of Climate Change and Urbanization. *CLEAN – Soil, Air, Water*, *45*(10), 1700111. https://doi.org/10.1002/clen.201700111

Weindorf, D. C., Zartman, R. E., and Allen, B. L. (2006). Effect of compost on soil properties in Dallas, Texas, Compost Science & Utilization, 14(1), 59–67.

Zhang, S., Grip, H., & Lövdahl, L. (2006). Effect of soil compaction on hydraulic properties of two loess soils in China. *Soil and Tillage Research*, *90*(1–2), 117–125. https://doi.org/10.1016/j.still.2005.08.012